

THERMAL-SHOCK INVESTIGATION

T. A. Hunter

L. L. Thomas

A. R. Bobrowsky

United States Air Force
Wright Air Development Center
Wright-Patterson Air Force Base, Ohio

1949-3-F

Prepared by
Engineering Research Institute
University of Michigan
for
Contract No. AF 33(038)-21254

TABLE OF CONTENTS

LIST OF FIGURES	iv
LIST OF TABLES	v
ABSTRACT	vi
SUMMARY	ii
INTRODUCTION	1
OTHER INVESTIGATIONS	3
THEORETICAL ANALYSIS	3
APPROACH TO THE PROBLEM	5
APPARATUS	6
SPECIMEN	17
TEST PROCEDURE	23
CRACK DEFINITION	23
MATERIALS	25
RESULTS	29
General	29
Early Work	29
Second Phase	30
Recent Work	33
DISCUSSION OF RESULTS	47
Material Comparison	47
Thermal-Shock Parameter Correlation	47
Effects of Temperature	48
Type of Crack	50
CONCLUSIONS	50
BIBLIOGRAPHY	52
APPENDIX	53
Key to Wiring Schematic	55
Component Parts of Thermal-Shock Apparatus	56
Miscellaneous Capital Items	57
Power Transformer (Specifications)	57
Key to Test Log	58
Test Log	60

LIST OF FIGURES

Figure	Page
1a. Photograph of Cracks in Vane of a Nozzle Diaphragm.	2
1b. Photograph of Three-Vane Assembly from the Nozzle Diaphragm from Which Fig. 1a Was Taken.	2
2a. Original Test Setup--Cooling Nozzle Directed at Specimen.	7
2b. Original Test Setup--Test Frame and Control Panel.	7
3. Original Test Setup	8
4. Interior of Old Test Rig Showing Setup with Two Specimens.	8
5. Details of Setup with Radiation Pyrometer and Specimen Supports.	9
6. Compressive Plastic Flow Produced by Tests in Rigid Specimen-Nozzle Holders. Specimen No. 39 (top) and No. 43 (bottom), about 2X scale. Specimen No. 39 shows the face at which the air jet pointed, whereas Specimen No. 43 shows the face adjacent to the cooled face.	10
7. Front View of Specimen Holder, Specimen, Air Nozzle, and Radiation Pyrometer, (Old Rig).	10
8. Exterior of Sound-Minimizing Chamber Surrounding Test Rig.	11
9. View of Specimen Holder with Measuring Telescope in Position to View Specimen.	11
10. Control Panel (WADC, Modified).	12
11. Control-Panel Assemblies.	13
12a. Operating Unit, View above Deck.	14
12b. Operating Unit, View below Deck.	14
12c. Precision Nozzle, Throat Side.	15
12d. Precision Nozzle, Back Removed to Show Water Channels	15
13. Automatic Camera Setup.	16
14. Helium Test Apparatus.	17
15. Thermal-Shock Specimen of Round Cross Section, Showing Grooves after Test; Type 347 Stainless Steel.	18
16. Thermal-Shock Specimen of Square Cross Section.	18
17. Diamond-Shaped Specimen of Type 304 Stainless Steel, Fractured during Overheating in Thermal-Shock Test. Axial load was caused by lower electrode and grip.	19
18. Thermal-Shock Specimens of Hollow-Cut Cross Section. Top specimen is Type 347 stainless steel; botton specimen is Inconel.	20
19. Thermal-Shock Specimen.	20
20. Triangular Specimens with Thermocouple Holes.	21
21. Fatigue Specimen.	21
22. Low-Speed Fatigue Machine (1800 rpm).	22
23. Enlargement of One Frame of Automatic 35-mm Camera Film Strip Showing Crack in Kennametal Type K-152 B, Specimen No. 2 at 261 Cycles.	24
24a. Specimen Showing Severe Oxidation. Visual crack inspection is difficult. Three cracks are present. Inconel, 1800°F.	26
24b. Kennametal Type 152 B No. 4, Showing Complete Fracture and Burning.	26
25a. Mechanical Crack in Type 304 Stainless Steel in Vicinity of Rupture Failure. X100.	27
25b. Thermal Crack in Type 304 Stainless Steel. X100.	27
25c. IN-5, 1819 Cycles, 100X.	28
25d. IN-7, 4706 Cycles, 100X.	28

LIST OF FIGURES (cont.)

Figure	Page
26. HS-21 at 2000°F after 673 Cycles.	32
27. Waspalloy at 2000°F after 784 Cycles.	32
28. Comparative Thermal-Shock Resistance--Temperature 1600°F.	34
29. Comparative Thermal-Shock Resistance--Temperature 1700°F.	35
30. Comparative Thermal-Shock Resistance--Temperature 1800°F.	36
31. Comparative Thermal-Shock Resistance--Temperature 1900°F.	37
32. Comparative Thermal-Shock Resistance--Temperature 2000°F.	38
33. Thermal-Shock Resistance--Nickel-Base Alloys.	42
34. Thermal-Shock Resistance--Iron-Base Alloys.	43
35. Thermal-Shock Resistance--Cobalt-Base Alloys.	44
36. Thermal-Shock Resistance--K-151-A and K-152-B Cermets.	45
37. Thermal-Shock Resistance--Battellalloy.	46
38. Hastelloy C at 2000°F, Air-Cooled for 291 Cycles.	49
39. Hastelloy C at 2000°F, Helium-Cooled for 624 Cycles.	49
A-1. Schematic Wiring Diagram of Test Rig. See Key.	54

LIST OF TABLES

Table	Page
I. Thermal-Shock Resistance at 1600°F.	39
II. Thermal-Shock Resistance at 1700°F.	39
III. Thermal-Shock Resistance at 1800°F.	40
IV. Thermal-Shock Resistance at 1900°F.	40
V. Thermal-Shock Resistance at 2000°F.	41
VI. Decreasing Order of Thermal-Shock Resistance.	51

ABSTRACT

Fourteen materials have been examined for their relative resistance to severe repeated thermal shock in the temperature range from 1600 to 2000°F, using a suitable specimen shape developed during the evaluation. It was found that thermal shocking by itself would produce cracking in all the materials tested.

SUMMARY

A program of investigation has been undertaken to evaluate the resistance of various materials to thermal shocking. A preliminary analysis of thermal-shock damage has been carried out on a theoretical basis. The results of this theoretical work indicate that the scope of the problem is so wide that purely analytical methods must be supplemented by experimental data.

An experimental program has therefore been set up to test several selected materials. Suitable apparatus has been constructed which gives reasonable reproducibility of results. A standard specimen shape has been devised after considerable experimentation. Excursions into the subjects of previous specimen history, mechanical fatigue, and thermal wiggling have been made.

FINAL REPORT

THERMAL-SHOCK INVESTIGATION

INTRODUCTION

Design of the turbine buckets is one of the most important problems of modern aircraft gas turbines. This design problem is complicated by the presence of high mechanical stresses, high temperatures, and a fatigue component. It is important that a reasonable method be found for bucket design, since the durability of the buckets appears to be one of the critical factors in the determination of the limiting overhaul time for the gas turbine aircraft engine.

The usual approach to bucket design is based on known centrifugal stresses interpreted from data on the short-time elevated-temperature tensile strength, creep rate, and stress-rupture life of the material. Until recently fatigue effects have usually been neglected because of lack of information about the fatigue-producing mechanism in the engine. Thermal effects can be included in the design if the operating temperatures of the turbine can be found; but this has been done only roughly and in a few cases.

Little attempt has been made to consider the effects of stress concentrations in bucket design. Stress raisers such as lateral cracks are known to be absent from the buckets, prior to their use, by virtue of 100-percent inspection of such parts before assembly. However, it has been shown by experience that cracks are initiated and developed in turbine parts during operation. These cracks act as stress raisers in three ways, first by furnishing a stress concentration, second by reducing the net section of material and thereby raising the nominal stress, and third by acting as surfaces for the growth of oxides which force the cracks open. Further, cracks may serve to nucleate fatigue failures. It has been observed that cracks have formed in the operation of turbine blades. These service cracks have been found to be distributed in such a manner that mechanical stresses alone would not have caused them to appear. These cracks indicate that the leading edges of turbine blades operate in tension, that the tension is almost uniform, and that cracks can be produced by repeated thermal straining. Examination of certain nonrotating parts of gas turbines also revealed cracks which could not have been mechanical in origin (see Figs. 1a and 1b).

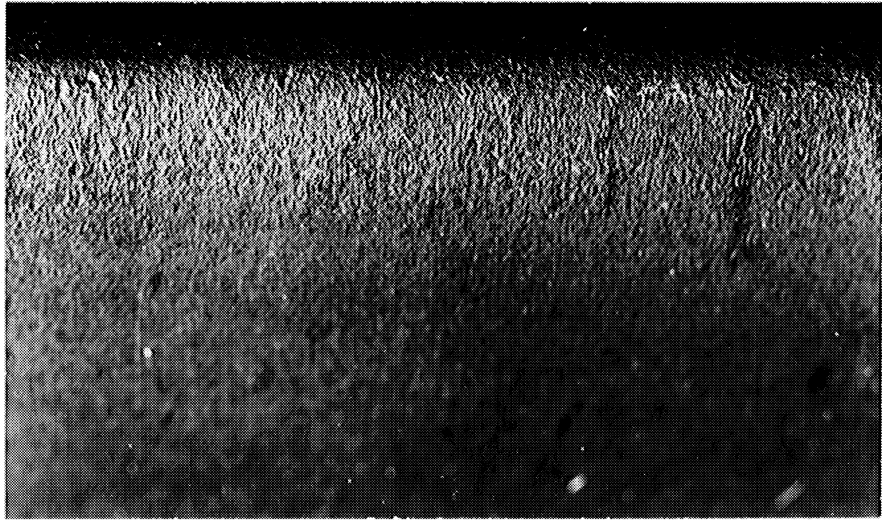


Fig. 1a. Photograph of Cracks in Vane of a Nozzle Diaphragm.



Fig. 1b. Photograph of Three-Vane Assembly from the Nozzle Diaphragm from Which Fig. 1a Was Taken.

In the light of this information, the Wright Air Development Center decided to sponsor research on the resistance of materials to repeated and severe thermal stressing. The basic test apparatus had been assembled by the Wright Air Development Center and was loaned to the University of Michigan for use. This basic apparatus has been redesigned and improved by several modifications. It uses an electrical resistance heating cycle of 60-second duration followed by a cold-air-blast shock-cooling cycle of 5-second duration. This operation has an effect on the specimen which is reasonably similar to that produced on a turbine blade during a flame-out or start-up in an aircraft.

This research was conducted at the University of Michigan Engineering Research Institute from April, 1951 to April, 1954.

OTHER INVESTIGATIONS

Previous investigations of cracking by thermal stress can be classified on the basis of the ductility of the material tested. Norton¹ and Lidman and Bobrowsky² worked on brittle ceramic materials. Whitman and others³ investigated metals which had a "reasonable" ductility. Avery and Matthews⁴ studied brittle castings. The work done on metals in reference 3 used a water coolant, a condition which does not prevail in gas turbine operation; therefore, this work was not considered strictly applicable to the present case.

It is understood that others are working on the thermal-shock problem concurrently with the present investigation; the Climax Molybdenum Company at Detroit, Allison Engine Division of General Motors Corporation at Indianapolis, General Electric Company at Schenectady, Allegheny Ludlum Steel Company, and the National Advisory Committee for Aeronautics are all reported to be interested in this problem.

THEORETICAL ANALYSIS

Since thermal shock is essentially a problem in heat transfer, the effects of conduction, convection, and radiation must be considered immediately. In the type of test which uses a blast of cold air to provide the thermal shock, the most important means of heat transfer is convection. Conduction is not negligible however, as a considerable amount of heat is drawn from the specimen into the water cooling system in the grips at the ends of the test piece. It is recognized that for the test piece, the ratio of the convection heat loss to the conduction heat loss is not so high as the same ratio for similar material in the shape of a turbine bucket because of the relatively larger conduction loss for the test piece. To allow for this, the velocity of the air blast has been made as high as possible (Mach 1) to maximize the convection effect. The effects of radiation are considered to be very small in contrast to conduction and convection and are ignored for both the test piece and the turbine bucket. In addition to the heat-transfer effects, certain specific properties of the materials must also be taken into consideration in evaluating thermal-shock

resistivity. Such factors as thermal-expansion coefficient, Poisson's ratio, yield point at the working temperature, thermal diffusivity, thermal conductivity, and ductility are involved in the analysis. Apparently, the material which develops the smallest thermal stress in proportion to the yield-point stress will be the best material in thermal-shock resistance. Such a material would then have a high thermal conductivity and diffusivity to prevent localized steep thermal gradients, a low expansion coefficient to reduce the thermal strains, a high yield stress and ductility to permit the maximum thermal stresses to be resisted, and a small value for Poisson's ratio to reduce lateral strains to a minimum. Generally, these specific properties of the material are most influential in the initiation of a crack in a thermal-shock specimen. Once a crack has been started, however, the phenomenon changes from crack initiation to crack propagation.

Corrosion resistance and oxidation are also of importance. It is known that single thermal shocks do not produce cracking in ductile materials and that the failure must therefore be progressive. Closely related factors are fatigue resistance and the deterioration of mechanical and metallurgical properties immediately prior to crack formation. It has been thought that the mechanism of mechanical fatigue and the mechanism of thermal fatigue are probably related.

In summary, the analysis of the problem may be set down in terms of the groups of variables which may be expected to affect the thermal-shock resistance of a material. The first group constitutes the external conditions of the test. These are usually referred to as the boundary conditions and are

External temperatures
Velocity of coolant
Properties of coolant
Specimen dimensions
Time

A second group of variables consists of the thermal, mechanical, and metallurgical properties of the material. These are

Thermal Properties

Specific heat
Thermal diffusivity
Emissivity
Thermal conductivity
Thermal expansion

Mechanical Properties

Elastic modulus
Poisson's ratio
Stress rupture
Fatigue strength
Creep
Yield strength
Ductility

Metallurgical Properties

Structure
Composition
Stresses and strains
Chemical reaction
Surface separations

APPROACH TO THE PROBLEM

Unfortunately, several of the twenty-two variables are related, and may even be related in several ways. It is believed that the combinations of external boundary conditions and material properties give rise to certain changes which lead to the production of micro-cracks and subsequent failure by fatigue. It does not appear feasible to analyze the thermal-shock phenomenon in terms of each of the twenty-two separate factors; therefore, the common approach of lumping several items together has been used in accordance with the method of concomitant variations.

All the external conditions have been taken as a unit by deciding on a certain size and shape of specimen for all tests, using a common coolant (air at 85 psi), and setting up a definite time sequence for all testing operations. The temperature of the specimen is the only variable in this group.

Of the thermal properties, only the conductivity and the expansion coefficient are thought to be important quantities in thermal shock. The metallurgical properties are largely dependent on previous conditions and are not subject to control in a series of subsequent experiments; therefore they are ignored. Of the mechanical properties, only the stress-rupture and fatigue-strength variables are considered for correlation with test results. Variation of any of the properties during the shocking process has not been considered.

Using this basic analysis as a reference, the attack on the problem was focussed on the following items:

1. The development of a reliable thermal-shocking apparatus using compressed air as the coolant.
2. The invention of a reasonably reproducible test, including a reasonable definition of thermal-shock failure.
3. The production of an ordered list of the thermal-shock resistances of various materials.

It is realized that the experimental method proposed cannot yield the fundamental parameters of the deterioration phenomenon which leads to cracking under thermal-shock conditions. However, it is possible, by experimental means, to obtain information of much practical use in the determination of economic overhaul intervals and in the evaluation of the merits of various materials. In this report most of the data are intended to serve as a datum for the thermal-shock resistance of a given material. This datum has been obtained by evaluating the material without previous exposure to stresses, fatigue, or elevated stress-temperature pretreatment.

It was hoped that a certain amount of work could be done on the deterioration process which accompanies failure by thermal cracking. It was planned to test the materials under both thermal-shock and stress-rupture conditions in order to produce

thermal-shock failure in a given number of cycles. An arbitrary number of cycles, about 100, was chosen for a working basis. Time did not permit any evaluations. Impact tests to measure deterioration could not be used, since they depend on bulk properties of the material and only a small portion near the shocked edge of the test specimens suffered appreciable deterioration. Rotating-beam fatigue tests required preparation of an excessive number of specimens and, thus, were impracticable.

APPARATUS

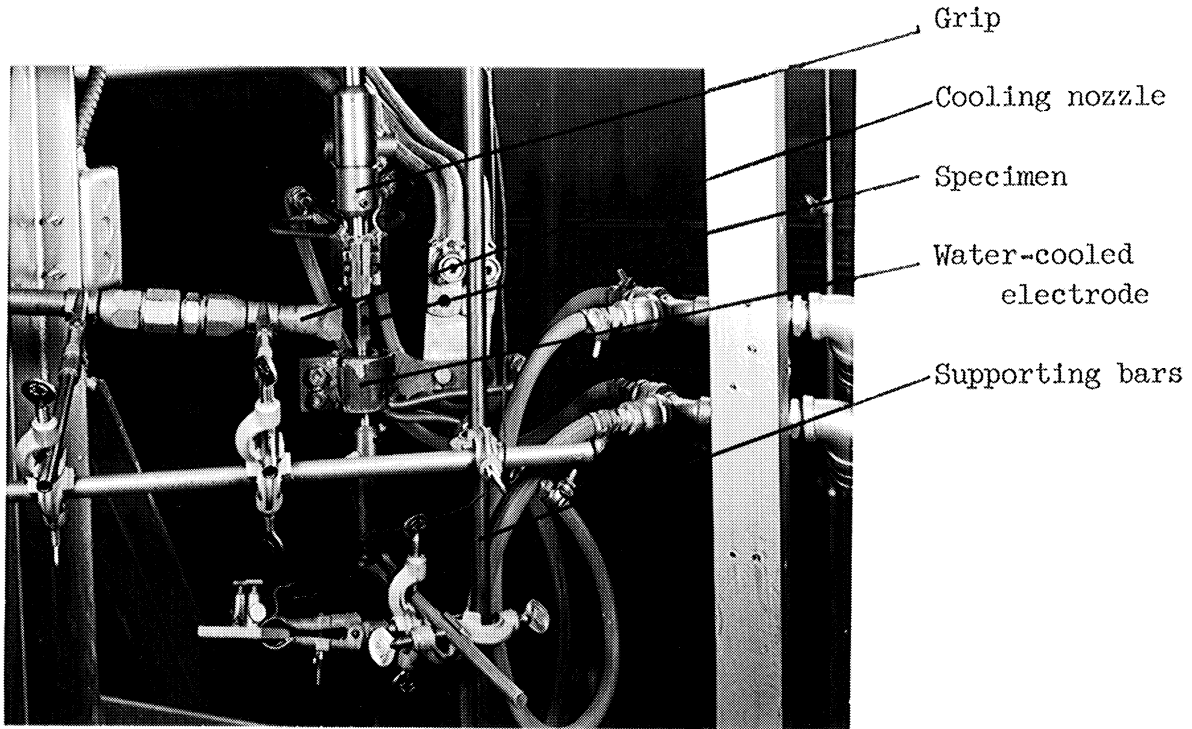
The testing rig which was originally used on this work was borrowed as a unit from Wright Air Development Center and subsequently altered a number of times to fit the immediate needs of the studies. Four new testing units were assembled using the Wright Air Development Center unit as a model, but incorporating extensive modifications.

Basically the units consist of two components, an operating part and a control part. The operating part holds the specimen, heats it as desired, cools it with an air blast, and has equipment for observing the specimen from time to time. The control unit contains the timers for maintaining uniformity of the heating and cooling cycles, temperature-regulating devices, power-supply controls, and a cumulative-cycle counter.

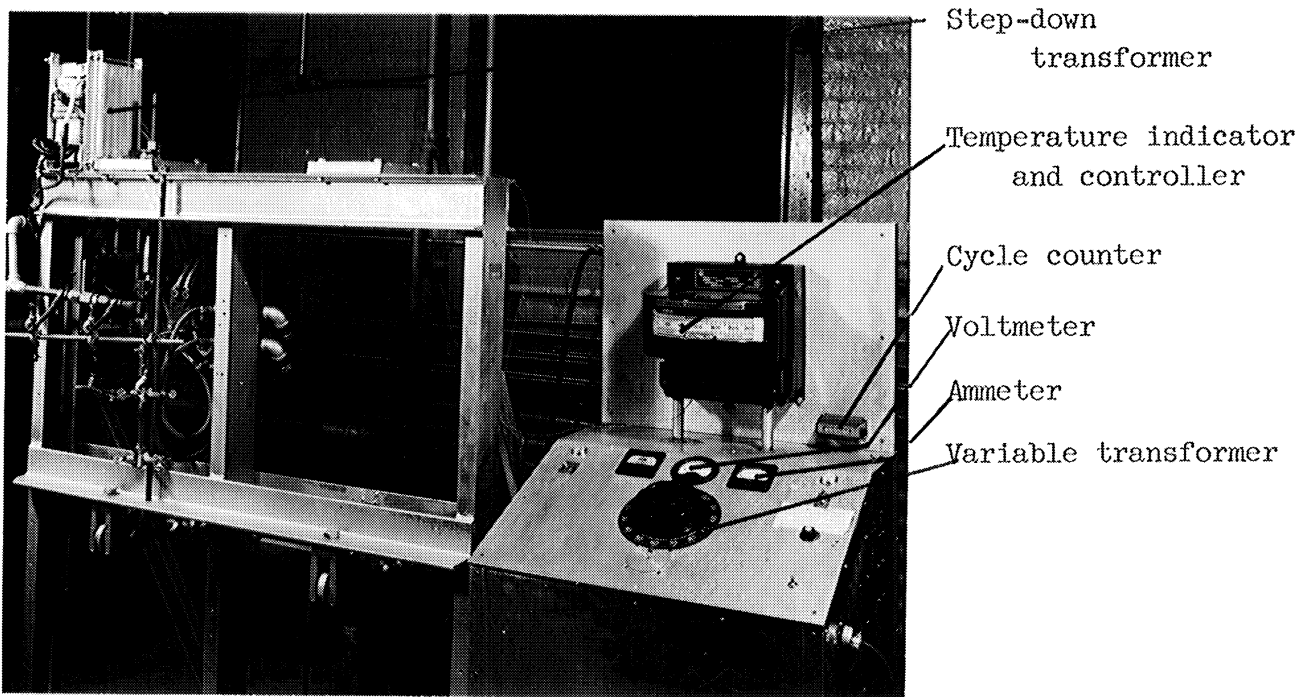
The testing cycle consists of a 1-minute heating period followed by a 5-second cooling blast of air. The specimen is heated by using the secondary circuit of a step-down transformer. Local heating of the test section results from a reduction in the area of the test piece at the test section, thus providing a higher local resistance for the heavy flowing currents. Control of the time of the heating cycle is obtained by setting a variac manually to fix the input voltage to the primary side of the transformer at such a value that the maximum desired specimen temperature is reached in one minute. The end of the heating cycle is determined by a Wheelco control which is actuated by a radiation pyrometer. When the pyrometer measures a specimen temperature corresponding to the setting of the Wheelco control, the heating current stops and the air blast turns on for 5 seconds. The duration of the air blast is controlled by an electric timer. At the end of 5 seconds the air blast is stopped, the heating current begun again, and the cycle repeated.

The original equipment is shown in Figs. 2a, 2b, and 3. The first alterations were the addition of a plenum chamber to improve the uniformity of the velocity of the air blast, and enlargement of the piping to reduce friction losses during the blast cycle. Also, a second operating setup was installed in the original test frame (Fig. 4). In this new device the temperature of the specimen was measured by a total-radiation pyrometer, instead of the thermocouple previously used, since the drilling of a thermocouple hole in the specimens had proved troublesome, and the hole also acted as an undesired stress raiser.

A further change was made at this time by integrating the air nozzle with the specimen holder as shown in Fig. 5. This resulted in better alignment of the air blast with the edge of the piece being tested. At this same time it was noted that



a. Cooling Nozzle Directed at Specimen.



b. Test Frame and Control Panel.

Fig. 2. Original Test Setup.

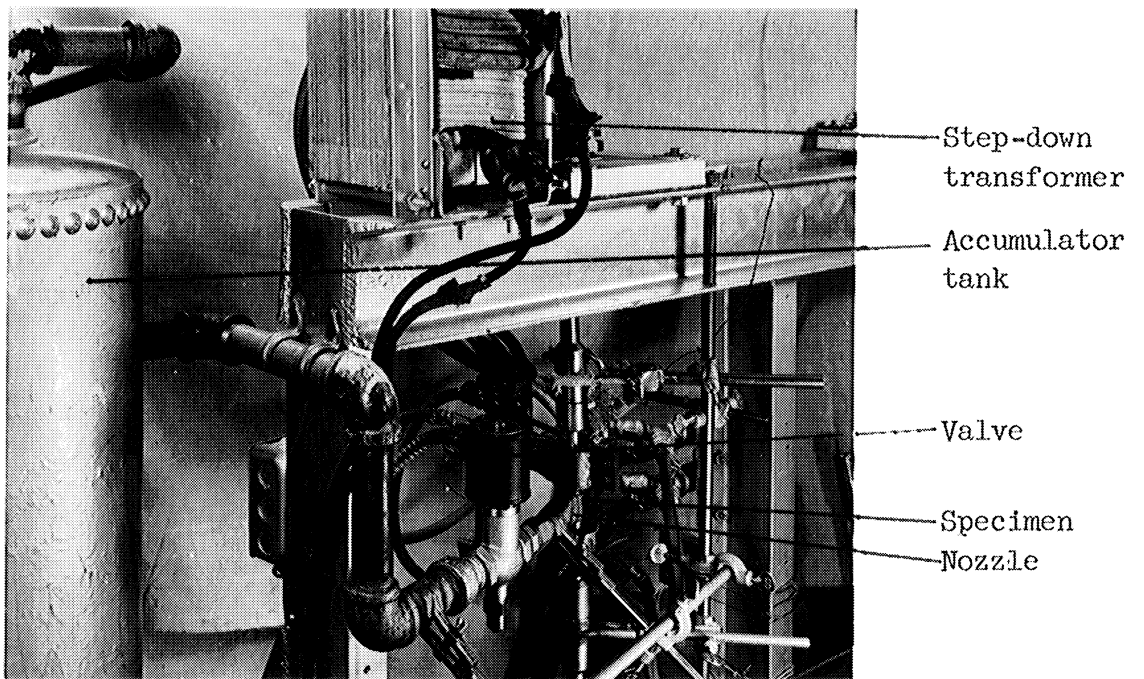


Fig. 3. Original Test Setup.

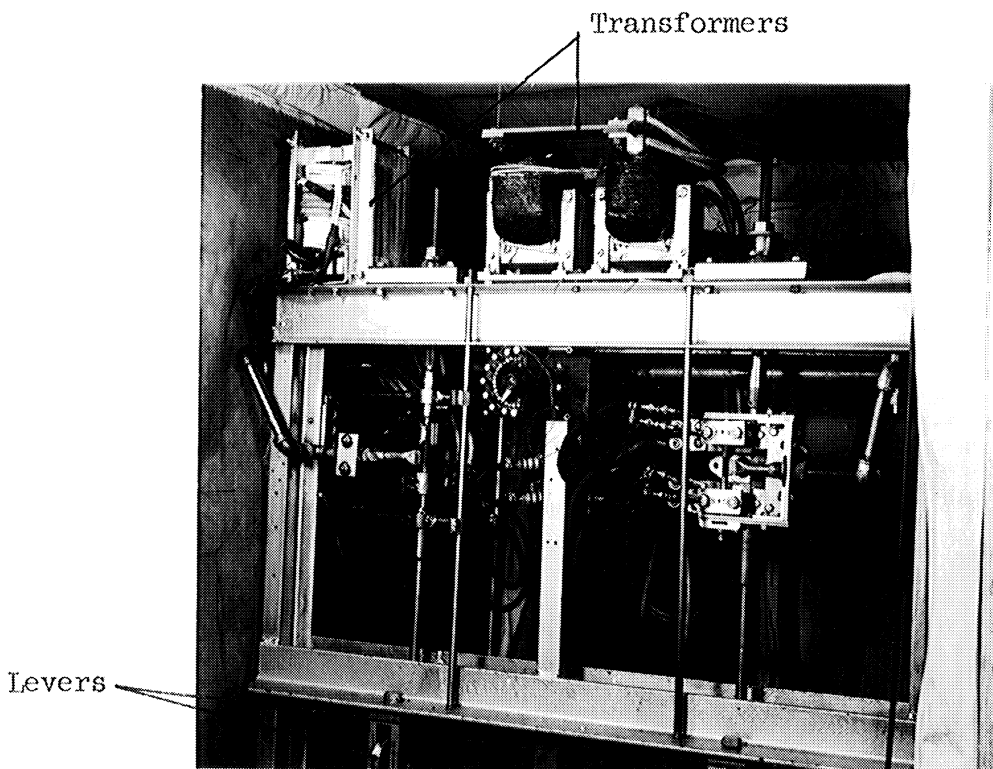


Fig. 4. Interior of Old Test Rig Showing Setup with Two Specimens.

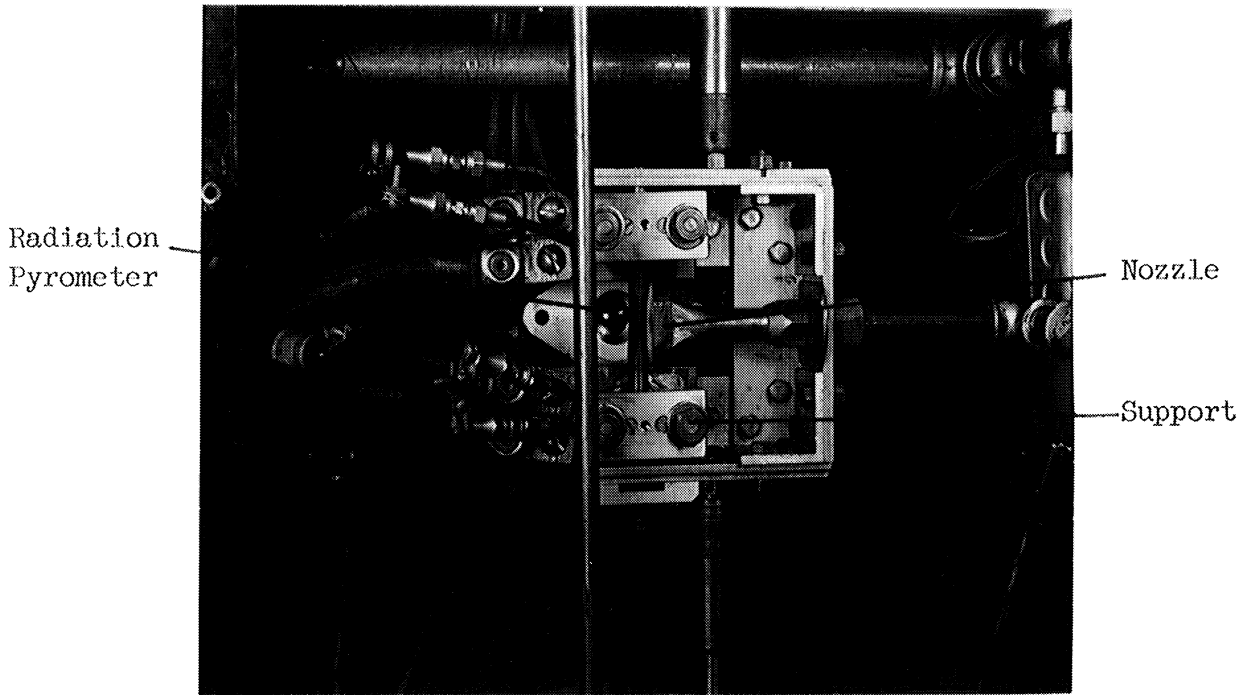


Fig. 5. Details of Setup with Radiation Pyrometer and Specimen Supports.

the test pieces were bulging badly when heated because thermal expansion was not permitted (Fig. 6). A redesign of the grips to permit axial motion was incorporated resulting in the arrangement shown in Fig. 7. This figure also shows a change from a flattened-tube type of air nozzle to a precision movable-wall type. This new nozzle provided for adjustment of the air velocity to about Mach 1, as determined by Schlieren means. Use of this nozzle required the construction of a sound-deadening chamber to surround the entire operating portion. This consisted of a framework filled with batts of slag wool (Fig. 8). The final addition to the operating rig was the installation of a telescope to permit the observation of the specimen during a test (Fig. 9). The control panel had to be rebuilt to accommodate two sets of controls; it is shown in Fig. 10.

It was soon realized that the use of only two test units would unduly prolong the investigations. The construction of four additional units was therefore begun, with the design based on the modified WADC equipment. A completely new design was worked out to permit rack mounting of the control equipment, as shown in Fig. 11. The operating rigs were redesigned to permit easier thermal expansion to take place, and the nozzles were provided with water-cooling passages, (Figs. 12c and 12d). Refinements were included which permitted more accurate positioning of the specimen, and the installation of automatic recording camera equipment to allow 24-hour-per-day operation (Figs. 12 and 13).

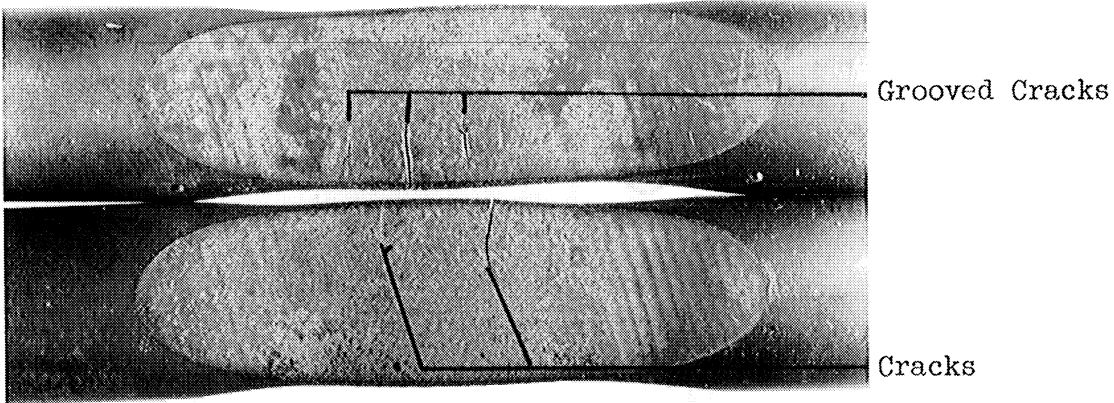


Fig. 6. Compressive Plastic Flow Produced by Tests in Rigid Specimen-Nozzle Holders. Specimen No. 39 (top) and No. 43 (bottom), about 2X scale. Specimen No. 39 shows the face at which the air jet pointed, whereas Specimen No. 43 shows the face adjacent to the cooled face.

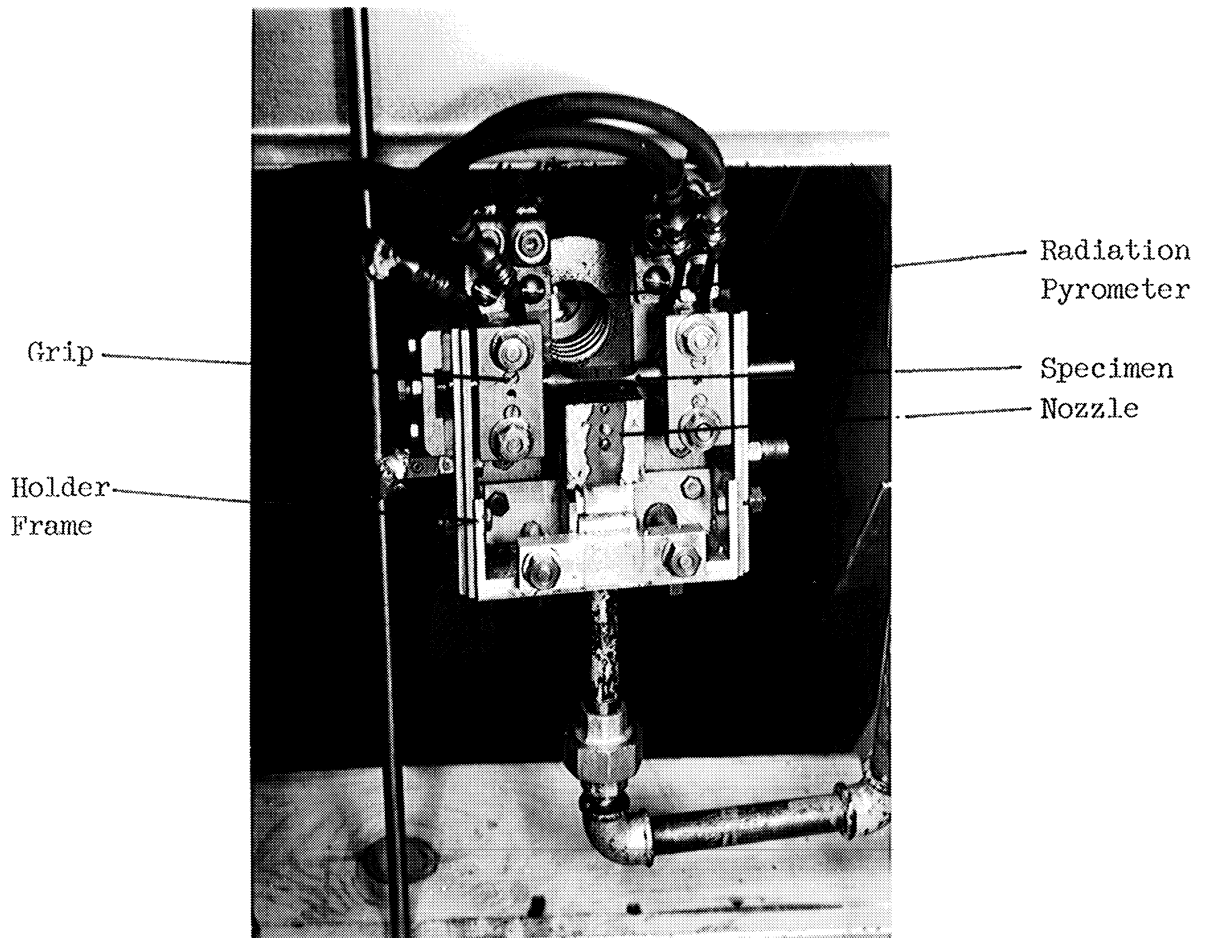


Fig. 7. Front View of Specimen Holder, Specimen, Air Nozzle, and Radiation Pyrometer, (Old Rig).

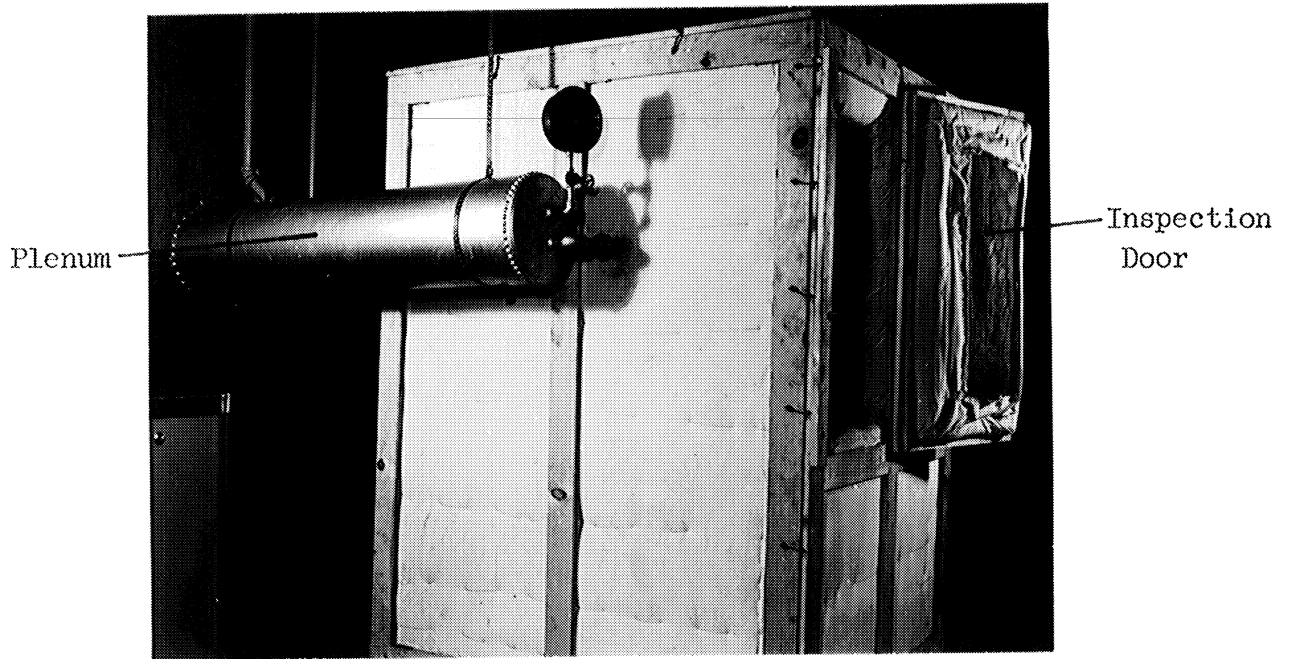


Fig. 8. Exterior of Sound-Minimizing Chamber Surrounding Test Rig.

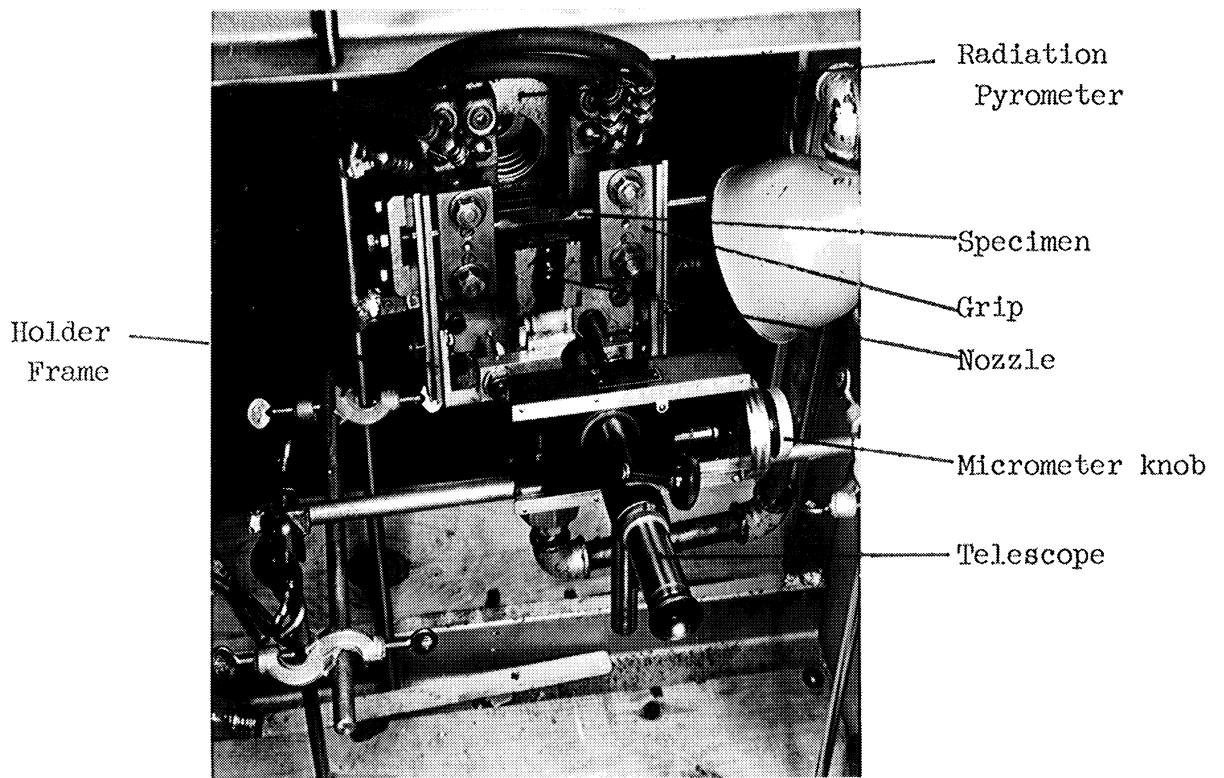


Fig. 9. View of Specimen Holder with Measuring Telescope in Position to View Specimen.

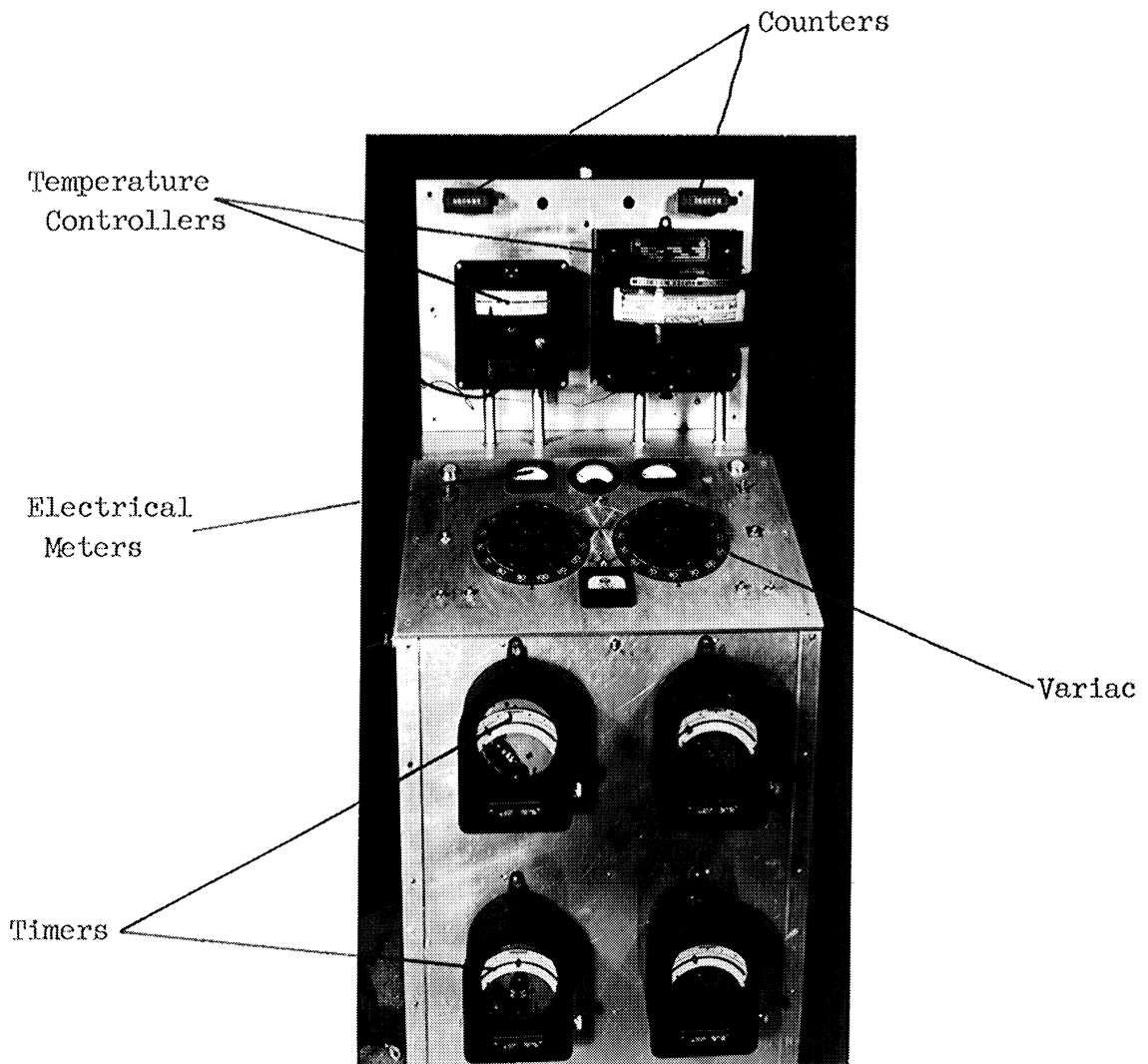


Fig. 10. Control Panel (WADC, Modified)

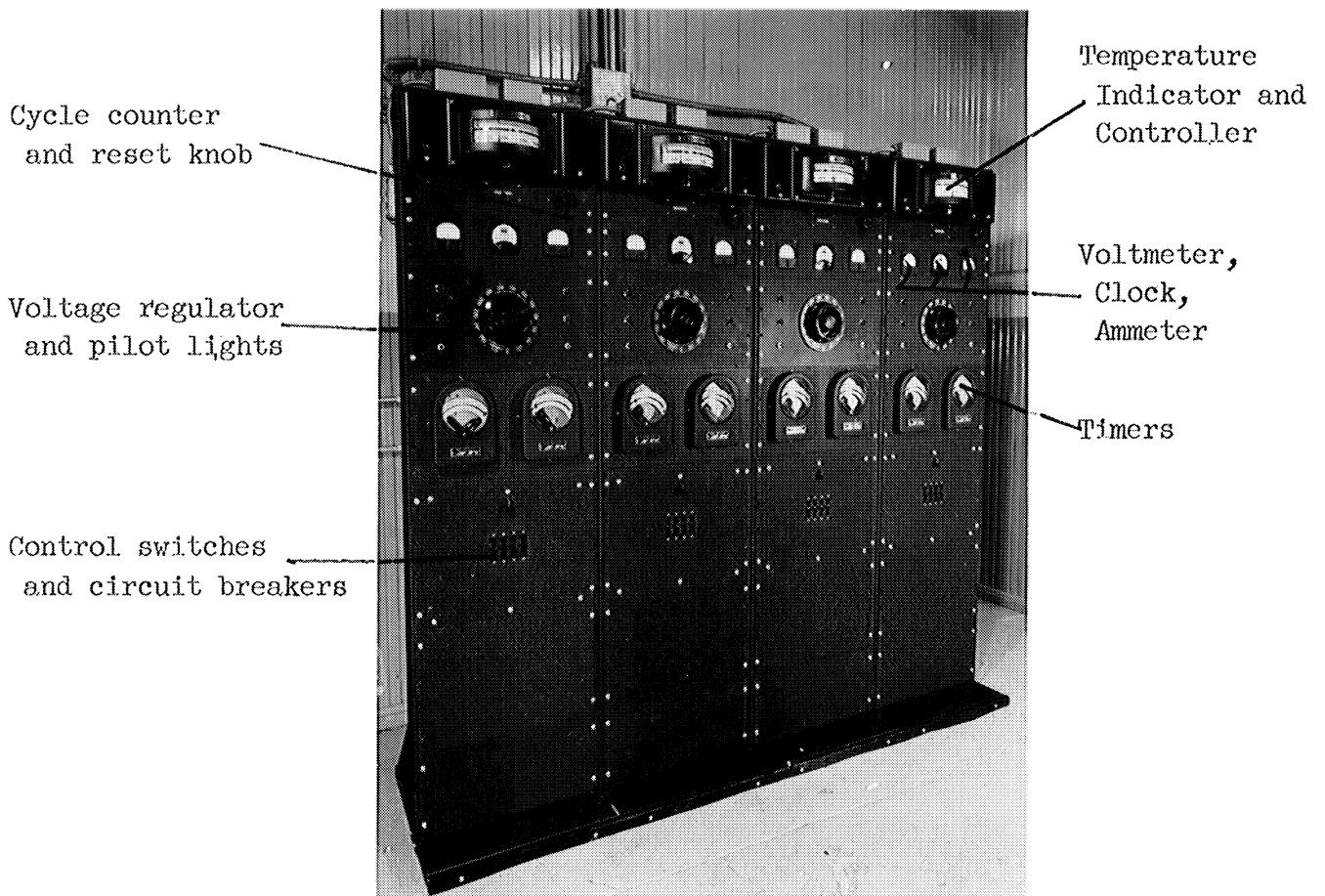


Fig. 11. Control-Panel Assemblies.

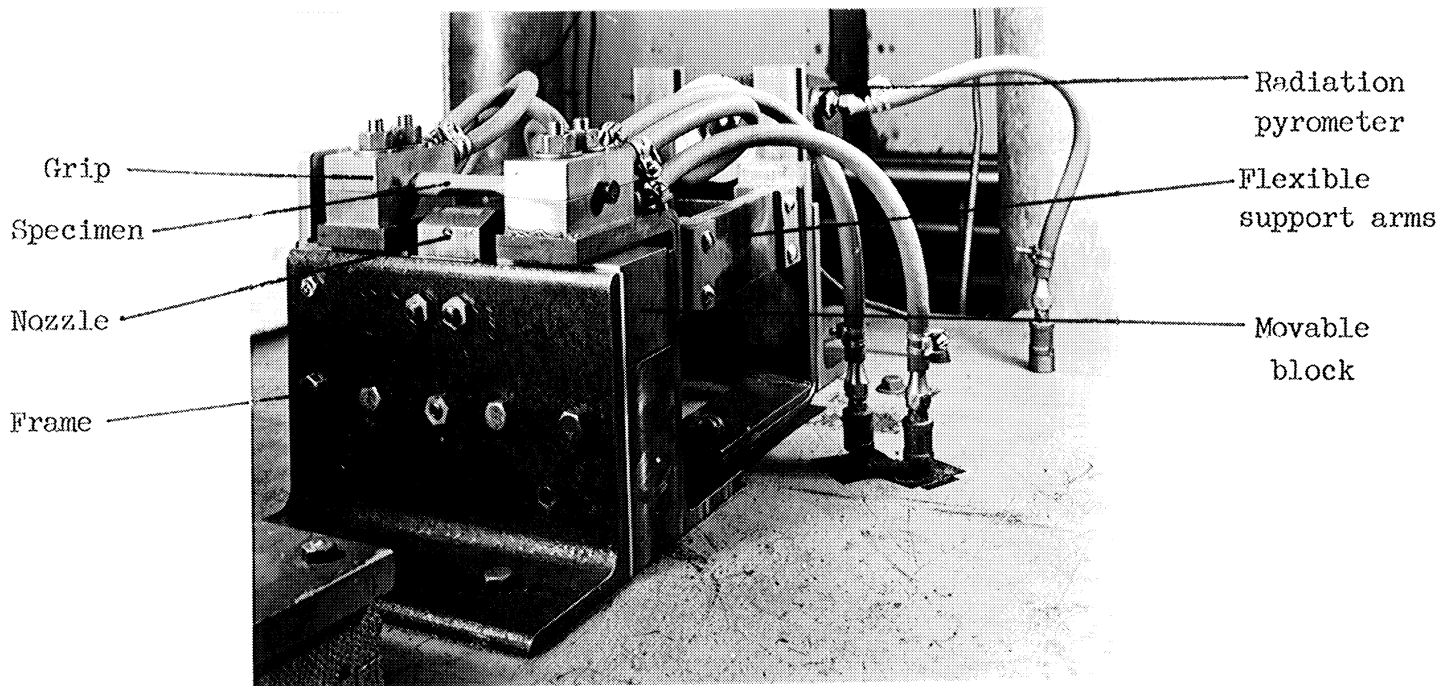


Fig. 12a. Operating Unit, View above Deck.

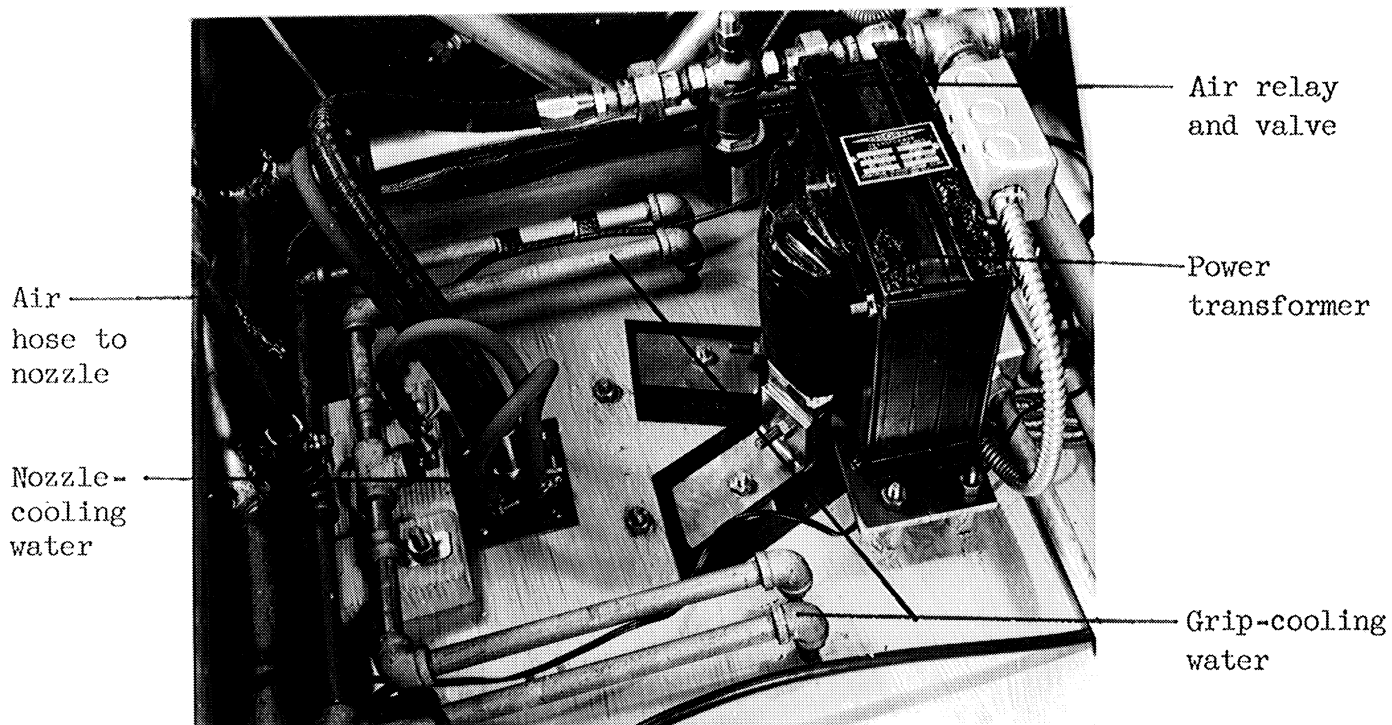


Fig. 12b. Operating Unit, View below Deck.

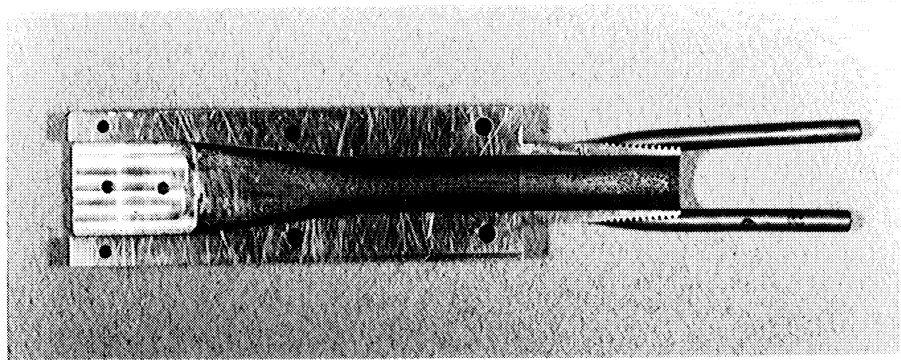


Fig. 12c. Precision Nozzle, Throat Side.

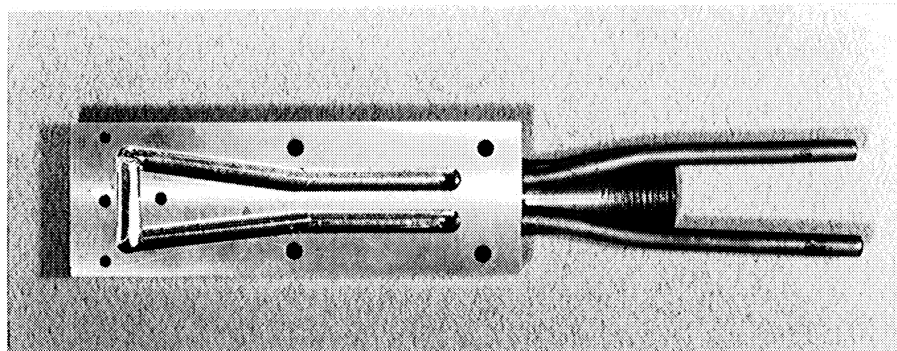


Fig. 12d. Precision Nozzle, Back Removed to Show Water Channels.

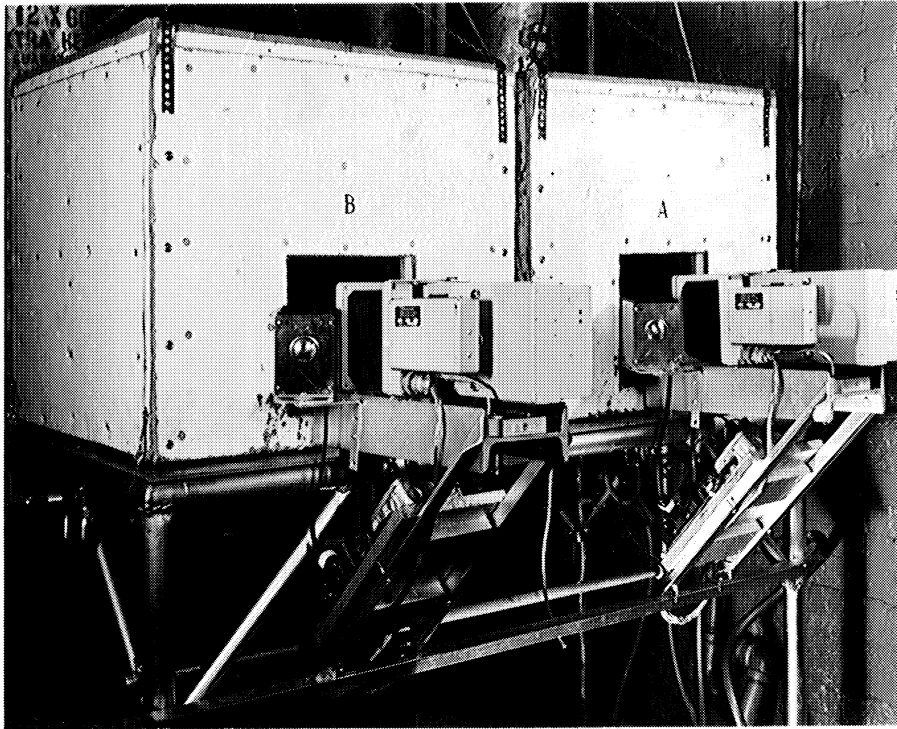


Fig. 13. Automatic Camera Setup.

Water cooling of the nozzles was necessary because of the closeness of the nozzle orifice to the heated specimen. It was found that radiation from the specimen was sufficient to heat the brass parts of the nozzle to such a temperature that the dimensions of the orifice would change appreciably and affect the performance of the air blast. The hot nozzle parts also adversely affected the uniformity of the air blast, since they had to be cooled by the air at the beginning of each blast. By keeping the nozzle at a uniform temperature with cooling water, both these adverse effects were reduced appreciably.

On one series of tests helium gas was used as the cooling medium. Tanks of the gas were connected to one of the plenum chambers as shown in Fig. 14, and a plastic liner was applied to the inside of the sound-deadening chamber to reduce the escape of gas during the tests.

A schematic diagram and parts list for the operating and control units are included in the appendix.

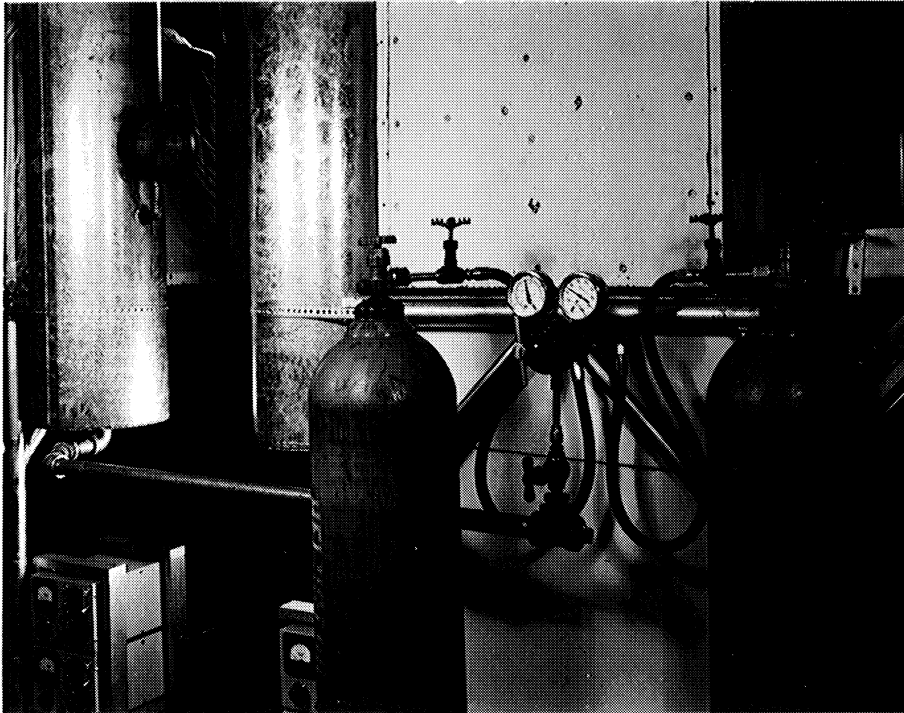


Fig. 14. Helium Test Apparatus.

SPECIMEN

One of the primary problems in this research was the design of a suitable test specimen. To be satisfactory, the specimen had to yield reasonably reproducible results, be simple to prepare, permit accurate temperature determinations while a test was in progress, and permit easy detection of cracks. The basic form of the test piece chosen was a cylindrical rod about $1/2$ inch in diameter and from 7 to 9 inches in length. The center portion of this piece was then machined to a desired cross section. Removal of material in the machining process provided the necessary local increase of electrical resistance to develop local heating of the test section.

Several cross-section shapes were investigated. A round section was first chosen because of its simplicity. As shown in Fig. 15, such a section does not possess any sharp edges; hence the tendency for a shallow crack to develop into a groove is pronounced. This grooving action made accurate crack detection very difficult, and pointed to the development of a cross section with a sharply defined edge. The use of an edge of finite width permitted a more accurate definition of cracking by setting an arbitrary standard of crack length. When a crack had progressed across the given edge, usually about 0.030 to 0.040 inch, it was said to be complete and failure by cracking

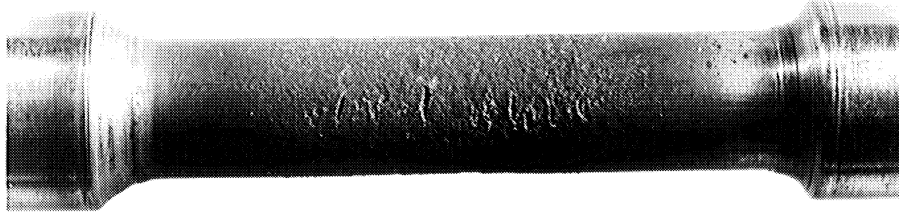


Fig. 15. Thermal-Shock Specimen of Round Cross Section, Showing Grooves after Test; Type 347 Stainless Steel.

to have occurred. Next a specimen of square cross section was developed and proved relatively easy to make. However, crack detection was still troublesome and the reproducibility was poor. This type of test piece is shown in Fig. 16.

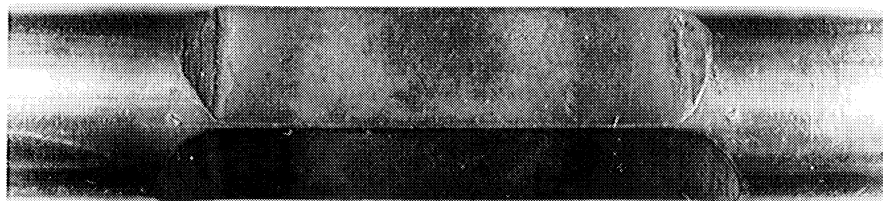


Fig. 16. Thermal-Shock Specimen of Square Cross Section.

From the square section it was learned that an edge sharper than a right angle was needed. This indicated that a triangular, diamond-shaped, or hollow-ground section might work. The hollow-ground specimen gave easily detectable cracks, but this shape was so hard to manufacture to specifications that it was abandoned. The diamond shape also gave easy crack detection, but it was very hard to measure the temperature of such a specimen with a radiation pyrometer. Hollow-ground and diamond shapes are shown in Figs. 17 and 18.

The triangular shape was finally developed and used throughout the remainder of the tests. This final specimen shape is shown in Fig. 19. It could be made at reasonable cost, permitted easy crack detection, and allowed temperature measurement by mounting the specimen so that the back face was perpendicular to the sight line of a radiation pyrometer.

In some of the early work the temperature was measured by inserting a thermocouple into a hole which was drilled along the axis of the piece. This hole was very difficult to drill in materials as hard as some of those tested. In addition, it acted as a stress raiser and thus interfered with the reproducibility of results. Some of these pieces with center holes are shown in Fig. 20.

Fatigue specimens were occasionally employed to determine mechanical properties at high stresses and room temperature. Figure 21 illustrates the shape of specimen used for this purpose. Some thermal-shock specimens were also prefatigued before shocking. The same machine (Fig. 22) was used for both types of fatigue work. It has a special low-speed drive to avoid overheating of the pieces, and loads the pieces in pure bending by the addition of dead weights.

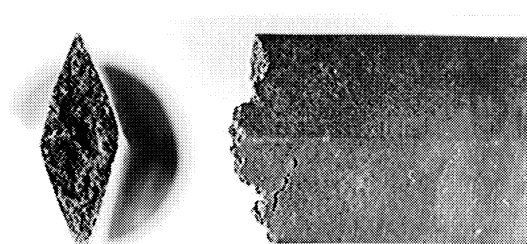


Fig. 17. Diamond-Shaped Specimen of Type 304 Stainless Steel, Fractured during Overheating in Thermal-Shock Test. Axial load was caused by lower electrode and grip.

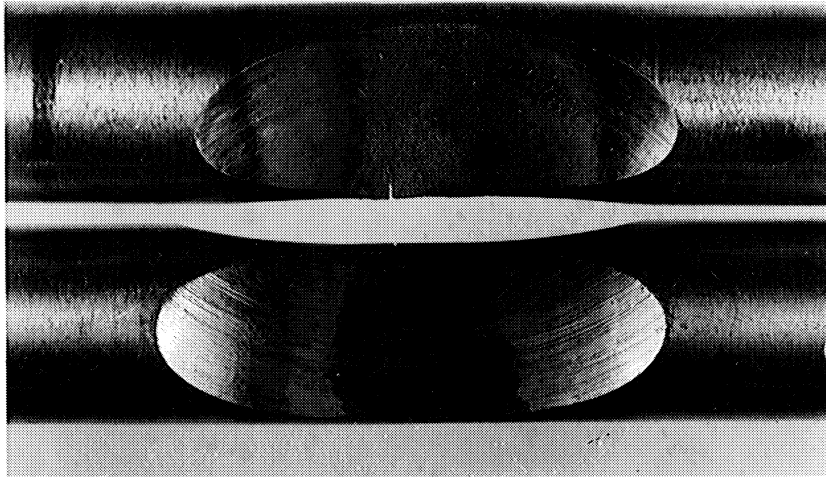


Fig. 18. Thermal-Shock Specimens of Hollow-Cut Cross Section. Top specimen is Type 347 stainless steel; bottom specimen is Inconel.

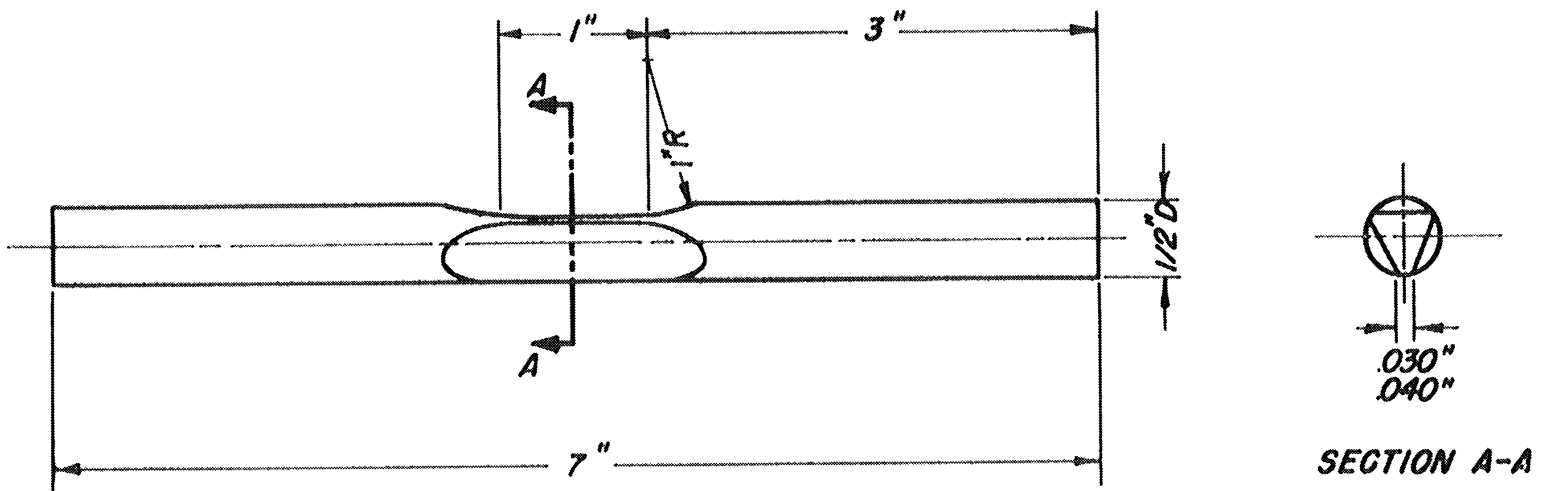
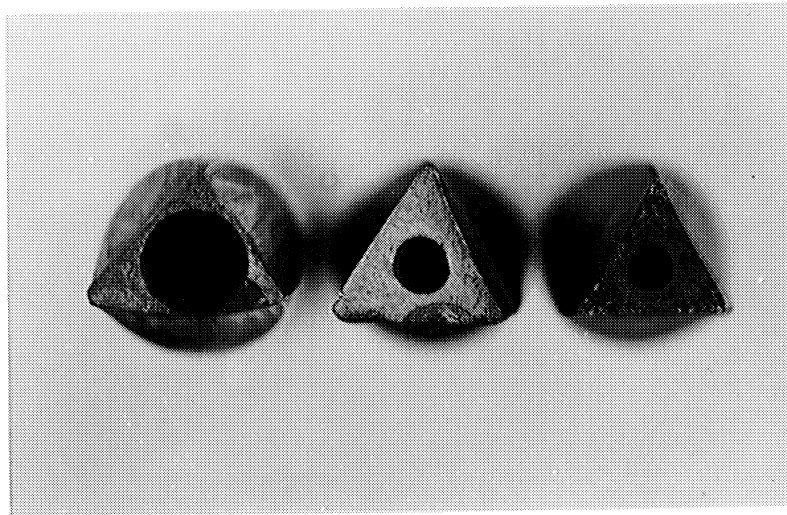


Fig. 19. Thermal-Shock Specimen



Oxide
Formation

- a. 1/4-inch Diameter Hole b. 1/8-inch Diameter Hole c. 1/8-inch Diameter Hole,
after Necking

Fig. 20. Triangular Specimens with Thermocouple Holes.

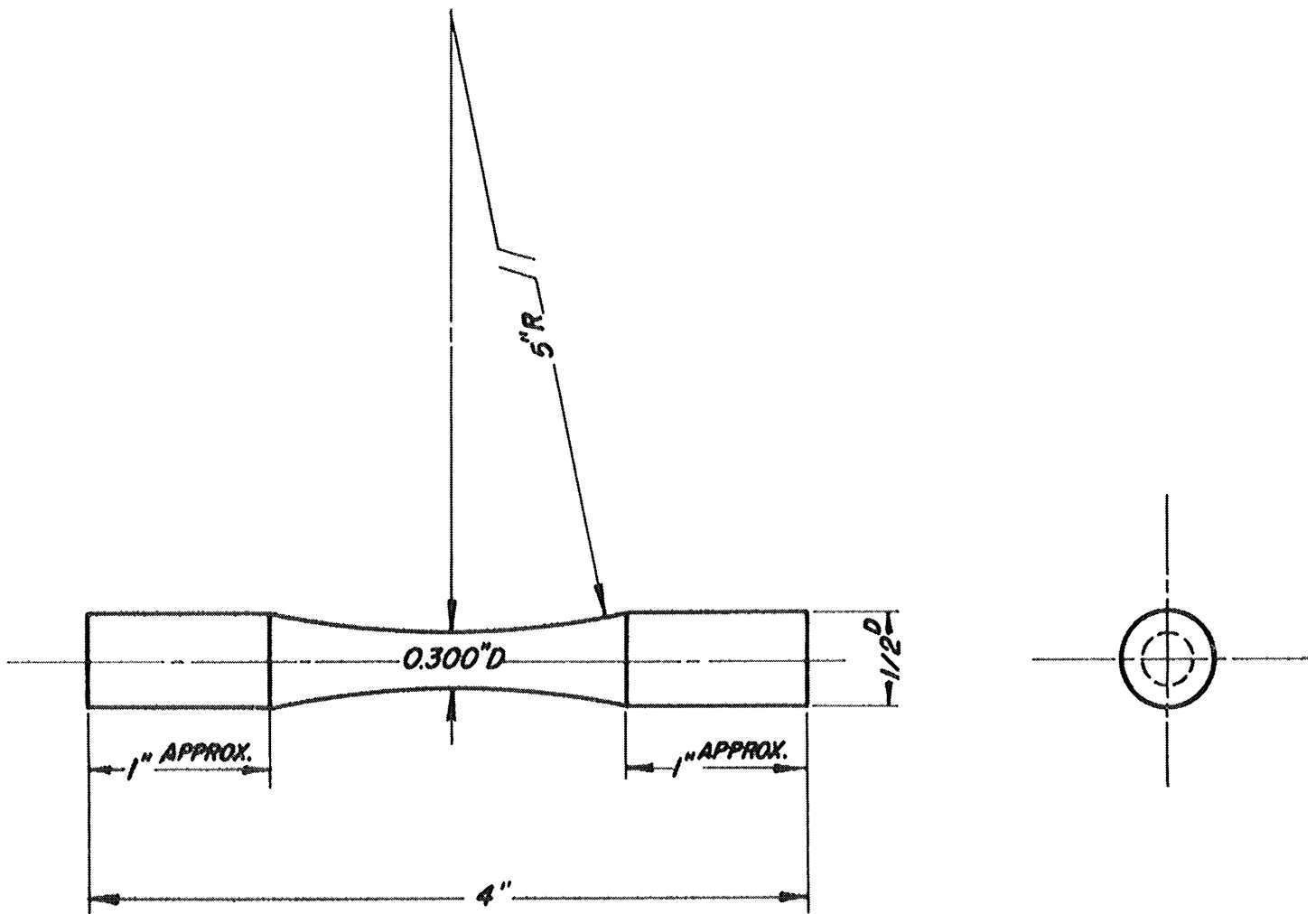


Fig. 21. Fatigue Specimen.

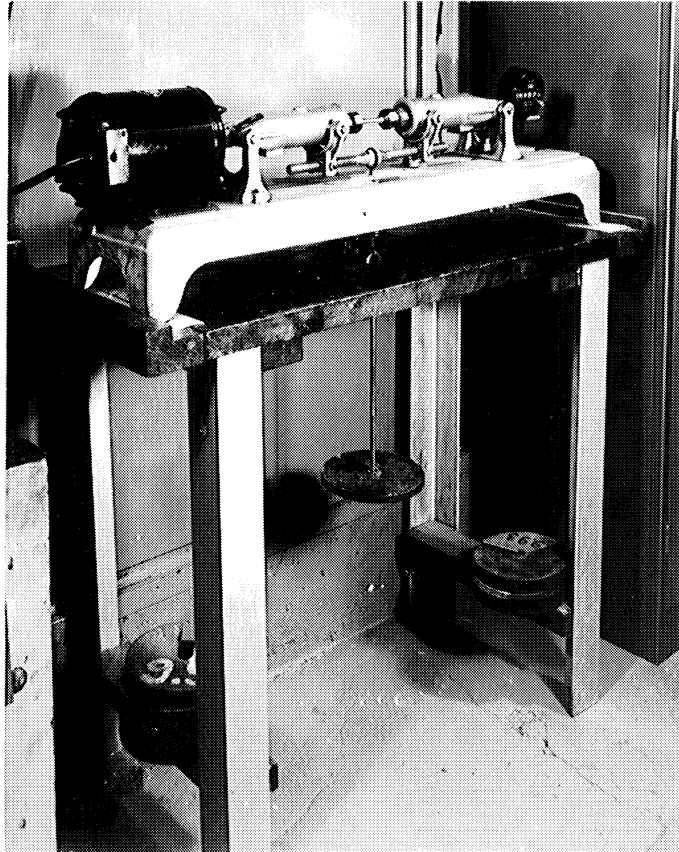


Fig. 22. Low-Speed Fatigue Machine (1800 rpm).

TEST PROCEDURE

The first step in conducting a test is calibration of the radiation pyrometer against a special specimen of the material under consideration which has an additional thermocouple. The specimen, after possible mechanical or thermal pretreatment, is then measured for edge width, inserted in the water-cooled chucks, and positioned in the holder. The radiation pyrometer is sighted on the back side of the specimen. The air nozzle is adjusted to give proper impingement of the air against the edge of the test piece, and the heating voltage is adjusted by setting the variac to give a 1-minute heating cycle. Any variations in the line voltage are compensated by manual adjustment of the variac. Thermal shocking is continued until a crack has formed and progressed across the measured edge width, defined as constituting a failure. In some cases failure by other means than cracking occurs, such as softening and sagging, upsetting, or gross erosion. These actions are allowed to continue to the point where the air blast no longer strikes the specimen at the proper place or angle.

When failure by some means has taken place, the specimen is removed from the test stand and the thermocouple specimen is reinserted for final calibration of the heat eye. The test temperature is taken as the mean of the initial and final calibration temperatures. Usually the final calibration temperature is higher than the initial temperature, due to contamination of the heat eye lens by dirt from the air blast.

On most tests the development and progress of a crack are easily visible with a 5X telescope. On some runs, however, the crack appears during the night or over a week-end period when no operator is on duty. In such cases an automatic recording camera is installed to take a picture of the specimen during each thermal shock. The time of the shock and the number of the shock are also recorded on the film strip, as shown in Fig. 23.

CRACK DEFINITION

In the process of developing a suitable specimen shape it became apparent that some sort of definition of what constitutes a failure would be needed. Failure was defined in terms of the cracking phenomenon, and thus the meaning of the term crack had to be set forth specifically.

The actual formation of a crack is presumably a process by which some combination of stress, temperature, and surroundings causes some of the specimen material to separate from its immediate neighbors by a distance which exceeds a few molecular diameters. After this initial separation has taken place the phenomenon of cracking changes from one of formation to one of growth.

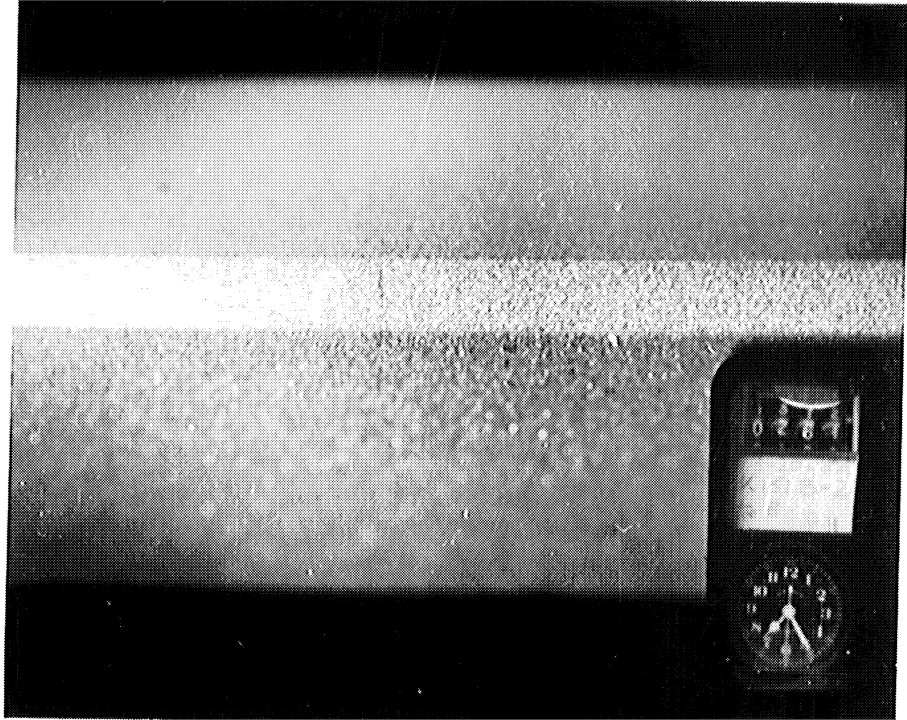


Fig. 23. Enlargement of One Frame of Automatic 35-mm Camera Film Strip Showing Crack in Kennametal Type K-152 B, Specimen No. 2 at 261 Cycles.

It is possible to recognize a crack by optical inspection methods only when it has grown to such a size as to be visible on the surface when viewed under reasonable magnification. Moreover, the crack must differ from the normal surface finish of the specimen in shape, texture, or size if it is to be noticed. It is therefore convenient to define a crack as a recognizable gap of a certain minimum length, realizing that such a gap is a combination of both initial separation and subsequent growth. In this work the minimum length has been taken as the width of the edge of the specimen, 0.030 to 0.040 inch. This definition proved suitable for all materials except the stainless steels, which had a tendency to form grooves, rather than cracks, and thus obscure the cracks.

Occasionally a crack would become filled with an oxide, which made it difficult to notice that a crack was present when the specimen was cold. In most cases, however, such oxides could be recognized as a dark line. In a typical case the crack could be seen with a 5X telescope during the air-blast portion of the cycle. The crack opened up when the air was turned on and then closed again as heating progressed. There were a few cases of tests at high temperatures in which formation of scale on the surface of the specimen made it almost impossible to decide if a crack was present (see Fig. 24a). In those cases the specimens were subjected to a metallographic examination. Occasionally a specimen cracked unexpectedly early in the test, and the cracks were not found until after they had progressed beyond the defined limits. In such instances an estimate of the number of cycles to failure was made.

One material, Kennametal, cracked in an unusual manner; the specimen broke completely into two pieces within a few cycles after the crack was initiated. Such a material was subject to very strong local heating in the region of the crack because of the increase of local electrical resistance at that place. For the last few cycles before complete rupture the material was subject to actual burning where contact was still maintained (see Fig. 24b).

Figures 25a, 25b, 25c, and 25d show the types of cracks developed by mechanical fatigue and thermal shock. It will be noted that in the thermal-shock crack there is little disturbance of the grain structure, except at the crack itself, and that the edges of the crack are not so sharp as those of the mechanical crack. The progress of the thermal crack seems to have been straight across the specimen, and was transgranular rather than following the grain boundaries. The sharp point on the end of the thermal crack is obviously a region of very high stress concentration.

MATERIALS

The materials which were tested in this program were special high-temperature metals. Classification of the types of materials may be made on the basis of the compositions. Basic groupings are:

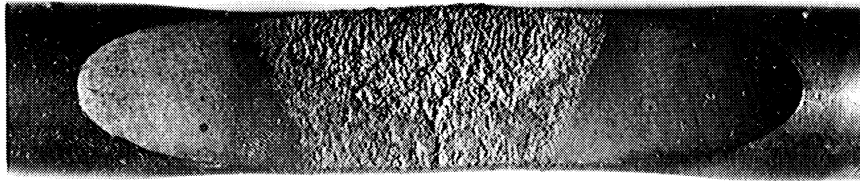


Fig. 24a. Specimen Showing Severe Oxidation. Visual crack inspection is difficult. Three cracks are present. Inconel, 1800°F.

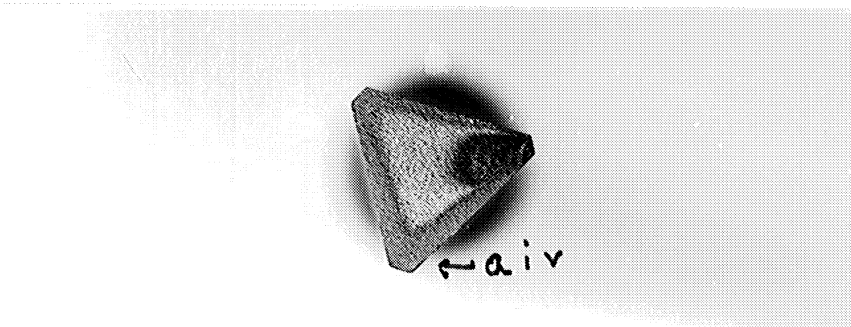
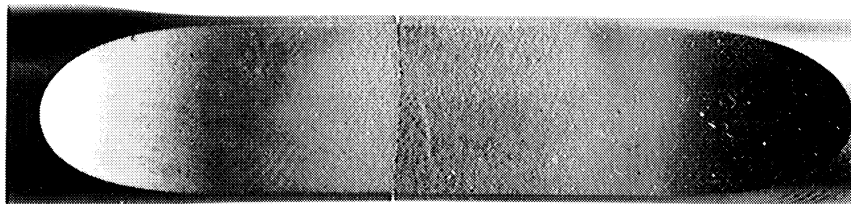


Fig. 24b. Kennametal Type 152 B No. 4, Showing Complete Fracture and Burning.

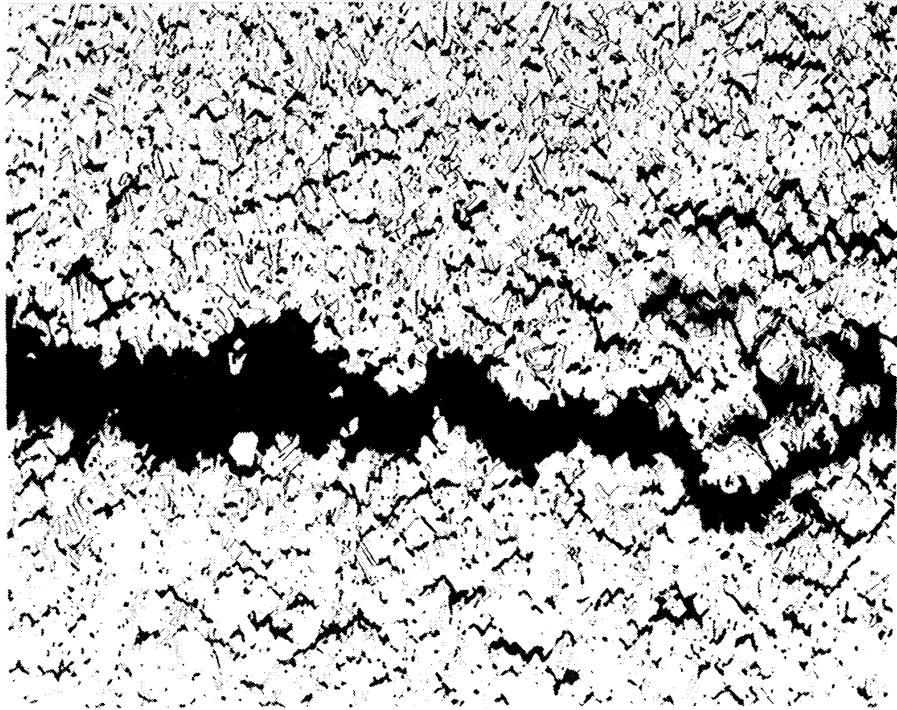
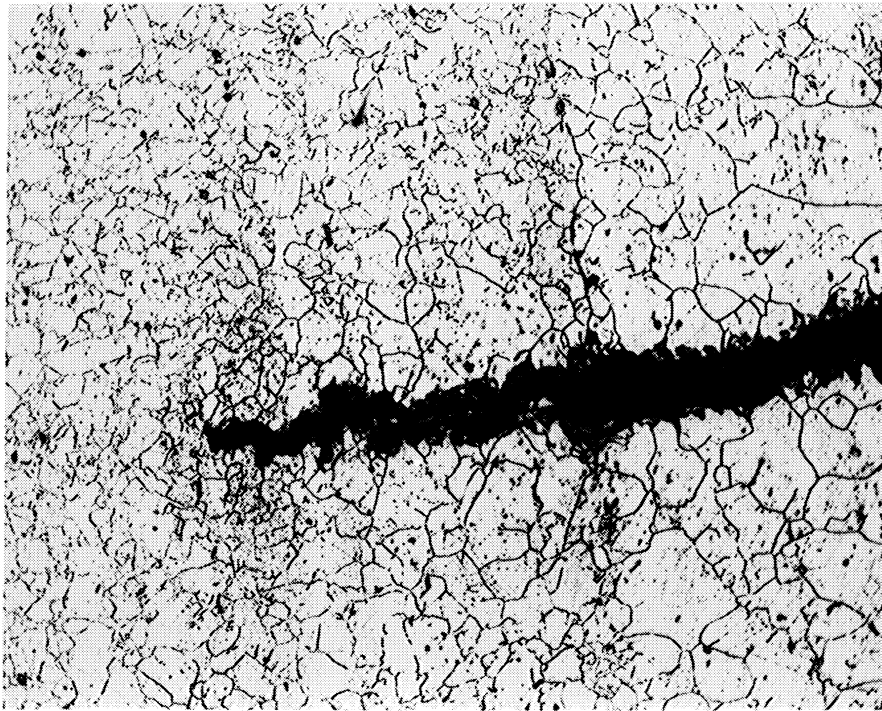


Fig. 25a. Mechanical Crack in Type 304 Stainless Steel in Vicinity of Rupture Failure. X100



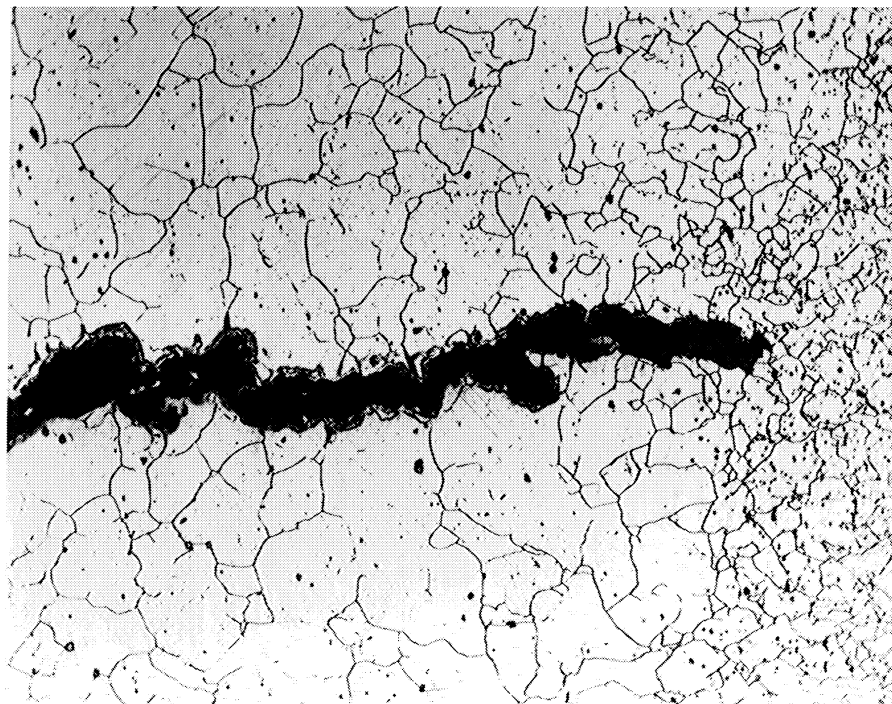
Fig. 25b. Thermal Crack in Type 304 Stainless Steel. X100



Cooled edge

Fig. 25c. IN-5, 1819 Cycles, 100X

Standard shock



Cooled
Edge

Fig. 25d. IN-7, 4706 Cycles, 100X

Standard Shock

<u>Cermets</u>	<u>Iron Base</u>	<u>Nickel Base</u>	<u>Cobalt Base</u>
K 151 A	N-155	Waspalloy	HS-21 (cast)
K 152 B	304 Stainless Steel	Hastelloy C	S-816 (cast)
	310 Stainless Steel	Inconel	S-816(wrought)
	347 Stainless Steel	Nimonic 80-A	
		M-252	

Five specimens of a special chromium-rich alloy, Battellalloy, were also examined. An attempt was made to test copper, but no satisfactory method of heating copper was found.

RESULTS

General

Results of this investigation may be divided roughly into three portions. In the early stages of the work the primary emphasis was on a theoretical analysis. The twenty-two relevant factors were examined, and the direct brute-force attack abandoned as impractically difficult. The experimental means of attack were then considered and a series of exploratory tests was run to get some idea of the limits of temperatures to be expected, specimen shapes, and methods of cooling.

The second phase of the work included such areas of study as the effects of temperature, prior fatigue damage, cold work, and thermal wiggling on thermal-shock resistance. In addition, a considerable effort was made to secure reproducibility of results.

The third stage of the program involved an extensive evaluation of the fourteen materials examined. New testing apparatus was constructed and over 200 tests run on thermal-shock resistance of materials without previous mechanical history, but under varying temperature conditions.

Early Work

As a beginning a theoretical attack was made on the problem in the hope that a dimensional analysis would yield some fundamental and useful parameters for the thermal-shock phenomenon. Brittle ceramic materials had been treated in this manner and suggested this attack for metals. It was found that twenty-two variables were involved and a few excursions into the theory of dimensions showed that the direct brute-force method could not yield much useful information. For this reason it was decided to use an experimental approach. This decision was the first important result.

In setting up the experimental program it was realized that several questions had to be answered before any really useful data could be expected. Most of these questions centered on the technique to be used. The technique was already fairly well defined by the equipment which was loaned by Wright Air Development Center, but the specimen shape to use, the temperature limits within which testing should be done, and the type of coolant to use remained to be selected.

The development of the standard specimen has already been described. Its design constituted the second important result. Concurrently with the tests to establish a workable specimen, work was conducted to find the temperature ranges for thermal heating. If the temperatures were too low, the testing time became exceedingly long and the conditions would not simulate turbine conditions accurately enough. Investigations showed that actual turbine temperatures were in the neighborhood of 1600°F, and tests on Inconel showed that such a testing temperature gave reasonable numbers of thermal-shock cycles to failure when applied to the standard specimen. It was decided to test further specimens in the temperature ranges of 1600° up to 1800°F. To reduce the number of cycles, and thus shorten the testing time, this was later revised upward to 2000°F as authorized by Wright Air Development Center.

The choice of coolant was determined by the operating conditions within an actual turbine. To duplicate these conditions the coolant had to be gaseous in nature, and compressed air was the obvious choice of medium. In order to get a cooling rate which would be high enough to make the test a true thermal shock, it was decided that the air should be applied through a nozzle at 85 psi. The design of this nozzle went through several stages and resulted in a high-precision rectangular-orifice type with movable walls to permit adjustments. The efflux velocity of the air was made as nearly Mach 1 as possible, as required by the theoretical analysis. Later developments in the nozzle design included a provision for water cooling to prevent dimensional changes by heat radiated from the test piece.

A certain amount of testing of materials under conditions of combined axial stress and thermal shock was undertaken. These tests were of a preliminary and exploratory nature, intended to establish the limits for the axial load values to be used. The results were so scattered that it was realized that the thermal-shock resistance would first have to be established for conditions of no axial stress before the combined-loading condition could be investigated. For this reason the combined-loading program was set aside with the intention of resuming it at a later time. It may be well to point out that this work still remains to be done.

Second Phase

In the second phase of the investigation several features of thermal-shock resistance in the absence of axial stresses were examined. Among these were the possibility of producing the thermal cracking by thermal means alone, the effect of changes in testing temperature, effects of prior mechanical-fatigue damage, effects of prior cold-work, reproducibility of results, and the nature of thermal crack.

Consideration of the production of cracks by purely thermal means led to the conclusion that such cracking must be a manifestation of progressive deterioration of the properties of the material. While there are some materials, usually brittle in nature, which can be cracked by a single severe quenching, the usual metals do not develop a thermal strain equal to the failure strain even when completely confined and cooled by as much as 2000°F. There was a question, then, as to whether repeated thermal shocking would develop the necessary deterioration of properties to permit cracking to develop in the absence of axial load. Several tests on HS-21, S-816, and N-155 established that it was possible to induce cracking by thermal shocking alone.

Increases in the maximum cycle temperature were also investigated and were found to result in a lowered resistance to thermal shock for most materials. The increases in temperature were made in 100°F steps from 1600° to 2000°F. At some of the higher temperatures, however, the material became so soft that plastic yielding was developed. This resulted in upsetting, sagging, and changes of shape so severe that failure was said to have occurred by means other than thermal cracking. In a turbine the blades would be so badly distorted that power output would be seriously affected. (See Figs. 26 and 27.)

Since the initiation of a crack is thought to be the result of the separation of a few particles by a few molecular distances, it would appear that either mechanical-fatigue damage or thermal-shock damage should have nearly the same effects on thermal-shock resistance. To test this hypothesis several specimens were run in thermal shock after having been prefatigued in a low-speed (1750-rpm) rotating-beam fatigue machine. Only a few samples of this kind were tested and the results were not conclusive except to indicate that prefatiguing reduced the sensitivity of the specimen to variations in edge width when tested in thermal shock. It is still thought that tests on prefatigued specimens should be made in order to find the correlation, if any, between mechanical and thermal damage.

Another type of mechanical damage which could easily be investigated was that due to cold-working of the material. Several Inconel specimens were subjected to cold-working of 1, 5, and 10 percent before thermal shocking. There was no significant change in the thermal-shock resistance with this cold-working.

After it was established that cracking could be produced by thermal shocking alone, the question of reproducibility of the results became important. It was realized that the initiation of a crack and its progress across the edge of a standard specimen would necessarily be a statistical phenomenon. Many random variations, particularly in the local properties of the test specimen, would be bound to show up in the results. In addition, there would be errors in machine operation and personal errors. After considerable effort most of the important machine errors were eliminated by changes in the design. Such developments as the precision water-cooled nozzle and the flexible laminated cantilever type of horizontal specimen mounting materially aided in narrowing the probable-error values of the data. It is felt, however, that the sizes of the samples used in this investigation were too small in many cases. Time limitations prevented obtaining the amount of data required for a good statistical analysis.

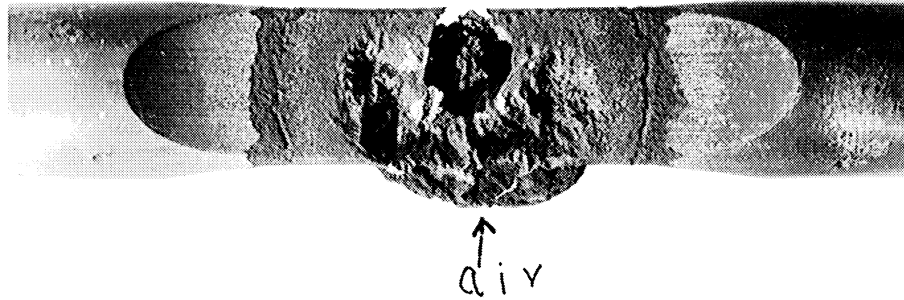


Fig. 26. HS-21 at 2000°F after 673 Cycles.

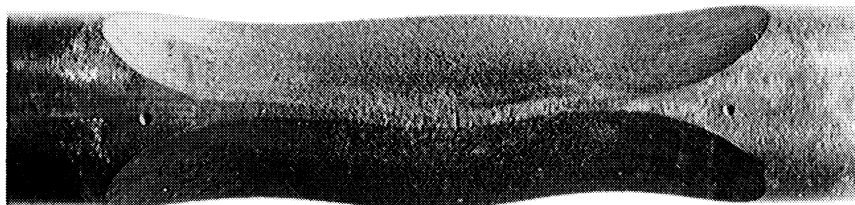


Fig. 27. Waspalloy at 2000°F after 784 Cycles.

Investigation into the nature of the thermal-cracking phenomenon was considered and a few photomicrographs were taken of cracks in Inconel and Type 304 stainless steel. These micrographs indicated that the cracks were essentially transgranular in character. Additional, more fundamental, research into the mechanism of thermal cracking is needed, but would be a separate investigation in itself.

Recent Work

As a result of the first two phases of the program, the investigation narrowed down to the testing of several different materials to determine their relative values of thermal-shock resistance in the absence of any previous mechanical history of axial loading. Four new testing rigs were constructed, tested, and placed in operation. They have operated almost continuously since their completion in December, 1953, and have proven to be very reliable.

The primary results of this portion of the investigation are the comparative performances of the various materials. The average number of thermal-shock cycles to failure for each material is shown in Figs. 28, 29, 30, 31, and 32, for temperatures of 1600°, 1700°, 1800°, 1900°, and 2000°F respectively. The results follow in Tables I-V. Graphical presentations of thermal-shock resistance by classes of materials are given in Figs. 33-37.

Tests were also performed to determine the effect of the heating and cooling action on S-816 (wrought) material in the absence of any thermal shock. This was an attempt to find out if the test cycle, by itself, had any influence on the results. It was found that the thermal "wiggling" action alone had no apparent effect on the thermal-shock resistance of the chosen material.

Another, rather special, type of test was performed to investigate the effect of corrosion on the rate of crack propagation. It was suspected that after a crack had been initiated, the progress of the crack would be hastened by the development of oxides between the sides of the crack. This would develop a wedging action, spread the crack sides, and cause the head end of the crack to progress. To check this hypothesis, a series of tests were run on Inconel using helium as the coolant in place of compressed air. The shock produced by the helium was visibly more severe than that from the air blast. No significant differences in thermal-shock resistance were revealed by use of the different, inert coolant, although the surface corrosion was considerably reduced.

Fig. 28. Comparative Thermal-Shock Resistance
 Temperature = 1600°F
 () = Number of Tests

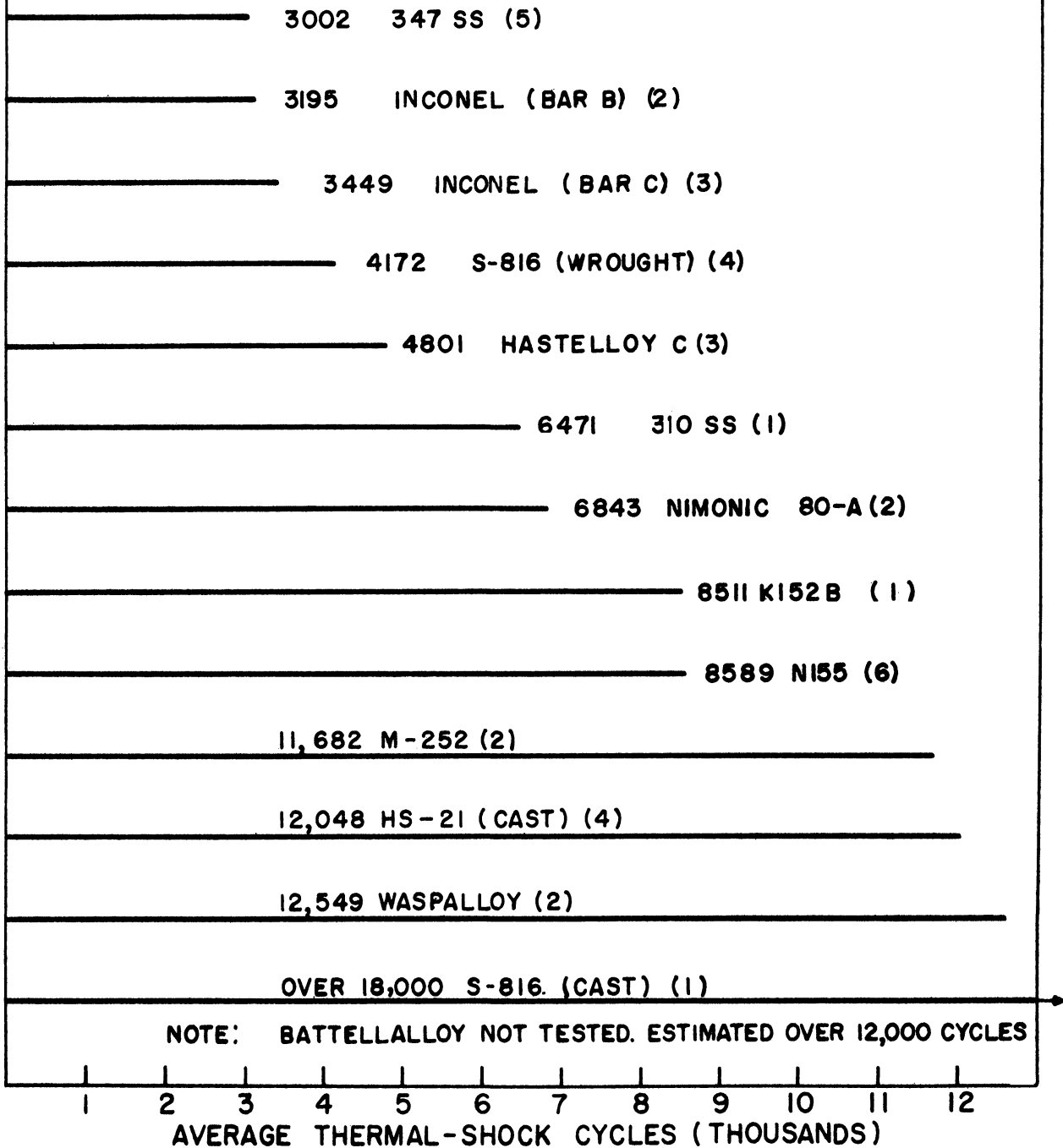


Fig. 29. Comparative Thermal-Shock Resistance

Temperature = 1700°F

() = Number of Tests

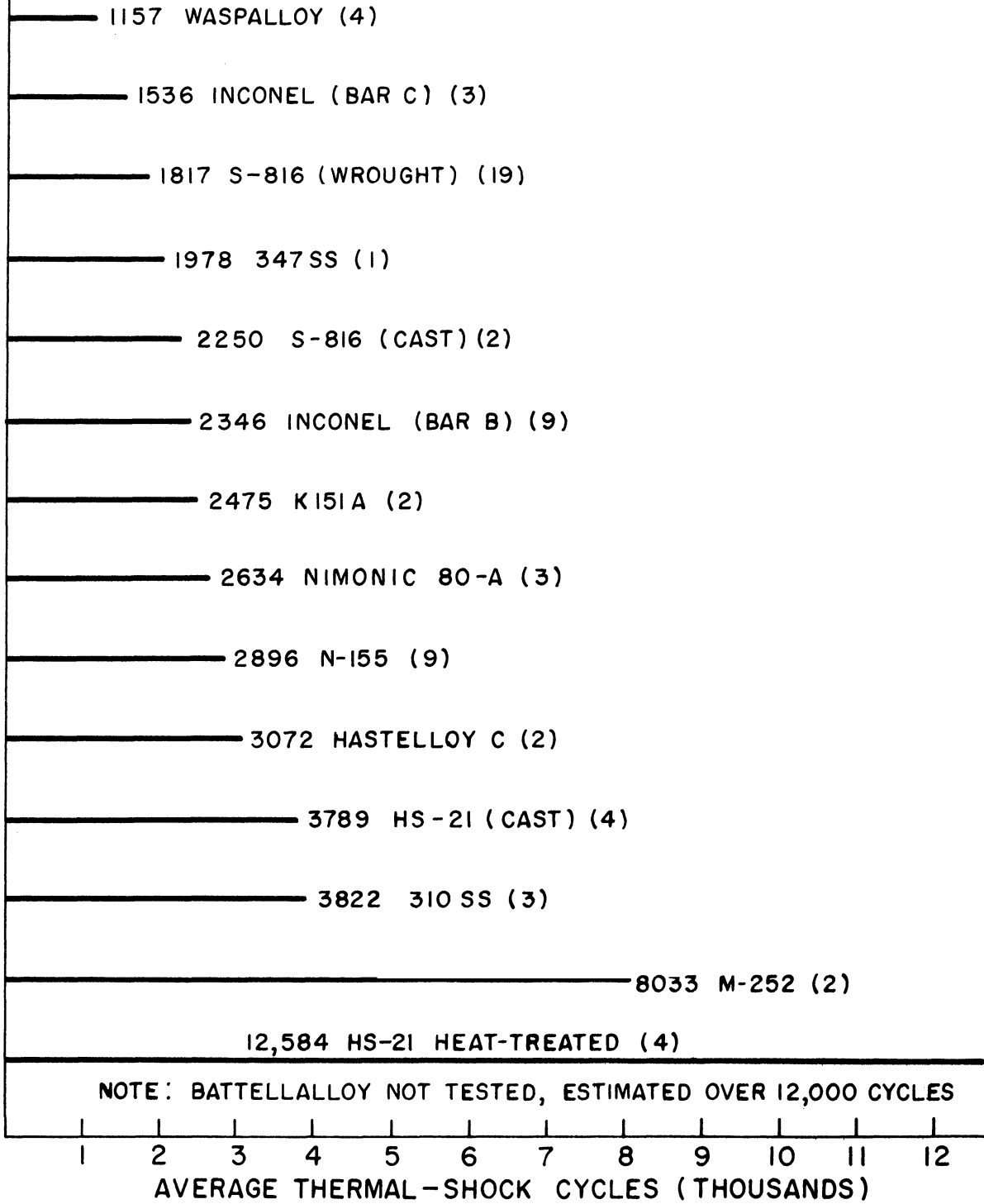


Fig. 30. Comparative Thermal-Shock Resistance

Temperature = 1800°F

() = Number of Tests

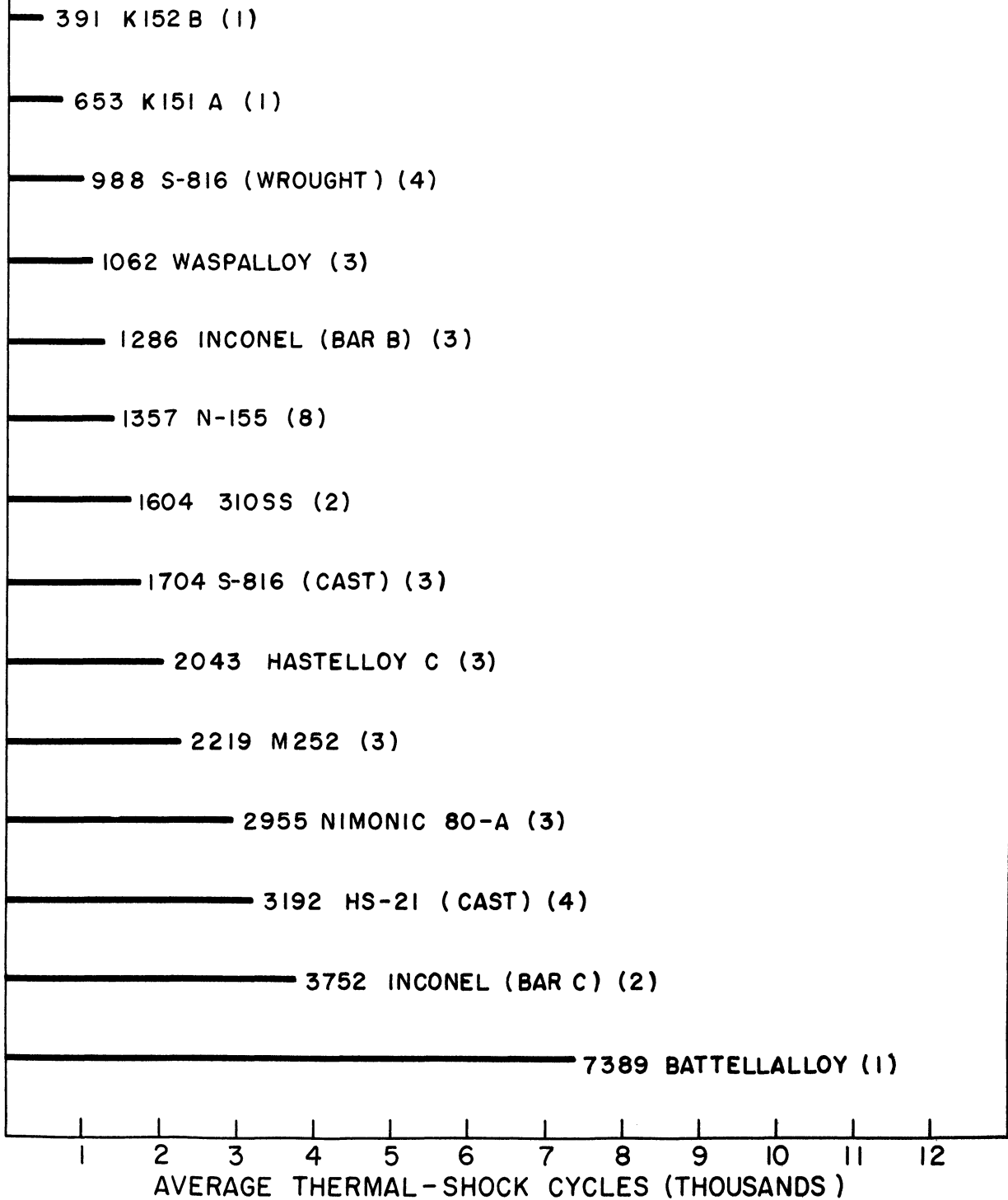


Fig. 31. Comparative Thermal-Shock Resistance
Temperature = 1900°F
() = Number of Tests

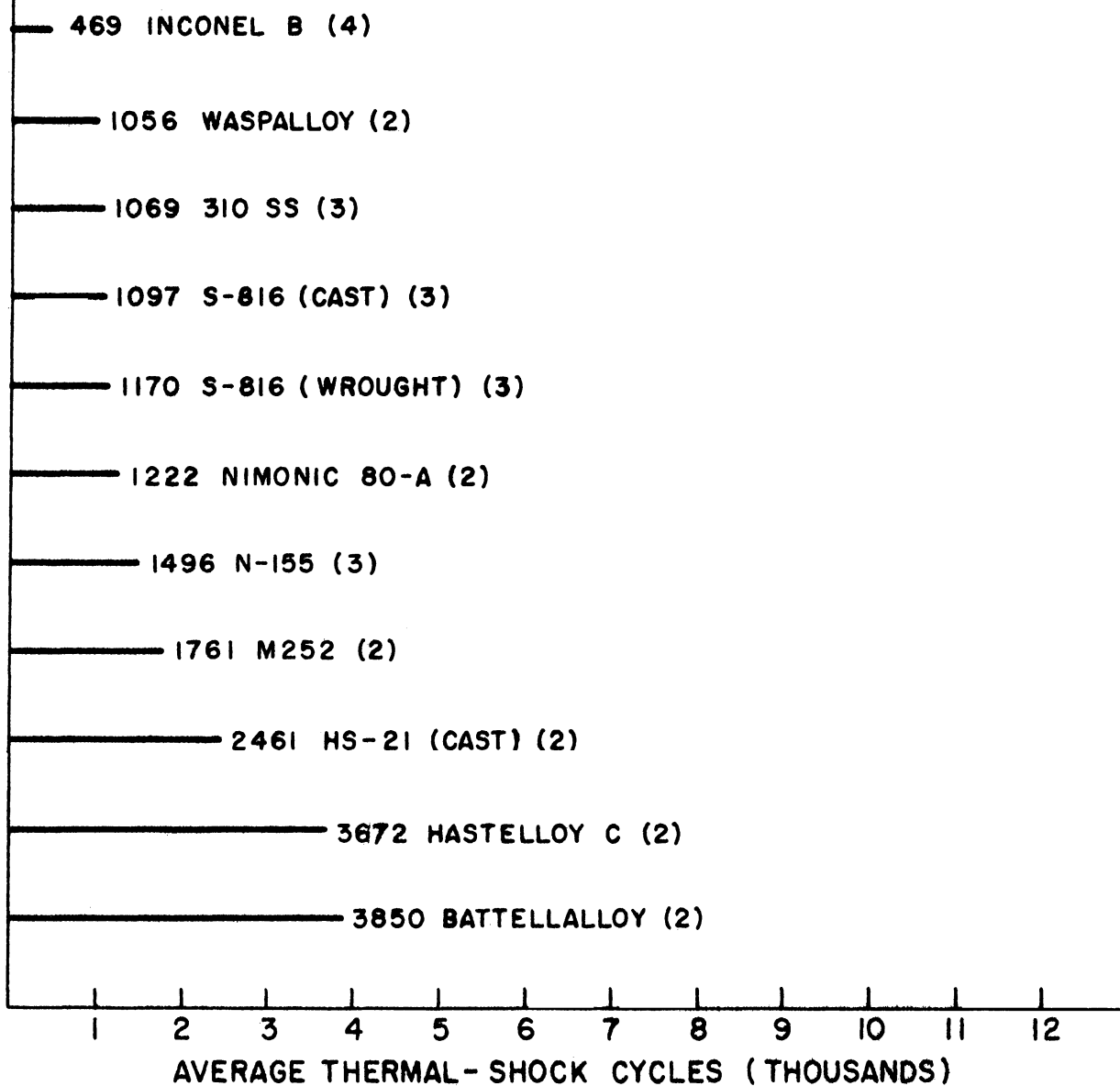


Fig.32. Comparative Thermal - Shock Resistance

Temperature = 2000 °F

()=Number of Tests

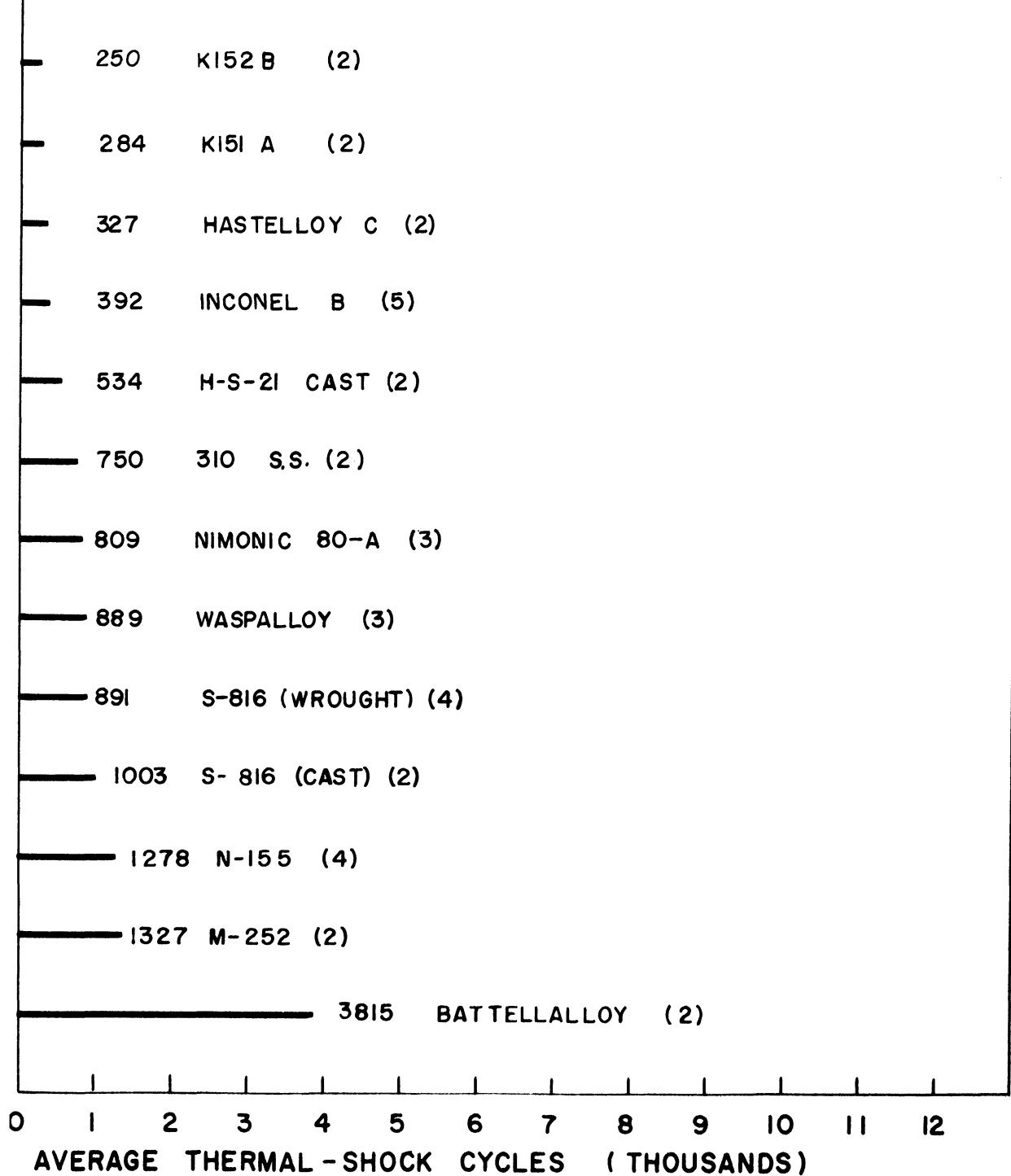


TABLE I

THERMAL-SHOCK RESISTANCE AT 1600°F

Material	Number of Tests	Average Thermal-Shock Cycle
Battellalloy	None	Estimated far over 12,000
S-816 (cast)	1	Over 18,000
Waspalloy	2	12,549
HS-21 (cast)	4	12,048
M-252	2	11,682
N-155	6	8,589
K-152	1	8,511
Nimonic 80-A	2	6,843
310 Stainless Steel	1	6,471
Hastelloy C	3	4,801
S-816 (wrought)	4	4,172
Inconel, Bar C	3	3,449
Inconel, Bar B	2	3,195
347 Stainless Steel	5	3,002

TABLE II

THERMAL-SHOCK RESISTANCE AT 1700°F

Material	Number of Tests	Average Thermal-Shock Cycle
Battellalloy	None	Estimated far over 12,000
HS-21 (50 hrs, 1350°F)	4	12,584
M-252	2	8,033
310 Stainless Steel	3	3,822
HS-21 (cast)	4	3,789
Hastelloy C	2	3,072
N-155	9	2,896
Nimonic 80-A	3	2,634
K-151 A	2	2,475
Inconel, Bar B	9	2,346
S-816 (cast)	2	2,250
347 Stainless Steel	1	1,978
S-816 (wrought)	19	1,817
Inconel, Bar C	3	1,536
Waspalloy	4	1,157

TABLE III

THERMAL-SHOCK RESISTANCE AT 1800°F

Material	Number of Tests	Average Thermal-Shock Cycles
Battellalloy	1	7,839
Inconel, Bar C	2	3,752
HS-21 (cast)	4	3,192
Nimonic 80-A	3	2,955
M-252	3	2,219
Hastelloy C	3	2,043
S-816 (cast)	3	1,704
310 Stainless Steel	2	1,604
N-155	8	1,357
Inconel, Bar B	3	1,286
Waspalloy	3	1,062
S-816 (wrought)	4	988
K-151 A	1	653
K-152 B	1	391

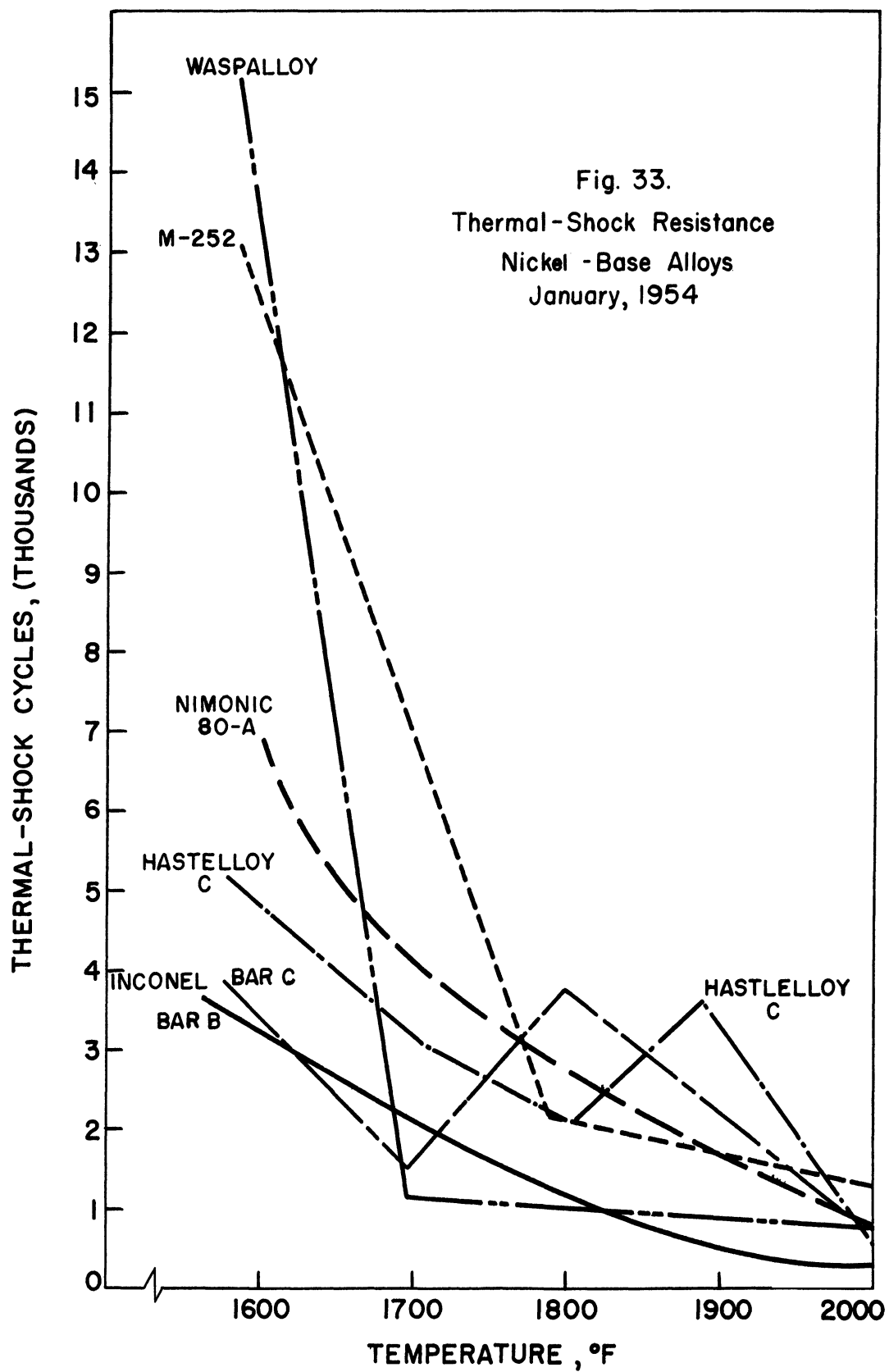
TABLE IV

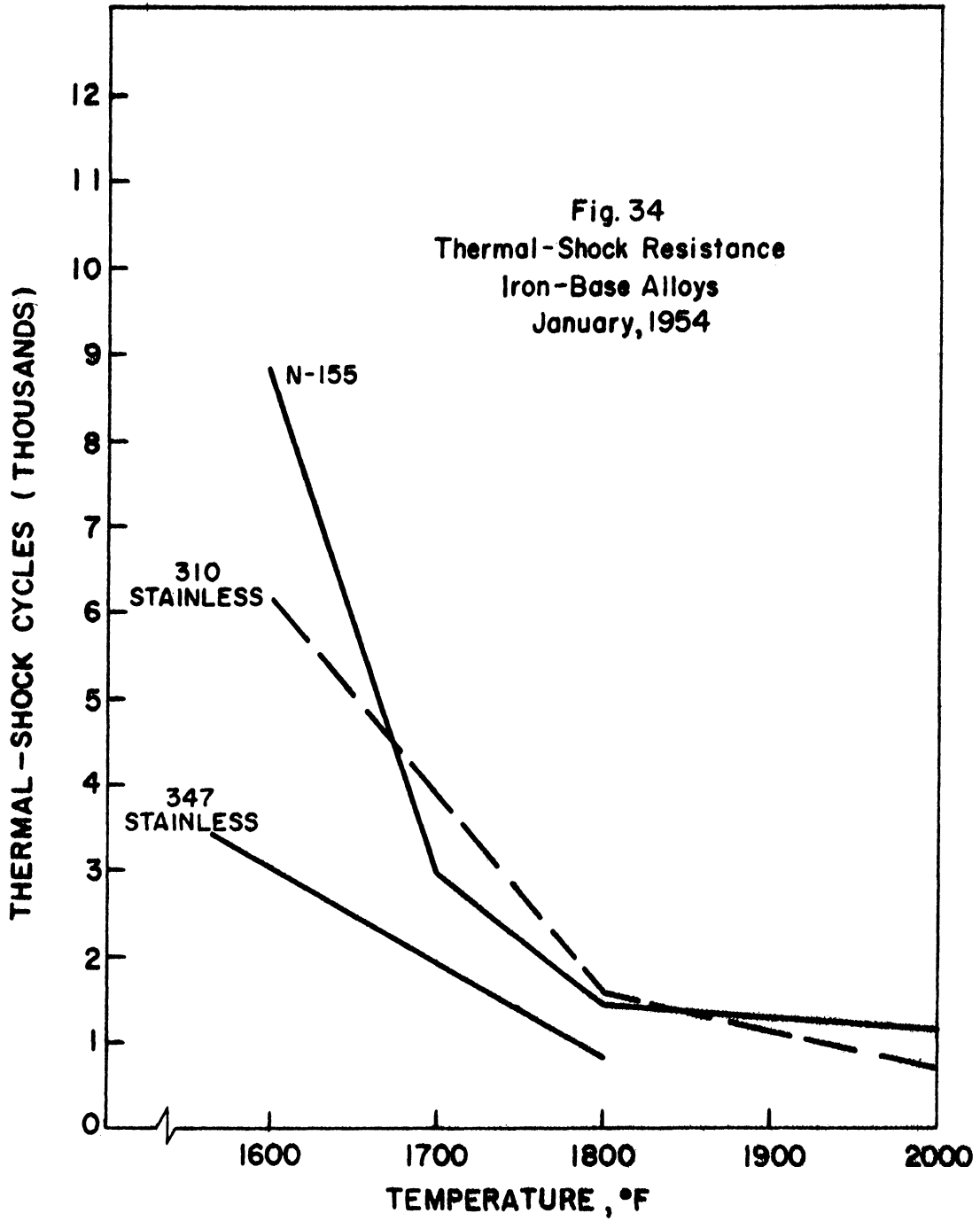
THERMAL-SHOCK RESISTANCE AT 1900°F

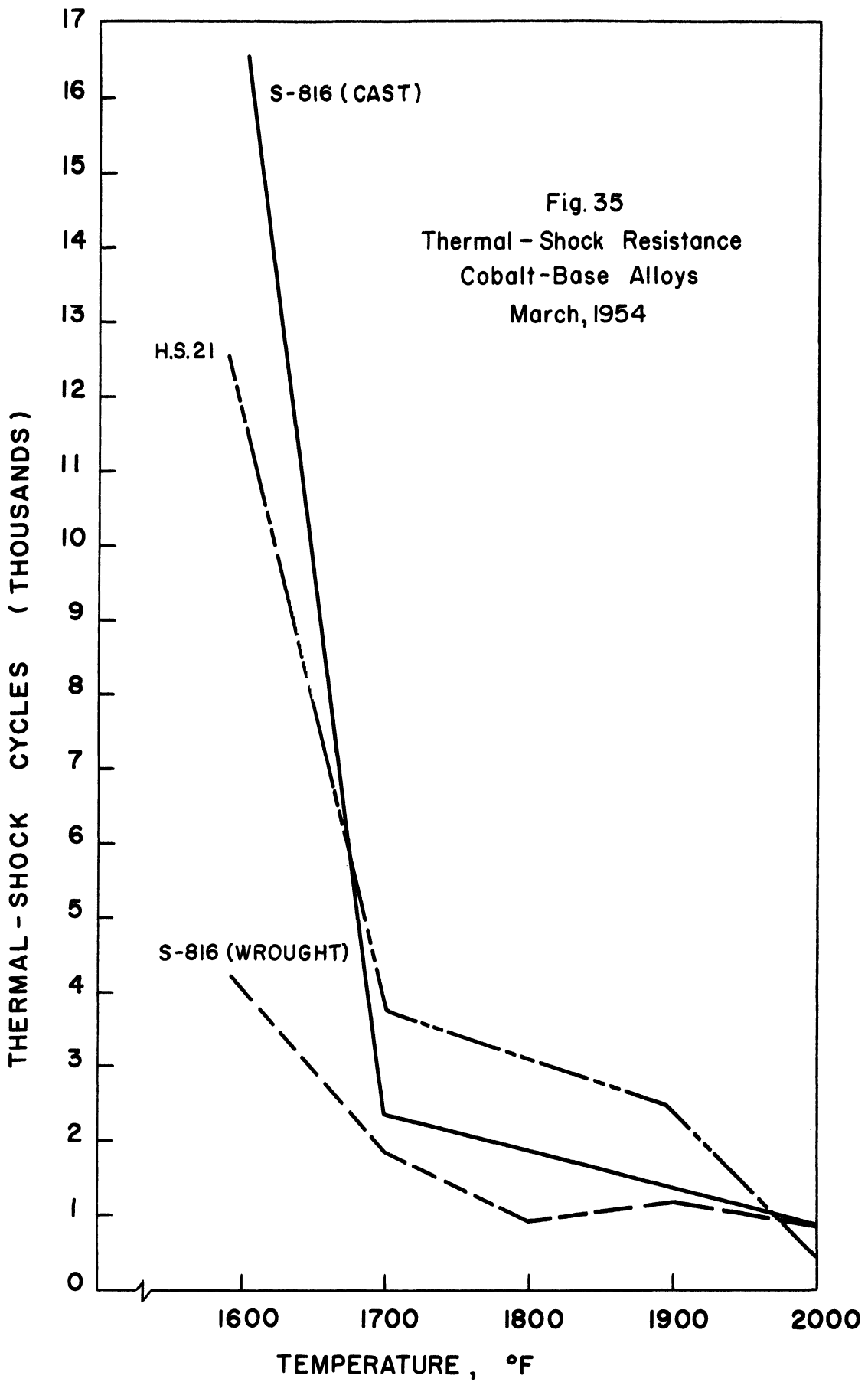
Material	Number of Tests	Average Thermal-Shock Cycles
Battellalloy	2	3,850
Hastelloy C	2	3,672
HS-21 (cast)	2	2,461
M-252	2	1,761
N-155	3	1,496
Nimonic 80-A	2	1,222
S-816 (wrought)	3	1,170
S-816 (cast)	3	1,097
310 Stainless Steel	3	1,069
Waspalloy	2	1,056
Inconel, Bar B	4	469

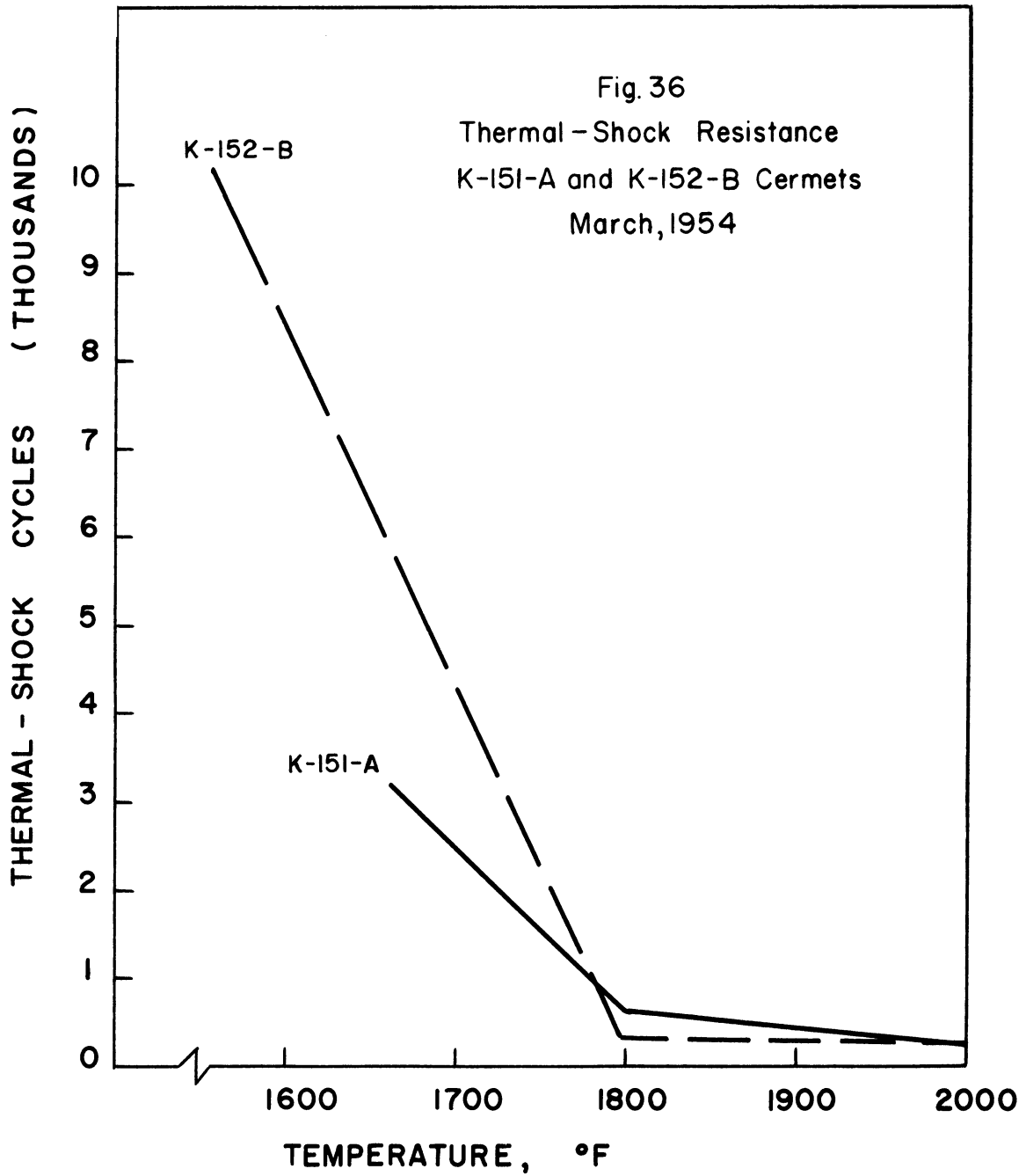
TABLE V
THERMAL-SHOCK RESISTANCE AT 2000°F

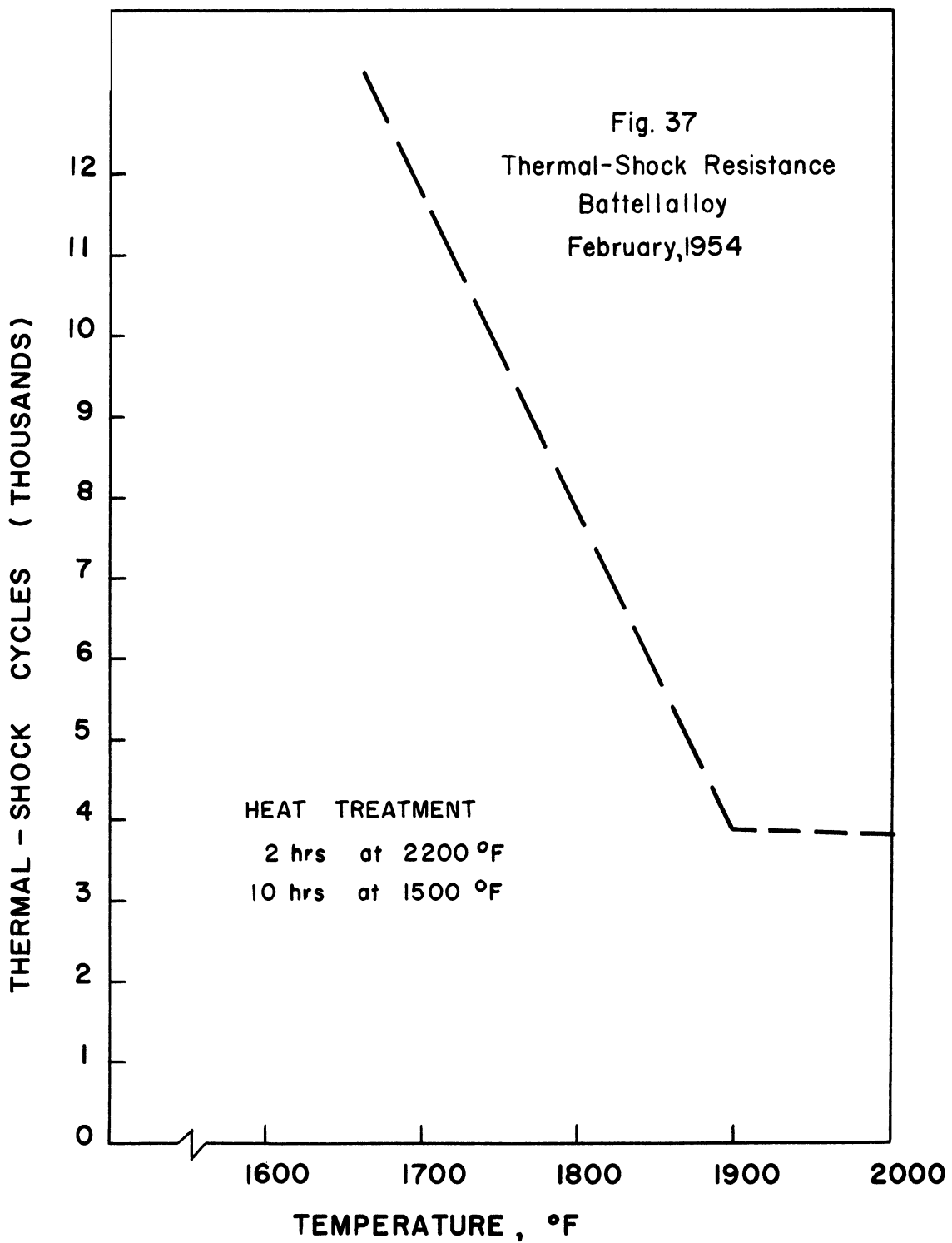
Material	Number of Tests	Average Thermal-Shock Cycles
Battellalloy	2	3,815
M-252	2	1,327
N-155	4	1,278
S-816 (cast)	2	1,003
S-816 (wrought)	4	891
Waspalloy	3	889
Nimonic 80-A	3	809
310 Stainless Steel	2	750
HS-21 (cast)	2	534
Inconel, Bar B	5	392
Hastelloy C	2	327
K-151-A	2	284
K-152-B	2	250











DISCUSSION OF RESULTS

Material Comparison

Inspection of the comparative performance charts shows that there is one outstanding material among those tested. This is the special Battellalloy, of which only five specimens were obtained. The first of these was tested at 2000°F in order to get the quickest evaluation. When the thermal-shock resistance proved to be far above that of any other material, a check test at the same temperature was conducted, with similar results. Two more tests were run at 1900°F; the results were comparable to the first two. With only one specimen left, it was decided to run it at 1800°F on the presumption that a test at any lower temperature would take many thousands of cycles to produce any results. Values for the lower temperatures are estimated. Little information as to the physical properties of this alloy is available to account for its remarkable behavior.

Of the other materials, only three, M-252, N-155, and S-816 (cast), had a thermal-shock resistance of over 1000 cycles when tested at 2000°F. The rest of the materials had values dwindling to 250 cycles for the cermet K-152 B. At 1600°F, the lowest temperature of testing, the materials had thermal-shock resistance ranging from 347 stainless steel, with 3002 cycles, up to S-816 (cast) which lasted more than 18,000 cycles.

Two different bars of Inconel, both from the same lot, were tested for comparison of properties within a material. The thermal-shock resistance was nearly the same for tests at 1600°F, where bar B had 3195 cycles and bar C withstood 3449 cycles. At 1700°F bar C took 1536 cycles whereas bar B required 2,346 cycles, an increase of almost 53 percent over bar C. At 1800°F the relative merit was reversed, bar C requiring 3752 cycles and bar B needing only 1296 cycles. This represents a difference of about 200 percent with respect to bar B. No comparisons were made for 1900° and 2000°F. The tests described seem sufficient to demonstrate the large variation in properties to be expected from what is said to be identical material. It would appear, therefore, that thermal-shock tests should involve statistical-sized sample groups if the results are to be reliable. On this basis, most of the tests performed in this investigation are only indications of thermal-shock resistance because of the small size of the sample groups.

Thermal-Shock Parameter Correlation

There have been several attempts to predict thermal-shock resistance on the basis of physical properties. Manson has proposed two similar parameters, the only difference between them being the omission of the thermal conductivity where the mass of the piece is large in contrast to the cooled portion. It is believed that this situation existed in these tests due to the direction of the coolant over the relatively small edge of the test piece. The parameter may be formulated as

$$\frac{\sigma}{E\alpha} \quad \text{or} \quad \frac{\epsilon}{\alpha} ,$$

where σ is the ultimate strength of the material, E is the elastic modulus, α is the thermal-expansion coefficient, and ϵ is the strain at the ultimate stress. Usually the first form is used because of the difficulty of measuring ϵ .

The correlation of the observed thermal-shock resistance with the Manson criteria was so poor it was of little value. The primary use of these thermal-shock resistance criteria has been on brittle materials, where single thermal-shock cycles can be made to produce failure; in the present investigation no such materials were examined. Also, a considerable portion of the discrepancy may lie in the obtainable values for the physical properties involved. Most tensile-test data are given for room-temperature conditions, or for temperatures up to about 1200°F. Thermal expansivities are usually given for ranges of values which are considerably removed from the test conditions. Further, it is known that all the terms in the parameter are variable with temperature. Until accurate values can be obtained for the quantities involved, any correlation with the proposed parameter will be doubtful.

Effects of Temperature

On all materials the raising of the test temperature lowered the thermal-shock resistance. In some materials, such as Waspalloy and S-816 (cast), this loss of resistance was very severe above 1600°F. In other materials the loss was more gradual, but they all tended to a smaller and smaller value with rising temperature. The reasons for this behavior may be found in the mechanical and metallurgical changes which take place in the materials at high temperatures. For most materials the coefficient of thermal expansion increases with higher temperatures, while the breaking strength decreases. Thus, it would appear that a given thermal quench would affect a relatively larger proportion of the breaking strength when applied at high temperatures than when applied at lower ones. Several such quenches would do a proportionately larger amount of damage to the specimen at the higher temperatures.

For some materials the higher temperatures resulted in actual softening to the point where the specimen sagged out of shape. In less drastic cases there was considerable upsetting on the hot (compression) side of the test piece, also indicating plastic action. Such plastic action undoubtedly helped in relaxing the thermal stresses induced by the quenching, but rapid failures were commonly produced.

At temperatures of 1900° and 2000°F materials such as the stainless steels and Inconel were very badly oxidized and were subject to severe pitting, erosion, and surface scaling. As a check to see what effect these conditions might have on thermal-shock resistance, tests were run on Hastelloy C and Inconel using a helium coolant instead of compressed air. While the surface corrosion was reduced, the thermal-shock resistance was not appreciably affected by this change in test conditions. (See Figs. 38 and 39.)

In several types of materials it is possible that certain metallurgical changes would also take place at the temperatures involved. These changes would fall into the categories of aging, hot-working, and grain growth. No metallographical examinations were made of the specimens after testing because of time and financial limitations. It may be pointed out that future investigations should include such examinations in their program.

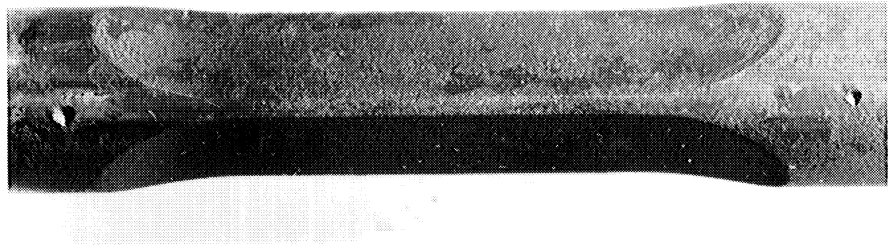


Fig. 38. Hastelloy C at 2000°F, Air-Cooled for 291 Cycles.

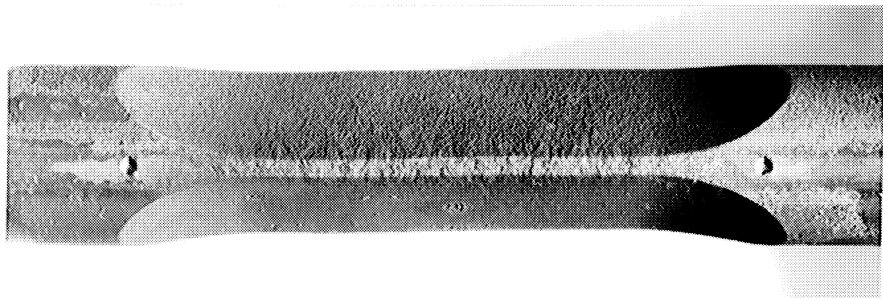


Fig. 39. Hastelloy C at 2000°F, Helium-Cooled for 624 Cycles.

Type of Crack

During this investigation there were no instances of cracking from a single thermal shock, in contrast to some reported tests on ceramic materials. This indicates that thermal-shock cracking was a progressive phenomenon for the materials tested, and shows that the action was one of thermal fatigue. On most specimens the crack or cracks were first visible under a 5X eyepiece as small hairlines at the top or bottom of the edge being shocked. Under continued shocking the cracks grew in length until they had crossed the edge, at which time failure was said to have taken place. Usually the rate of crack development was a very irregular thing, but a fortuitous set of observations on the one specimen of N-155 at 1600°F showed a rather uniform crack development at a rate of 0.0001 inch per cycle, after initiation of the crack at 6574 cycles.

Except for HS-21 and the Kennametals, this cracking rate is thought to be of the right order of magnitude for the other materials. HS-21 cracked at a higher rate than this once a crack was started. The Kennametals exhibited very rapid crack progression; in one case the specimen cracked completely into two pieces within 20 cycles, whereas the usual test involves the development of a crack only about 0.040 inch long.

CONCLUSIONS

1. In the usual metallic materials intended for high-temperature service, thermal-shock cracking is produced by thermal fatigue except for shapes of greatly varying section.
2. Thermal fatigue is a cumulative process which continues until a crack is initiated; then the failure process becomes a combination of fatigue effects and stress-concentration effects.
3. The order of decreasing resistance to thermal shock at the test temperatures was as shown in Table VI.
4. Correlation of thermal-shock resistance with the ϵ/α criterion was poor, but the available data on which it is based is considered of doubtful value.
5. Large variations of thermal-shock resistance occur within a given material. For reliable results a statistical-sized sample group must be used.
6. Increasing the temperature lowers the thermal-shock resistance of the materials tested.
7. Mechanical fatiguing of type 347 stainless steel prior to thermal-shock testing resulted in a decrease in the sensitivity of this material to variations in edge width, and a decrease in the width of the scatter band of the data.
8. Mechanical cold stretching of 1, 5, and 10 percent prior to thermal-shock testing of Inconel developed no significant change in the thermal-shock resistance of this material.

9. Thermal heating and cooling without thermal shock has a negligible effect on the thermal-shock resistance of S-816 (wrought) at 1700°F.
10. Coolant tests on Inconel at 2000°F showed little difference in thermal-shock resistance between helium or air coolant.

TABLE VI
DECREASING ORDER OF THERMAL-SHOCK RESISTANCE

2000°F	1900°F	1800°F	1700°F	1600°F
Battellalloy	Battellalloy	Battellalloy	Battellalloy	Battellalloy
M-252	Hastelloy C	HS-21 (cast)	HS-21 heat-treated	S-816 (cast)
N-155	HS-21 (cast)	Nimonic 80-A	M-252	Waspalloy
S-816 (cast)	M-252	Inconel	310 stainless steel	HS-21 (cast)
S-816 (wrought)	N-155	M-252	HS-21 (cast)	M-252
Waspalloy	Nimonic 80-A	Hastelloy C	Hastelloy C	N-155
Nimonic 80-A	S-816 (wrought)	S-816 (cast)	N-155	K-152 B
310 stainless steel	S-816 (cast)	310 stainless steel	Nimonic 80-A	Nimonic 80-A
HS-21 (cast)	310 stainless steel	N-155	K-151 A	310 stainless steel
Inconel	Waspalloy	Waspalloy	S-816 (cast)	Hastelloy C
Hastelloy C	Inconel	S-816 (wrought)	Inconel	S-816 (wrought)
K-151 A		K-151 A	347 stainless steel	Inconel
K-152 B		K-152 B	S-816 (wrought)	347 stainless steel
			Waspalloy	

BIBLIOGRAPHY

1. Norton, F. H., Refractories, McGraw-Hill Book Company, 2nd ed., 1942.
2. Lidman, W. G., and Bobrowsky, A. R., "Correlation of the Physical Properties of Ceramic Materials with Resistance to Fracture by Thermal Shock", N.A.C.A. TN 1918, 1949.
3. Whitman, M. J., Hall, R. W., and Yaker, C., "Resistance of Six Cast High-Temperature Alloys to Cracking by Thermal Shock", N.A.C.A. TN 2037, 1950.
4. Avery, Howard S., and Matthews, Norman A., "Cast Heat-Resistant Alloys of the 16% Chromium - 35% Nickel Type", Trans. A.S.M. 38, 957 (1947).
5. Manson, S. S., "Behavior of Materials under Conditions of Thermal Stress", N.A.C.A. TN 2933, July, 1953.
6. Hoffman, C. A., and Cooper, A. L., "Investigation of Titanium Carbide Base Ceramals Containing Either Nickel or Cobalt Base for Use as Gas Turbine Blades", N.A.C.A., RM E 52 H05, 1952.
7. Crandall, W. B., "Evaluation Techniques for High Temperature Metal-Ceramic Materials" Paper 30, WADC TR 52-127, 1952.
8. Baker, N. I., "Recent Thermal Shock Testing Results", Progress Report for N.A.C.A. Subcommittee on Heat Resistant Materials, Edited by W. L. Badger, General Electric Company, Thompson Laboratories, 1953.
9. Cooper, A. L., and Colteryahn, L. E., "Elevated Temperature Properties of Titanium Carbide Base Ceramals Containing Nickel and Iron", N.A.C.A., RM E 51 I10, 1951.

APPENDIX

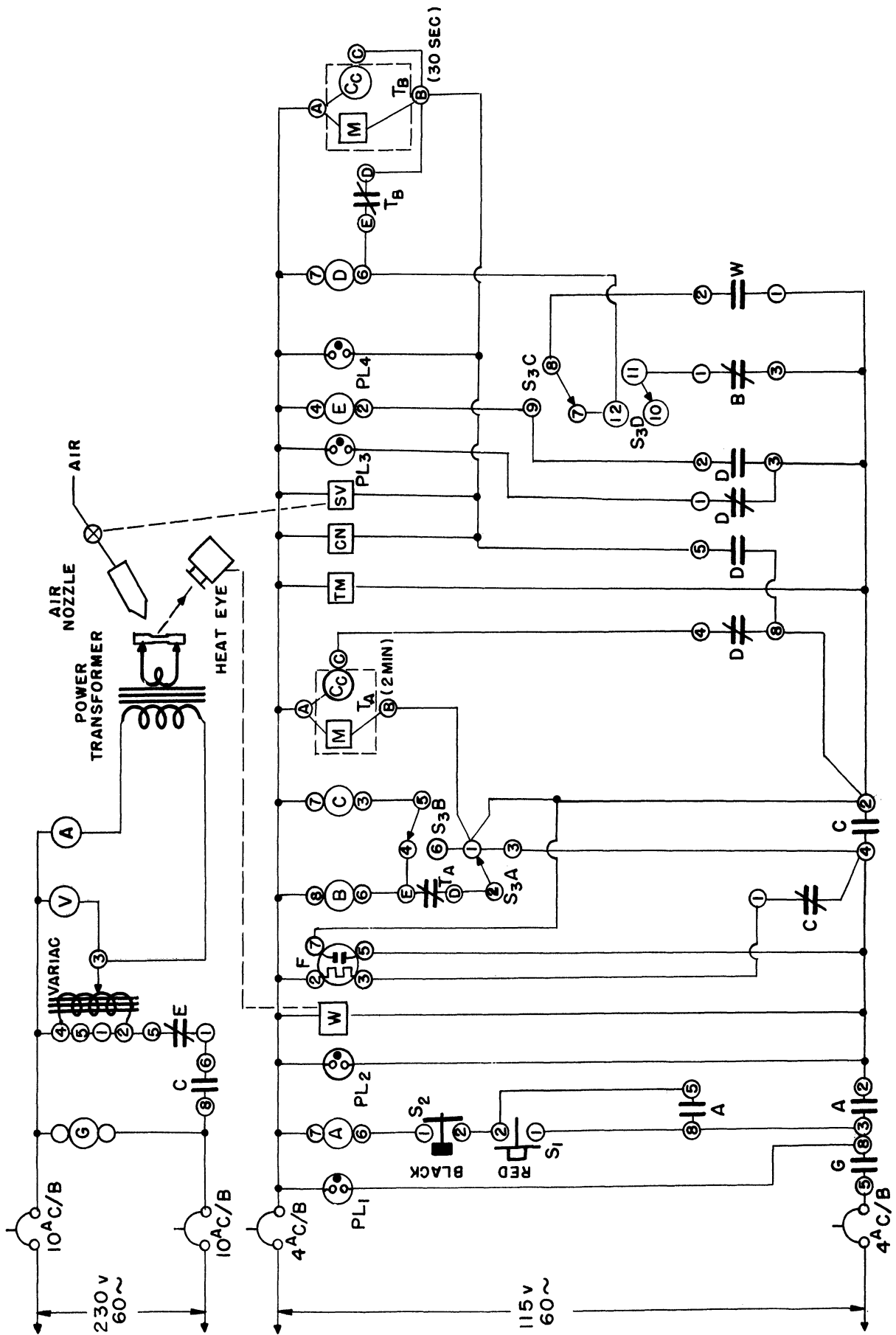




Fig. A-1 Schematic Wiring Diagram of Test Rig. See Key.

KEY TO WIRING SCHEMATIC

- (A) DPDT 115^V 60[~] Relay (Potter and Brumfield MR11A)
- (B) DPDT 115^V 60[~] Relay (Potter and Brumfield MR11A)
- (C) DPDT 115^V 60[~] Relay (Potter and Brumfield PR11A)
- (D) DPDT 115^V 60[~] Relay (Potter and Brumfield MR11A)
- (E) SPDT 115^V 60[~] Relay (Potter and Brumfield PR5A)
- (F)  20-sec Thermal Time-delay Relay (Amperite 115NO20)
- (G) DPDT 230^V 60[~] Relay (Potter and Brumfield MR11A)
- (PL)  Neon Pilot Light 115^V

(W) Wheelco 241-P Capacitrol

(TM) Running Time Meter (GE 8KT9D2)

(CN) Counter (Veeder-Root BL20506)

(SV) Solenoid Valve (Detroit Lubricator No. 681)


(TA) Timer, 2 min (GE 3TSA10 AF9)

(TB) Timer, 30sec (GE 3TSA10 AF5)

S₁ N.O. Push Button

S₂ N.C. Push Button

* S₃ 4 Pole 2 Pos. Rotary Switch (Mallory 3242J)

 Heinemann Circuit-breaker Switch: $\left\{ \begin{array}{l} 10^A: 0411-10, 230^{VAC} \\ 4^A: P0411-4, 115^{VAC} \end{array} \right.$

\neq Normally closed contacts

\perp Normally open contacts

* Cut-off Selector Switch; shown in Temp position on schematic
 (Beginning of cooling portion of cycle controlled by Wheelco Capacitrol)
 In Time position, beginning of cooling controlled by TA (0-2 min)

COMPONENT PARTS OF THERMAL-SHOCK APPARATUS

Quantity	Unit	Component Parts (per unit)		
		Quantity	Name	
2	Dual Test Stand	2	Specimen Holder Assembly †	
		2	Air Nozzle †	
		2	Wheelco A0429 Heat Eye*	
		2	Heat Eye Support †	
		2	Power Transformer ‡	
		2	Det. Lub. No. 681 Solenoid Valve*	
		2	4-cu-ft Air Tank	
		1	Steel Table †	
4	Control Unit	1	ICA/3912 Relay Rack	
		1	ICA/3601RS Panel, 3-1/2 x 19	
		1	ICA/3605RS Panel, 8-3/4 x 19	
		2	ICA/3605RS Panel, 10-1/2 x 19	
		1	ICA/3606RS Panel, 12-1/4 x 19	
		1	ICA/3607 Panel, 14 x 19	
		1	ICA/3654RS Panel, 3-Meters, 5-1/4 x 19	
		1	ICA/4031 Chassis, 13 x 17 x 4	
		1	ICA/4070 Bottom Plate 13 x 17	
		1	Wheelco 241-P Capacitrol	
		1	V-R B120506 Magnetic Counter	
		1	Simpson Mod 57 Voltmeter, 0-300 ^V	
		1	Simpson Mod 57 Ammeter, 0-10 ^a	
		1	G.E. 8KT803 Time Meter 1/10 hr	
		1	G.R. V20HM Variac	
		1	G.E. 3TSA10AF5 Timer 30 sec	
		1	G.E. 3TSA10AF9 Timer 2 min	
		2	Heinemann PO411-4 Circuit Breaker	
		2	Heinemann O411-10 Circuit Breaker	
		1	Potter and Brumfield PR5A Relay 115 ^V	
		1	Potter and Brumfield PR11A Relay 115 ^V	
		3	Potter and Brumfield MR11A Relay 115 ^V	
		1	Potter and Brumfield MR11A Relay 230 ^V	
		1	Amperite 115N020 Relay 115 ^V	
		4	Pilot light, assem. 115 ^V	
		2	Push button switch	1-4001 NO
				1-4002 NC
		1	Mallory 3242J 4PDT Switch	
		-	Wire, plugs, receptacles and hardware	

† Fabricated locally

* Purchased

‡ Built per our specifications by Osborne Transformer Corp., Detroit, Mich. (Type No. 22384)

MISCELLANEOUS CAPITAL ITEMS
Net Physical Parts of Above Units

Quantity	Name
1	Mercoild DA31 Pressure Control
1	Allen Bradley BA22 Contactor
-	Wire, cables, plugs and receptacles to connect Control Units to Test Stands

POWER TRANSFORMER

Specifications

Primary: 140 T. [No. 8 AWG Copper]

Secondary: 1 T. [12 pcs. .020 x 4 Copper Sheet, in parallel]

Leads: Primary; No. 8 stranded

Secondary; 2 1/4 x 2 Copper bar in parallel

Core: Shell-Type, 4% Si, Cross-section 12.5 in²
(Or equivalent grain-oriented spiral core)

Construction: Open (core and coil)

Dimensions: 9 in. wide x 9-1/4 in. high x 7 in. deep (overall)

Built by: Osborne Transformer Corporation, Detroit, Michigan

Type No. 22384

Rating: 1920 V.A.

KEY TO LOG

Column (1)

- (1) Relative position on bar stock
- 1 Specimen number

Column (2)

- Arrow indicates direction and location of cooling jet; cooling medium is air unless otherwise stated
- W Cooling medium is water
- *0.45 Width of cooled edge, inches
- P.F.* Previously subjected to rotating beam fatigue as shown in column (6)
- X Failed during pre-fatigue
- 1700/5 Number in parentheses indicates average of calibrations at beginning and end of test (Mean max test temp)

Column (3)

- M Thermal shock cycle manually controlled
- 1500/5 Automatic cycle control; maximum temperature, °F, and length of cooling period, seconds
- P1800 Dead load, 1800 lbs
- +10/100 Starting with stated maximum temperature, maximum temperature was increased 10°F after each 100 cycles
- 40.5K Reversed-bending (rotating-beam) fatigue tests; maximum stress, 40,500 psi
- to 1800 Maximum temperature held constant after 1800°F was reached

Column (4)

- A Air cooling for stated number of cycles
- W Water cooling for stated number of cycles
- no symbol Air cooling for stated number of cycles

Column (5)

- O No failure visible
- F Fracture
- C Cracks
- G Grooves
- FC Face crack
- PC Possible crack

Column (6)

- B Specimen warped due to thermal strains
- A 0.14 Area of cross section, square inch
- T300/1600 Heat treated before testing 300 hr at 1600°F
- G1500 Grooves first appeared at 1500 cycles
- OH Stated maximum temperature was exceeded due to malfunction of control unit
- BT Broke through to thermocouple hole

$P \left\{ \begin{array}{l} 1700/60 \\ 1200/23 \end{array} \right\}$ Previously subjected to cyclic heating and cooling
 (Max temp) $\frac{1700}{60}$ (Heating time, seconds)
 (Min temp) $\frac{1200}{23}$ (Cooling time, seconds)
 (Number of cycles) 1000

40.5K/
 82000 Previously subjected to 82000 cycles at 40,500 psi

R Reproducibility test

N Specimen formed a neck due to tensile strain

+100/5108 Maximum temperature was increased 100°F at 5108 cycles

Check II Second test to determine the effect of alteration of testing procedure

P Study of crack propagation

PT1 Previously subjected to tensile strain of 1% at room temperature

LRS1 Long-time test at reduced severity, Test No. 1

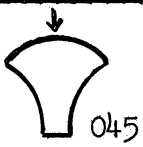
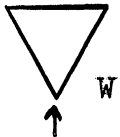


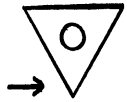
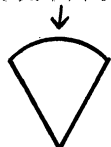

T{ }I Heat treated as shown in braces { }, Lot No. I

C20/1700 Heat treated for 20 hours by heating to 1700°F and allowing to cool for 5 seconds by natural convection

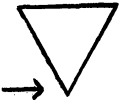



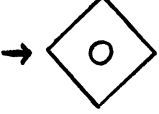


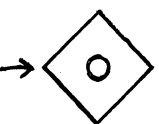
Column (2) Letter at tail of arrow indicates test unit on which test was run. Two arrows indicate two separate tests with cooling on different edges. Horizontal arrow indicates first test

Column (3) Number [e.g., (1)] indicates edge number, shown in Column (2), on which test was run



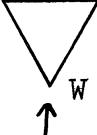
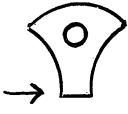
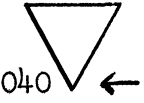
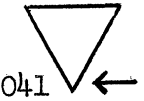


TEST LOG

Specimen Number (1)	Cross Section (2)	Cycle (3)	Number of Cycles (4)	Type of Failure (5)	Remarks (6)
Type 304 Stainless Steel					
1		M	---	O	B
2		1600/10	4400A 300W	O C	B
3		1600/4 +10/100	1783	C	
4a	Fatigue Specimens	40.5K	3300	F	
4b		40.5K	2600	F	
5		1700/4 1800/4	1100 675	O C	
6		1600/4 1900/4	6240 1240	O C	G6500
7		1500/5 P600	4130	F	A0.16
8		1600/5 1800/4	3082 517	O C	T 300/1600

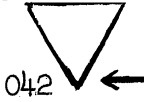

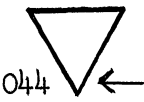
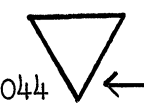




TEST LOG (cont.)

Specimen Number (1)	Cross Section (2)	Cycle (3)	Number of Cycles (4)	Type of Failure (5)	Remarks (6)
Type 304 Stainless Steel (cont.)					
9		1500/3	5753	O	
10		1600/4 1700/4 1800/4	1000 1000 80	O O C	
11		1500/5 P1800	1000	F	A0.132
12		1500/5 P600 P900 P1800	5200 1200 203	O O F	A0.133
13		1600/4	1284	C	G1115
14		1500/4	1000	F	OH
15		1600/5	1900	C	T 300/1600
16		1600/5	409	C	



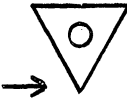
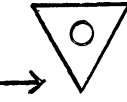
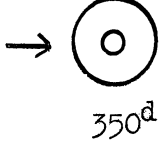
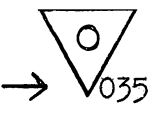
TEST LOG (cont.)

Specimen Number (1)	Cross Section (2)	Cycle (3)	Number of Cycles (4)	Type of Failure (5)	Remarks (6)
Type 304 Stainless Steel (cont.)					
17		1500/5 P1800	300	F	A0.140
18		1800/4	1950	C	G1500
19		1700/3	530	C	
20		1500/3	1000	O	BT
Type 310 Stainless Steel					
B9-1		1900/5 (1907)	1024	C	T 2/2100
B9-2		1900/5 (1907)	1008	C	T 2/2100
B9-3		1900/5 (1885)	1177	C	T 2/2100
B9-4		2000/5 (1990)	707	C	T 2/2100

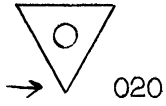
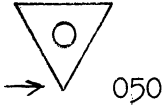


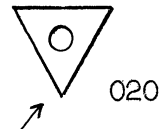
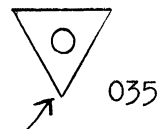
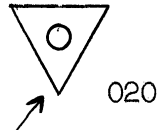
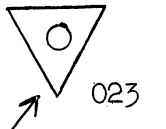
TEST LOG (cont.)

Specimen Number (1)	Cross Section (2)	Cycle (3)	Number of Cycles (4)	Type of Failure (5)	Remarks (6)
Type 310 Stainless Steel (cont.)					
B9-5		2000/5 (2012)	794	C	T 2/2100
B9-6		1800/5 (1770)	1873	C	T 2/2100
B9-7		1800/5 (1810)	1435	C	T 2/2100
B9-8		1700/5 (1720)	2770	C	T 2/2100
B9-9		1700/5	3500	C	T 2/2100
B9-10		(1692)	5197	C	T 2/2100
B9-11		1600/5 (1583)	6471	C	T 2/2100
Type 347 Stainless Steel					
1		1600/4 +10/100	866	C	


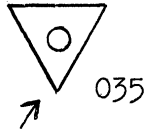

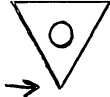
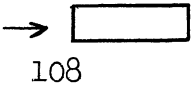
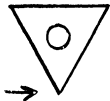

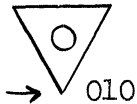
TEST LOG (cont.)

Specimen Number (1)	Cross Section (2)	Cycle (3)	Number of Cycles (4)	Type of Failure (5)	Remarks (6)
Type 347 Stainless Steel					
2		1600/4 +10/100	1147	C	
3		1500/4 +10/100	575	C	B.T.
4a	Fatigue Specimens	54K	5200	F	40.5K/ 82000
4b		54K	10400	F	
5		1500/4 +10/100	1326	C	
6		1500/4 +10/100	1990	C	
7		1600/4 +10/100 to 1800	2700	G	
8	(Defective)	Used for bend test			
9		1600/4	2863	C	R

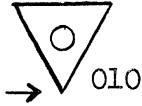

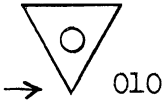


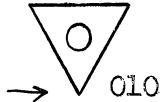
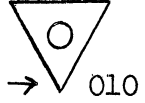

TEST LOG (cont.)

Specimen Number (1)	Cross Section (2)	Cycle (3)	Number of Cycles (4)	Type of Failure (5)	Remarks (6)
Type 347 Stainless Steel					
10	 020	1600/4	3787	C	Check II
11	 050	1600/4	2580	C	
12	 020	1600/4	3162	C	G736
13	 020	1600/4	2204	C	G2072
14	 020	1600/4	2707	C	G2604
15	 035	1600/4	3003	C	G2820 R
16	 020	1600/4	2518	C	R
17	 023	1600/4	4850	O	Check I



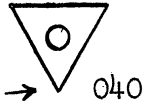
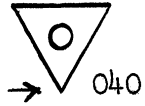
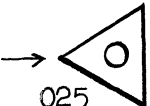
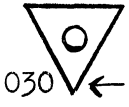

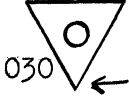
TEST LOG (cont.)

Specimen Number (1)	Cross Section (2)	Cycle (3)	Number of Cycles (4)	Type of Failure (5)	Remarks (6)
Type 347 Stainless Steel (cont.)					
18		Fatigue 64K	7200	F	54K 103300
19		1600/4	1825	C	R
20		Fatigue 64K	4300	F	37K/217100 42K/11000 48K/35600 54K/10000 59K/10400
21		1600/4	4430	C	
22		1600/5	1423	C	T 2/2000
23		1600/5	2962	C	
24		Fatigue 59K	52900	F	
25		1600/5 PF	1562	C	54K/50000




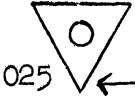



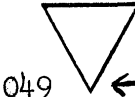
TEST LOG (cont.)

Specimen Number (1)	Cross Section (2)	Cycle (3)	Number of Cycles (4)	Type of Failure (5)	Remarks (6)
Type 347 Stainless Steel (cont.)					53K/52000
26	 010	1600/5 PF	1960	C	59K/12000 64K/1000 70K/1000 75K/500
27	 010	X PF		F	53K/52000 59K/11300
28	 010	1600/5 PF	1594	C	53K/52000 59K/12000 64K/1000 70K/1000 75K/500
29	 010	X PF		C	53K/52000 59K/12000 64K/1000 70K/1000 75K/300
30	 010	1600/5	1973	C	
31	 010	1600/5	2764	C	
32	 010	1600/5	1500	C	
33 (4)	 040	X PF		F	59K/32600


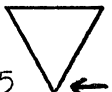






TEST LOG (cont.)

Specimen Number (1)	Cross Section (2)	Cycle (3)	Number of Cycles (4)	Type of Failure (5)	Remarks (6)
Type 347 Stainless Steel (cont.)					
34 (3)		1600/5 PF	1811	C	60K/39000
35 (2)		Use for Calibration of Heat Eye			
36 (1)		1600/5 PF	1859	C	58K/30000
37 (5)		1600/5	4635	C	
38		1600/5	2114	C	T 2 / 2000
39 (7)		1600/5	2440	G	G2440
40		1600/5	3143	G	
41		1600/5	2710	C	G2000

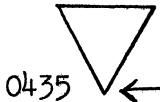




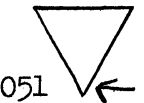

TEST LOG (cont.)

Specimen Number (1)	Cross Section (2)	Cycle (3)	Number of Cycles (4)	Type of Failure (5)	Remarks (6)
Type 347 Stainless Steel (cont.)					
42		Used for Calibration			
43 (11)		1600/5	10708	C	P
44 (12)		1600/5	2046	C	T2/2000
45 (13)		1600/5	1956	C	T2/2000
H.S. 21					
1		1500/3.5 +10/100	1000	C	BT
2		1700/5 (1718)	3552	C	
3		1900/5 (1917)	2625	C	
4		1700/5 (1719)	6820	C	FC 6003 *4C 6561




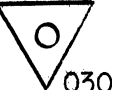




TEST LOG (cont.)

Specimen Number (1)	Cross Section (2)	Cycle (3)	Number of Cycles (4)	Type of Failure (5)	Remarks (6)
H.S. 21 (cont.)					
5	045 	1800/5 ✓	1252	C	
6	035 	1900/5 (1862)	2309	C	
7	*0485 	1700/5 (1720)	1506	C	
8	047 	1800/5 ✓	3468	C	
9	0375 	1600/5 (1603)	5305	C	
10	039 	2000/5	673	C	
11	0430 	1600/5 (1605)	17615	C	
12	049 	1700/5	7375	C	51/1350









TEST LOG (cont.)

Specimen Number (1)	Cross Section (2)	Cycle (3)	Number of Cycles (4)	Type of Failure (5)	Remarks (6)
H.S. 21 (cont.)					
13	0435 	1800/5 ✓	3902	C	
14	Used for Fatigue Specimen				
15	035 	1600/5	15334	O	
16	038 	1700/5 ✓	14489	C	T 51/1350
17	0395 	1700/5 (1708)	3279	C FC.004	
18	038 	2000/5 (1990)	396	C	
19	051 	1700/5	10060	C	T 51/1350
20	039 	1800/5 ✓	4147	C	









TEST LOG (cont.)

Specimen Number (1)	Cross Section (2)	Cycle (3)	Number of Cycles (4)	Type of Failure (5)	Remarks (6)
H.S. 21 (cont.)					
21	0355 	1600/5 (1613)	9938	C	
22	049 	1700/5 ✓	18411	C	T 51/1350
Inconel					
1	 015	1500/3 +10/100	1450	C	G1150
2	 030	1500/3 +10/100	2730	C	
3	 035	1500/3-1/2	428	C	
4	035 	1700/5	3167	C	2/500 T 1/3/1400
5	035 	1700/5	1819	C	2/500 T 1/3/1400
6	 035	1600/4	7449	C	








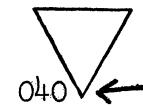
TEST LOG (cont.)

Specimen Number (1)	Cross Section (2)	Cycle (3)	Number of Cycles (4)	Type of Failure (5)	Remarks (6)
Inconel (cont.)					
7		1700/5	4706	C	2/500 T 1/3/1400
8		1700/5	2090	C	T 1/3/1400 PT 1
9		1700/5	6465	C	2/800 T 1/3/1400
10		1700/5	3685	C	T 1/3/1400 PT 10
11		1700/5	2860	C	T 1/3/1400 PT 5
12		1700/5	1884	C	1/3/1400 T/20/1700
13		1700/5	2500	C	T 1/3/1400 PT 1
14		1700/5	2527	C	T 1/3/1400 PT 5

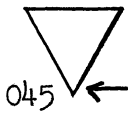
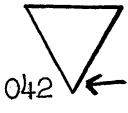
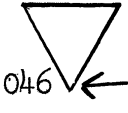
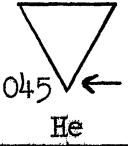
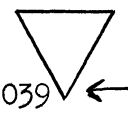
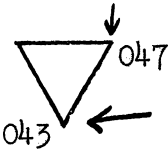
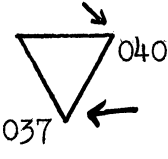
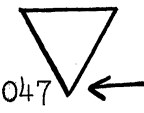
EST LOG (cont.)

Specimen Number (1)	Cross Section (2)	Cycle (3)	Number of Cycles (4)	Type of Failure (5)	Remarks (6)
Inconel					
15		1700/5	2804	C	T 1/3/1400 PT 10
16		1700/5	3590	C	T 1/3/1400
17		1700/5	2270	C	T 1/3/1400 PT 1
18		1700/5	3015	C	T 1/3/1400 PT 5
19		1700/5	1830	C	T 1/3/1400 PT 10
20		1700/5	2898	C	T 1/3/1400
21		1700/5	7498 11265	FC? C	T 1/3/1400 LRSI
22		1700/5	4339 6866	FC? C	T 1/3/1400 (RS) a/c Flex. pipe to nozzle

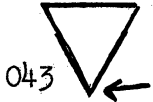
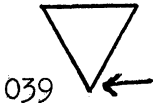
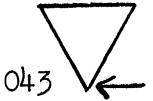

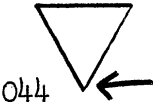
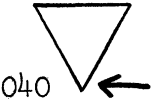

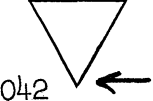
TEST LOG (cont.)

Specimen Number (1)	Cross Section (2)	Cycle (3)	Number of Cycles (4)	Type of Failure (5)	Remarks (6)
Inconel (cont.)					
23		1700/5	2250	C	T 1/3/1400
24		1700/5	8145	C	T 1/3/1400 LRS II
25		1700/5	3538 4229	FC C	T 1/3/1400
Inconel Lot II					
C-1		1600/5	4358-	C	T 1/3/1400
C-2		1600/5	3416-	C	T 1/3/1400
C-3		1600/5	2572-	C	T 1/3/1400
C-4		1700/5	1693+	C 0.9	T 1/3/1400
C-5		1700/5	1378-	C	T 1/3/1400

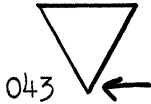
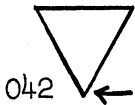
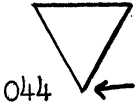
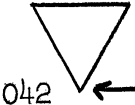

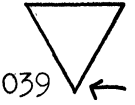

TEST LOG (cont.)

Specimen Number (1)	Cross Section (2)	Cycle (3)	Number of Cycles (4)	Type of Failure (5)	Remarks (6)
Inconel Lot II					
C-6		1700/5	1537	C	T 1/3/1400
C-7		1800/5 (1845)	3854	C	T 1/3/1400
C-8		1800/5 (1790)	3204 3651	C 3C	T 1/3/1400
C-9		2000/5 (1998)	732	0	T 1/3/1400 Spec. upset in middle- shortened 1/4 inch
C-10		2000/5 (1950)	732	0	T 1/3/1400 Air removes scale from cooled area
Inconel Lot II (1/2-inch Diameter Rod)					
B-1		1700/5 1700/5	2267 1760	C C	
B-2		1700/5 1700/5	2344 2527	C C	
B-3		1700/5	2622	C	

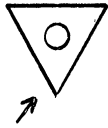
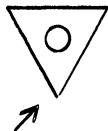
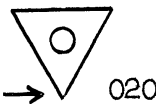
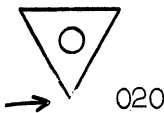
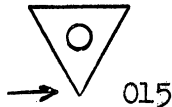
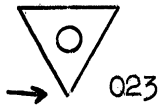
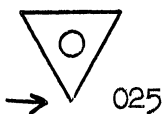
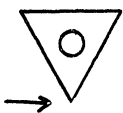
TEST LOG (cont.)

Specimen Number (1)	Cross Section (2)	Cycle (3)	Number of Cycles (4)	Type of Failure (5)	Remarks (6)
Inconel Lot II (1/2-inch Diameter Rod) (cont.)					
B-4		2000/5	958-	C	
B-5		2000/5	398	C	
B-6		2000/5	212	C	
B-7		2000/5	140? 299	C	
B-8		1700/5	2560	C	
B-9		1700/5	2283	C	
B-10		1700/5	2206	C	
B-11		Not Used			

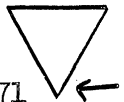
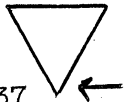
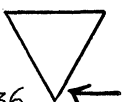



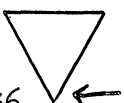
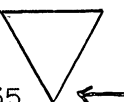
TEST LOG (cont.)

Specimen Number (1)	Cross Section (2)	Cycle (3)	Number of Cycles (4)	Type of Failure (5)	Remarks (6)
Inconel Lot II (1/2-inch Diameter Rod) (cont.)					
B-12		2000/5	110? 143	C	
B-13		1900/5	580		
B-14		1900/5	463		
B-15		1900/5	659	C	
B-16		1900/5	175		
B-17		1800/5	480		
B-18		1800/5	1962	C	

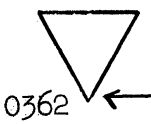
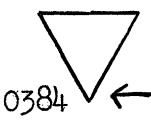
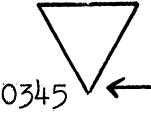
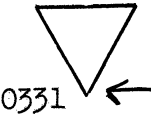

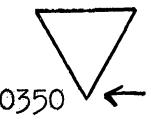
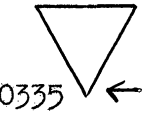
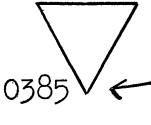
TEST LOG (cont.)

Specimen Number (1)	Cross Section (2)	Cycle (3)	Number of Cycles (4)	Type of Failure (5)	Remarks (6)
S-816 Alloy (Wrought)					
1		1500/4 P700 No load	1788 18391	O C	A 0.08 N +100/5108 +100/10000
2		1500/4 P1100 to P700	2657	F	A 0.08 N
3		1700/4	2256	C	
4		1700/4	2550	C	
5		1600/4	3870	C	
6		1500/4	2630	C	
7		1500/4	13280	C	
8		1600/4	7497	C	

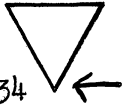
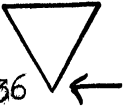
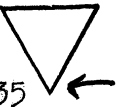
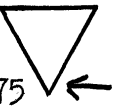
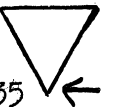
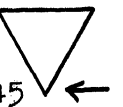
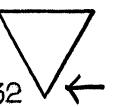
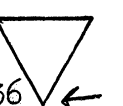
TEST LOG (cont.)

Specimen Number (1)	Cross Section (2)	Cycle (3)	Number of Cycles (4)	Type of Failure (5)	Remarks (6)
S-816 Alloy (Wrought) (cont.)					
9	0371 	1800/5 (1805)	1069 ⁻	C	T { 1/2150W } 16/1800
10	037 	1700/5 (1700)	2426	C	T { 1/2150W } 16/1800
11	036 	1600/5 (1606)	5130	C	T { 1/2150W } 16/1800
12	0388 	1800/5 (1797)	956 ⁻	C	T { 1/2150W } 16/1800
13	034 	1700/5 (1705)	1903 ⁺	C (0003 short) (003 short)	T { 1/2150W } 16/1800
14	0350 	1800/5 (1793)	1146 ⁻	C	T { 1/2150W } 16/1800
15	036 	1600/4 (1613)	4600	C	T { 1/2150W } 16/1800 } I
16	0335 	1600/4 (1607)	3620	C	T { 1/2150W } 16/1800

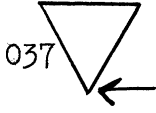
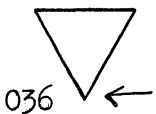
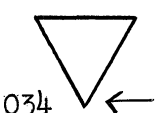
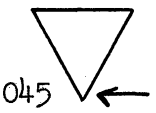
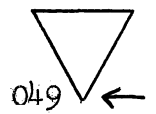

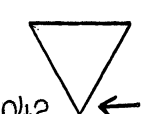

TEST LOG (cont.)

Specimen Number (1)	Cross Section (2)	Cycle (3)	Number of Cycles (4)	Type of Failure (5)	Remarks (6)
S-816 Alloy (Wrought) (cont.)					
17	 0362	1700/5 (1713)	1956 ^m	C	T $\left\{ \begin{array}{l} 1/2150W \\ 16/1800 \end{array} \right\}$ I
18	 0384	1800/5 (1790)	784	C	T $\left\{ \begin{array}{l} 1/2150W \\ 16/1800 \end{array} \right\}$ I
19	 0345	1700/5 (1713)	2300 ^m	C	T $\left\{ \begin{array}{l} 1/2150W \\ 16/1800 \end{array} \right\}$ I
20	 0331	1600/5 (1630)	3100 ^m	C	T $\left\{ \begin{array}{l} 1/2150W \\ 16/1800 \end{array} \right\}$ I
21	 0325	1700/5 (1697)	2190	C	T $\left\{ \begin{array}{l} 1/2150 \\ 16/1800 \end{array} \right\}$ II P $\left\{ \begin{array}{l} 1700 / 60 \\ 1200 / 23 \\ 1000 N \end{array} \right\}$
22	 0350	1700/5 (1692)	2190	C	T $\left\{ \begin{array}{l} 1/2150 \\ 16/1800 \end{array} \right\}$ II P $\left\{ \begin{array}{l} 1700 / 60 \\ 1200 / 23 \\ 600 N \end{array} \right\}$
23	 0335	1700/5 (1685)	1414	C	T $\left\{ \begin{array}{l} 1/2150 \\ 16/1800 \end{array} \right\}$ II P $\left\{ \begin{array}{l} 1700 / 60 \\ 1200 / 23 \\ 1182 N \end{array} \right\}$
24	 0385	1700/5 (1699)	1697	C	T $\left\{ \begin{array}{l} 1/2150 \\ 16/1800 \end{array} \right\}$ II P $\left\{ \begin{array}{l} 1700 / 60 \\ 1200 / 23 \\ 1040 N \end{array} \right\}$

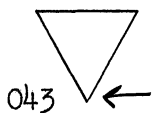
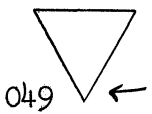
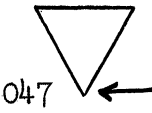
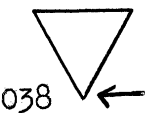

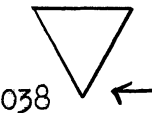
TEST LOG (cont.)

Specimen Number (1)	Cross Section (2)	Cycle (3)	Number of Cycles (4)	Type of Failure (5)	Remarks (6)
S-816 Alloy (Wrought) (cont.)					
25	034 	1700/5 (1702)	2328	C	T $\left\{ \begin{array}{l} 1/2150 \\ 16/1800 \end{array} \right\}$ II
26	036 	1700/5 (1713)	2239	C	T $\left\{ \begin{array}{l} 1/2150 \\ 16/1800 \end{array} \right\}$ II
27	035 	1700/6 (1690)	1967	C	T $\left\{ \begin{array}{l} 1/2150 \\ 16/1800 \end{array} \right\}$ II
28	0375 	1700/5 (1705)	1598	C	T $\left\{ \begin{array}{l} 1/2150 \\ 16/1800 \end{array} \right\}$ II
29	035 	1700/5 (1695)	1122	C	T $\left\{ \begin{array}{l} 1/2150 \\ 16/1800 \end{array} \right\}$ II P $\left\{ \begin{array}{l} 1700/60 \\ 1200/23 \\ 2000 N \end{array} \right\}$
30	0345 	1700/5 (1700)	2110	C	T $\left\{ \begin{array}{l} 1/2150 \\ 16/1800 \end{array} \right\}$ II P $\left\{ \begin{array}{l} 1700/60 \\ 1200/23 \\ 2000 N \end{array} \right\}$
31	032 	1700/5 (1702)	1542	C	T $\left\{ \begin{array}{l} 1/2150 \\ 16/1800 \end{array} \right\}$ II P $\left\{ \begin{array}{l} 1700/60 \\ 1200/23 \\ 2000 N \end{array} \right\}$
32	036 	1700/5 (1698)	2110-	C	T $\left\{ \begin{array}{l} 1/2150 \\ 16/1800 \end{array} \right\}$ II P $\left\{ \begin{array}{l} 1700/60 \\ 1200/23 \\ 1000 N \end{array} \right\}$


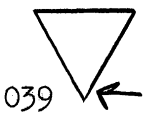
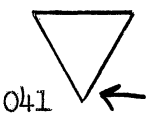
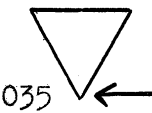

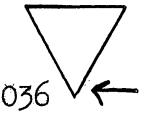

TEST LOG (cont.)

Specimen Number (1)	Cross Section (2)	Cycle (3)	Number of Cycles (4)	Type of Failure (5)	Remarks (6)
S-816 Alloy (Wrought) (cont.)					
33	037 	1700/5 (1715)	1700	C	T $\left\{ \begin{array}{l} 1/2150 \\ 16/1800 \end{array} \right\}$ II P $\left\{ \begin{array}{l} 1700/60 \\ 1200/23 \\ 3121 \text{ N} \end{array} \right\}$
34	036 	1700/5 (1719)	1543	C	T $\left\{ \begin{array}{l} 1/2150 \\ 16/1800 \end{array} \right\}$ II P $\left\{ \begin{array}{l} 1700/60 \\ 1200/23 \\ 3110 \text{ N} \end{array} \right\}$
35	034 	1700/5 ✓	2150	C	T $\left\{ \begin{array}{l} 1/2150 \\ 16/1800 \end{array} \right\}$ II P $\left\{ \begin{array}{l} 1700/60 \\ 1200/23 \\ 3000 \text{ N} \end{array} \right\}$
S-816 Alloy (Wrought) Lot II					
P6-1	045 	1900/5	1082	C	T $\left\{ \begin{array}{l} 1/2150 \\ 16/1800 \end{array} \right\}$
P6-2	049 	1900/5	1351	C	T $\left\{ \begin{array}{l} 1/2150 \\ 16/1800 \end{array} \right\}$
P6-3	038 	1900/5	1077	C	T $\left\{ \begin{array}{l} 1/2150 \\ 16/1800 \end{array} \right\}$
P6-4	042 	2000/5	786	C	T $\left\{ \begin{array}{l} 1/2150 \\ 16/1800 \end{array} \right\}$
P6-5	048 	2000/5	1001	C	T $\left\{ \begin{array}{l} 1/2150 \\ 16/1800 \end{array} \right\}$

TEST LOG (cont.)

Specimen Number (1)	Cross Section (2)	Cycle (3)	Number of Cycles (4)	Type of Failure (5)	Remarks (6)
S-816 Alloy (Wrought) Lot II (cont.)					
P6-6		2000/5	800	C	T {1/2150 } {16/1800 }
P6-7					
P6-8		2000/5	976	C	T {1/2150 } {16/1800 }
S-816 (Cast)					
6-1		1800/5 (1805)	1557	C	
6-2		1800/5 (1840?)	3005	C	
6-3		1900/5 (1880)	1522	C	
6-4		1800/5 (1805)	549	C	


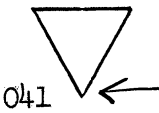
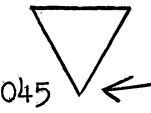
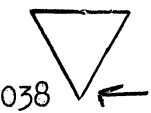
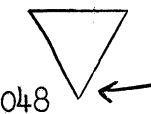
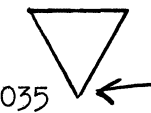
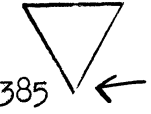
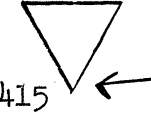
TEST LOG (cont.)

Specimen Number (1)	Cross Section (2)	Cycle (3)	Number of Cycles (4)	Type of Failure (5)	Remarks (6)
S-816 (Cast) (cont.)					
6-5		1900/5 (1927)	1040	C	
6-6	Used for Fatigue Specimens				
6-7		1900/5 ✓	729	C	
6-8		2000/5 (1982)	1370	C	
6-9		2000/5 (2017)	636	C	
6-10		1700/5 (1717)	2090	C	
6-11		1700/5 (1710)	2509	C	
6-12		1600/5 ✓	18700	0	No Crack-stopped

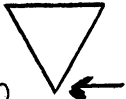
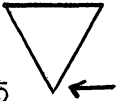

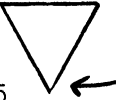
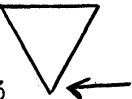
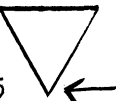

TEST LOG (cont.)

Specimen Number (1)	Cross Section (2)	Cycle (3)	Number of Cycles (4)	Type of Failure (5)	Remarks (6)
N-155 Alloy (Wrought)					
1	038	1700/5	3764 3878 4949	C TR (1) FC 2C	T {1/3/2200W } I 50/1400
2	040	1700/5	3211	C	T {1/3/2200W } I 50/1400
3	038	1700/5	3248	C	T {1/3/2200W } I 50/1400
4	034	1800/5	1508	C	T {1/3/2200W } I 50/1400
5	036	1600/5	3886	O	T {1/3/2200W } I 50/1400 Removed 11-15 for check-no crack
6	040	1700/5	3105	C	T {1/3/2200W } I 50/1400
7	042	1800/5	1818	C	T {1/3/2200W } I 50/1400
8	039	1700/5	3195	C	T {1/3/2200W } I 50/1400

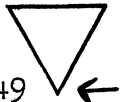
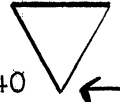
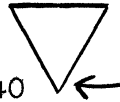
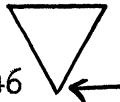
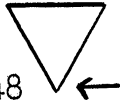


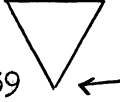
TEST LOG (cont.)

Specimen Number (1)	Cross Section (2)	Cycle (3)	Number of Cycles (4)	Type of Failure (5)	Remarks (6)
N-155 Alloy (Wrought)					
9	037 	1700/5	2888	C	T $\left\{ \begin{array}{l} 1/3/2200W \\ 50/1400 \end{array} \right\}$ I
10	041 	1600/5	10124	O	T $\left\{ \begin{array}{l} 1/3/2200W \\ 50/1400 \end{array} \right\}$ I
11	045 	1800/5	2052	C	T $\left\{ \begin{array}{l} 1/3/2200W \\ 50/1400 \end{array} \right\}$ I
12	038 	1800/5	1228	C	T $\left\{ \begin{array}{l} 1/3/2200W \\ 50/1400 \end{array} \right\}$ II
13	048 	1800/5	1095	C	T $\left\{ \begin{array}{l} 1/3/2200W \\ 50/1400 \end{array} \right\}$ II
14	035 	1800/5	1042	C	T $\left\{ \begin{array}{l} 1/3/2200W \\ 50/1400 \end{array} \right\}$ II
15	0385 	1800/5	990	C	T $\left\{ \begin{array}{l} 1/3/2200W \\ 50/1400 \end{array} \right\}$ II
16	0415 	1800/5	1130	C	T $\left\{ \begin{array}{l} 1/3/2200W \\ 50/1400 \end{array} \right\}$ II

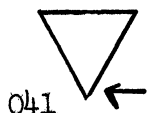

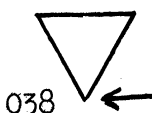
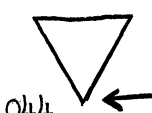

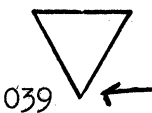
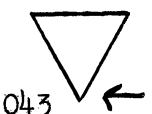
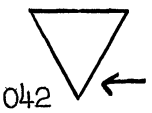
TEST LOG (cont.)

Specimen Number (1)	Cross Section (2)	Cycle (3)	Number of Cycles (4)	Type of Failure (5)	Remarks (6)
N-155 Alloy (Wrought) (cont.)					
17	040 	1700/5	2229	C	T $\left\{ \begin{array}{l} 1/3/2200W \\ 50/1400 \end{array} \right\}$ II
18	0365 	1700/5	1995	C	T $\left\{ \begin{array}{l} 1/3/2200W \\ 50/1400 \end{array} \right\}$ II
19	0395 	1600/5	5153	C	T $\left\{ \begin{array}{l} 1/3/2200W \\ 50/1400 \end{array} \right\}$ II
20	0465 	1700/5	2320	C	T $\left\{ \begin{array}{l} 1/3/2200W \\ 50/1400 \end{array} \right\}$ II
21	0433 	1600/5	3530	C	T $\left\{ \begin{array}{l} 1/3/2200W \\ 50/1400 \end{array} \right\}$ II
22	045 	1600/5	7000	C	T $\left\{ \begin{array}{l} 1/3/2200W \\ 50/1400 \end{array} \right\}$ II
23	0466 	1600/5	6728	C	T $\left\{ \begin{array}{l} 1/3/2200W \\ 50/1400 \end{array} \right\}$ II

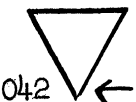




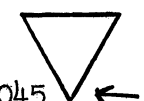
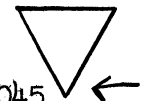
TEST LOG (cont.)

Specimen Number (1)	Cross Section (2)	Cycle (3)	Number of Cycles (4)	Type of Failure (5)	Remarks (6)
N8155 Alloy (Wrought) Lot II					
C5-1	049 	2000/5	1287-	C	T { 1/3/2200 } 50/1400 }
C5-2	040 	2000/5	1083	C	T { 1/3/2200 } 50/1400 }
C5-3	040 	2000/5	1775-	C	T { 1/3/2200 } 50/1400 }
C5-4	046 	2000/5	966	C	T { 1/3/2200 } 50/1400 }
C5-5	048 	1900/5	1495	C	T { 1/3/2200 } 50/1400 }
C5-6	046 	1900/5	1458	C	T { 1/3/2200 } 50/1400 }
C5-7	047 	1900/5	1535	C	T { 1/3/2200 } 50/1400 }
C5-8	039 	1600/5	19000	O	T { 1/3/2200 } 50/1400 }

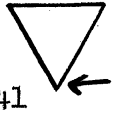
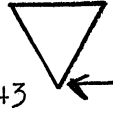
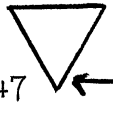


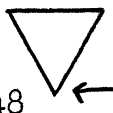
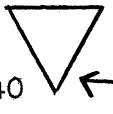
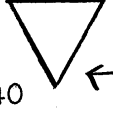
TEST LOG (cont.)

Specimen Number (1)	Cross Section (2)	Cycle (3)	Number of Cycles (4)	Type of Failure (5)	Remarks (6)
Waspalloy					
A3-1	041 	1600/5	10050	C	T { 4/1975 } 16/1400 }
A3-2	038 	1600/5	15048	C	T { 4/1975 } 16/1400 }
A3-3	038 	1800/5 (1798)	1789 ⁻	C	T { 4/1975 } 16/1400 }
A3-4	044 	1800/5 (1795)	613	C	T { 4/1975 } 16/1400 }
A3-5	041 	1800/5 (1805)	784	C	T { 4/1975 } 16/1400 }
A3-6	039 	1700/5 (1695)	1319 ⁻	C	T { 4/1975 } 16/1400 }
A3-7	043 	1700/5 (1705)	742	C	T { 4/1975 } 16/1400 }
A3-8	042 	1700/5 (1695)	879	C	T { 4/1975 } 16/1400 }


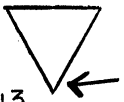

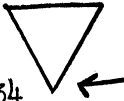
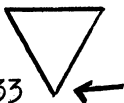
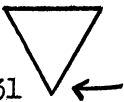
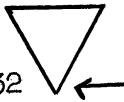

TEST LOG (cont.)

Specimen Number (1)	Cross Section (2)	Cycle (3)	Number of Cycles (4)	Type of Failure (5)	Remarks (6)
Waspalloy (cont.)					
A3-9	042 	1650/5 (1680)	1690	C	T { 4/1975 } 16/1400
A3-10	038 	1900/5 (1880)	1102	C	T { 4/1975 } 16/1400
A3-11	039 	1900/5 (1920)	1010	C	T { 4/1975 } 16/1400
A3-12	035 	2000/5 (2002)	784	C	T { 4/1975 } 16/1400
A3-13	042 	2000/5 (1990)	622	C	T { 4/1975 } 16/1400
A3-14	045 	2000/5	1263	C over	T { 4/1975 } 16/1400
A3-15	Not Used				
A3-16	045 	2000/5 (1982)	1263	C over	

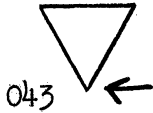
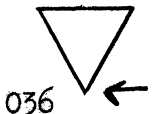
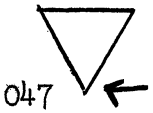
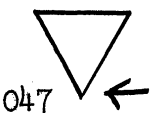
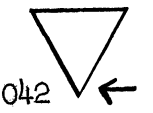
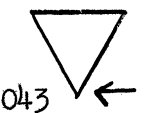
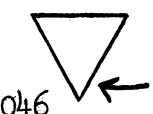
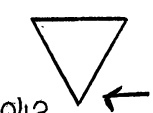
TEST LOG (cont.)

Specimen Number (1)	Cross Section (2)	Cycle (3)	Number of Cycles (4)	Type of Failure (5)	Remarks (6)
M-252 Alloy					
B2-1	041 	1600/5 (1575)	15648	C *.5/13964 Fix	T { 4/1950 } 15/1400
B2-2	043 	1600/5 (1595)	7717	C .2 over .1 over	T { 4/1950 } 15/1400
B2-3	047 	1700/5 (1745?)	3747	C	T { 4/1950 } 15/1400
B2-4	043 	1700/5 (1690)	12318	C	T { 4/1950 } 15/1400
B2-5	046 	1900/5 (1890)	1872	C	T { 4/1950 } 15/1400
B2-6	048 	1800/5 (1982)	2375	C	T { 4/1950 } 15/1400
B2-7	040 	1800/5 (1805)	2342	C	T { 4/1950 } 15/1400
B2-8	040 	1800/5 (1800)	1941	C	T { 4/1950 } 15/1400

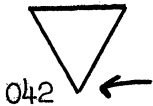
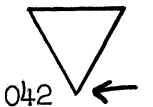
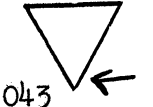
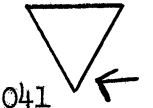

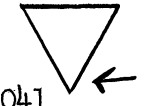
TEST LOG (cont.)

Specimen Number (1)	Cross Section (2)	Cycle (3)	Number of Cycles (4)	Type of Failure (5)	Remarks (6)
M-252 Alloy (cont.)					
B2-9	041 	2000/5 (1998)	1229	C	T { 4/1950 } 15/1400 }
B2-10	043 	2000/5 (1975)	1425	C	T { 4/1950 } 15/1400 }
B2-11	040 	2000/5 (1892)	1650	C	T { 4/1950 } 15/1400 }
Battellalloy					
D-1	034 	2000/5 (2032)	3552	C	T { 2/2200 } 10/1500 }
D-2	033 	1900/5 (1920)	2745	C	T { 2/2200 } 10/1500 }
D-3	031 	2000/5 (1980)	4079	C	T { 2/2200 } 10/1500 }
D-4	032 	1900/5 (1920)	4956	C	T { 2/2200 } 10/1500 }
D-5	035 	1800/5	7839	C	T { 2/2200 } 10/1500 }

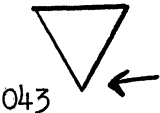
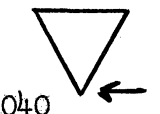
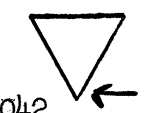
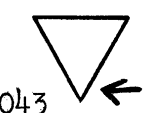
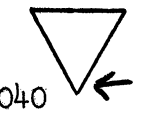

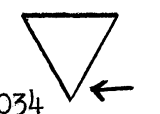

TEST LOG (cont.)

Specimen Number (1)	Cross Section (2)	Cycle (3)	Number of Cycles (4)	Type of Failure (5)	Remarks (6)
Hastelloy C (Cast)					
C-1	 043	1600/5 (1607)	4618	C	$T \left\{ \begin{matrix} 1/2200 \\ 16/1600 \end{matrix} \right\}$
C-2	 036	1600/5 (1595)	2240	C	$T \left\{ \begin{matrix} 1/2200 \\ 16/1600 \end{matrix} \right\}$
C-3	 047	1600/5 (1585)	7546	C	$T \left\{ \begin{matrix} 1/2200 \\ 16/1600 \end{matrix} \right\}$
C-4	 047	1700/5 (1683)	2737	C	$T \left\{ \begin{matrix} 1/2200 \\ 16/1600 \end{matrix} \right\}$
C-5	 042	1700/5 (1719)	3098	O	$T \left\{ \begin{matrix} 1/2200 \\ 16/1600 \end{matrix} \right\}$
C-6	 043	1700/5 (1702)	3408	C	$T \left\{ \begin{matrix} 1/2200 \\ 16/1600 \end{matrix} \right\}$
C-7	 046	1800/5 (1825)	2922	C	$T \left\{ \begin{matrix} 1/2200 \\ 16/1600 \end{matrix} \right\}$
C-8	 042	1800/5 (1798)	1338	C	$T \left\{ \begin{matrix} 1/2200 \\ 16/1600 \end{matrix} \right\}$

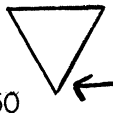
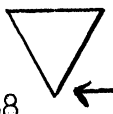
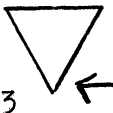
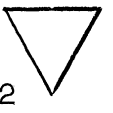
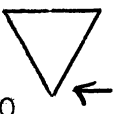

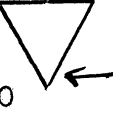
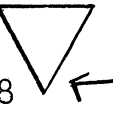
TEST LOG (cont.)

Specimen Number (1)	Cross Section (2)	Cycle (3)	Number of Cycles (4)	Type of Failure (5)	Remarks (6)
Hastelloy C (Cast) (cont.)					
C-9		1800/5 (1810)	1872	C	$T \left\{ \begin{array}{l} 1/2200 \\ 16/1600 \end{array} \right\}$
C-10		1900/5 (1860)	4325	C	$T \left\{ \begin{array}{l} 1/2200 \\ 16/1600 \end{array} \right\}$
C-11		1900/5 (1880)	3020	C	$T \left\{ \begin{array}{l} 1/2200 \\ 16/1600 \end{array} \right\}$
C-12		2000/5 (2010)	364	C	$T \left\{ \begin{array}{l} 1/2200 \\ 16/1600 \end{array} \right\}$
C-13		2000/5 (1990)	291	C	$T \left\{ \begin{array}{l} 1/2200 \\ 16/1600 \end{array} \right\}$
C-14		Not Used			
C-15	 He	2000/5 (1988)	624	C	$T \left\{ \begin{array}{l} 1/2200 \\ 16/1600 \end{array} \right\}$


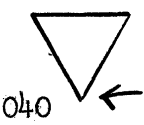
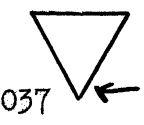
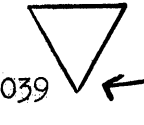
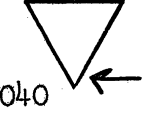
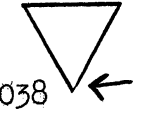
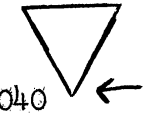
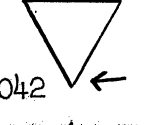
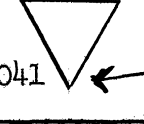
TEST LOG (cont.)

Specimen Number (1)	Cross Section (2)	Cycle (3)	Number of Cycles (4)	Type of Failure (5)	Remarks (6)
Kennametal K-151-A					
1	043 	2000/5 (1975)	300	C	Fractured
2	040 	2000/5 (2000)	269	C	
3	042 	1700/5 (1686)	2626	C	Fractured
4	043 	1700/5 (1719)	2325	C	Fractured
5	040 	1600/5 (1592)	18020+	O	Stopped
6	050 	1800/5 (1800)	653	C	Fractured
Kennametal K-152-B					
1	034 	2000/5	154	C	Fractured
2	057 	2000/5	345	C	Fractured

TEST LOG (cont.)

Specimen Number (1)	Cross Section (2)	Cycle (3)	Number of Cycles (4)	Type of Failure (5)	Remarks (6)
Kennametal K-152-B (cont.)					
3	050 	1800/5	391	C	Fractured
4	038 	1600/5	8511	C	Fractured
5	043 	1800/5	251	C	Fractured
6	042 	1700/5	535	C	Fractured
Nimonic 80-A					
B4-1	040 	1700/5 (1728)	3574	C	T {8/1965 } {16/1300 }
B4-2	043 	1800/5 (1775)	2919	C	T {8/1965 } {16/1300 }
B4-3	040 	2000/5 (2020)	789	C	T {8/1965 } {16/1300 }
B4-4	048 	2000/5 (1990)	849	C	T {8/1965 } {16/1300 }

TEST LOG (cont.)

Specimen Number (1)	Cross Section (2)	Cycle (3)	Number of Cycles (4)	Type of Failure (5)	Remarks (6)
Nimonic 80-A (cont.)					
B4-5	037 	2000/5 (1982)	1078	C	T { 8/1965 } 16/1300 }
B4-6	040 	1900/5 (1972)	1755	C	T { 8/1965 } 16/1300 }
B4-7	037 	1900/5 (1895)	1910	C	T { 8/1965 } 16/1300 }
B4-8	039 	1700/5 (1720)	1770	C	T { 8/1965 } 16/1300 }
B4-9	040 	1800/5 (1817)	2918	C	T { 8/1965 } 16/1300 }
B4-10	038 	1700/5 (1710)	2560	C	T { 8/1965 } 16/1300 }
B4-11	040 	1800/5 (1825)	3029	C	T { 8/1965 } 16/1300 }
B4-12	042 	1600/5 (1600)	7177	C	T { 8/1965 } 16/1300 }
B4-13	041 	1600/5 (1600)	6510	C	T { 8/1965 } 16/1300 }

